Integrated *in situ* U-Pb age and Hf-O analyses of zircon from Suixian Group in northern Yangtze: New insights into the Neoproterozoic low-$\delta^{18}O$ magmas in the South China Block

Ya-Nan Yang[a, b], Xuan-Ce Wang[c, d], Qiu-Li Li[a], Xian-Hua Li[a,*]

[a] State Key Laboratory of Lithospheric Evolution, Institute of Geology and Geophysics, Chinese Academy of Sciences, Beijing 100029, China

[b] University of Chinese Academy of Sciences, Beijing 100049, China

[c] The Institute for Geoscience Research (TIGeR), Department of Applied Geology, Curtin University, GPO Box U1987, Perth, WA 6845, Australia

[d] The School of Earth Science and Resources, Chang'an University, Xi'an, 710054, China

* Corresponding author.
Tel: +86 10 82998512
Fax: +86 10 62010846
E-mail address: lixh@gig.ac.cn (X.-H. Li).

Abstract

The mid- to late-Neoproterozoic magmatic rocks from the northern margin of the Yangtze Block are major protoliths of high-pressure (HP) and ultrahigh-pressure (UHP) metamorphic rocks in the Dabie-Sulu orogenic belt along the northern margin of the South China Block. Oxygen isotopic compositions of these mid- to late-Neoproterozoic magmatic rocks hold a key to understanding the origin of large-scale ^{18}O-depletion in the HP and UHP metamorphic rocks. We report here the integrated *in situ* U-Pb dating and Hf-O isotope analyses of zircon grains from sedimentary and volcanic rocks in the Neoproterozoic Suixian Group along the northern margin of the Yangtze Block, South China. This study shows that the Suixian Group was deposited at 740-720 Ma, corresponding to late stage of the second deposition cycle (820-720 Ma) of the Neoproterozoic deposition in the Yangtze Block. Detrital zircon grains from the Suixian Group display age peaks at 0.73-0.74 Ga, 0.79 Ga, and 2.0 Ga. Zircon U-Pb ages together with Hf-O isotopic compositions indicate provenance of the Suixian Group dominantly from the proximal Neoproterozoic igneous rocks with possible contribution from Paleoproterozoic rocks along the northern margin of the South China Block. Zircon $\delta^{18}O$ values from the Suixian Group have a large range from 10.5‰ to 1.3‰. Zircon grains with negative $\delta^{18}O$ values, typical index of magma-meteoric water interaction, were not identified in this study. The major phase of low-$\delta^{18}O$ magmas ($\delta^{18}O_{zircon}$ < 4.6‰) initiated at ca. 800 Ma, long before the first glaciation event arising at about 715 Ma in the South China Block, and lasted for over 100 m.y.. The $\varepsilon_{Hf}(t)$ values of the low-$\delta^{18}O$ zircon grains

from the Suixian Group range between -15.5 and 10.7. About seventy-four percent of low-$\delta^{18}O$ zircon grains have negative $\varepsilon_{Hf}(t)$ values varying from -15.5 to -0.02. This strongly argues against the possibility that the low-$\delta^{18}O$ magma was generated dominantly by partial melting of high-T hydrothermally altered oceanic lower crust. This study emphasizes that high-T water-rock interaction and continental rifting tectonic setting are essential to produce the abundant low-$\delta^{18}O$ magmas, and confirms that most of negative $\delta^{18}O$ signature identified in zircon grains from HP and UHP metamorphic rocks may not have been inherited from their Neoproterozoic protoliths.

Keywords

Zircon, Low-$\delta^{18}O$ magma, U-Pb age, Lu-Hf isotopes, South China, Neoproterozoic

1 Introduction

Hydrothermal interaction between rocks and meteoric water offers the most viable mechanism to imprint low-$\delta^{18}O$ values on the rocks (Bindeman, 2011). Low-$\delta^{18}O$ magmatic zircon grains have commonly been identified in high-temperature (high-T) rhyolites, A-type granites and rare arc magmas (e.g. Muñoz et al., 2012). The best example of high-T rhyolites is from the Yellowstone volcanic field with zircon $\delta^{18}O$ values varying from 2‰ to 6‰ (e.g., Bindeman, 2008; Bindeman and Valley, 2001; Watts et al., 2010). Recent discoveries of isotopically diverse minerals from the Snake River Plain, Iceland, Kamchatka Peninsula, and other environments show that high-T water-rock interaction and subsequent recycling of hydrothermally altered subsolidus predecessors during the magma evolution are important to produce low-$\delta^{18}O$ magmatic zircon grains (Bindeman and Simakin, 2014). Well-documented examples of low-$\delta^{18}O$ A-type granites come from western Scotland and southeastern China: zircon grains from granites in western Scotland have $\delta^{18}O$ values varying from ~0‰ to 7.2‰ (e.g., Monani and Valley, 2001); Mesozoic A-type granites from southeastern China also have low-$\delta^{18}O$ zircon grains ($\delta^{18}O$ = 3.1‰ to 5.4‰, Wei et al., 2008). Thus hotspot and rift environments with high magma and heat fluxes are ideal settings to produce low-$\delta^{18}O$ magmas (e.g., Bindeman and Simakin, 2014; Wang et al., 2011). Partial melting of subducted oceanic gabbro can also generate low-$\delta^{18}O$ magmas (Wei et al., 2002). The low-$\delta^{18}O$ magmas produced by partial melting of subducted lower crust are expected to possess MORB-like radiogenic isotope signatures such as positive $\varepsilon_{Hf}(t)$ and $\varepsilon_{Nd}(t)$ values.

Thus, combination of zircon O and Hf isotopes is crucial for examination of the origin of low-$\delta^{18}O$ magmas.

Large-scale ^{18}O-depletion has been identified in HP and UHP metamorphic rocks in the Dabie-Sulu orogenic belt along the northern margin of the South China Block (Fu et al., 2013; Rumble et al., 2002; Yui et al., 1995; Zheng et al., 1996; Zheng et al., 2004). The depletion and ultra-depletion of ^{18}O in these UP and UHP metamorphic rocks has significant implications not only for understanding fluid rock interaction during deep subduction of continental crust, but also for identifying the Neoproterozoic Snowball Earth events (Chen et al., 2003; Rumble et al., 2002; Tang et al., 2008; Zheng et al., 2004; Zheng et al., 2007; Zheng et al., 2003).

Oxygen isotope and U-Pb ages of detrital zircon grains from the Neoproterozoic sedimentary sequences in the Nanhua rift basin along the Sibao orogen in the South China Block show that low-$\delta^{18}O$ magmatic zircon grains started from ca. 870 Ma. This coincides with the tectonic switching from the Sibao orogenesis to post-orogenic extension and is more than 150 Ma prior to the first episode of mid-Neorpoterozoic glaciation event (Wang et al., 2011; Yang et al., 2015). Therefore, nonglacial origin for the low-$\delta^{18}O$ Neoproterozoic magmas in the South China was proposed, and a two-stage mechanism with high magma and high heat flux in continental rifting environment was advanced to explain the low-$\delta^{18}O$ magmas (Wang et al., 2011; Yang et al., 2015). Alternative mechanisms for such a low-$\delta^{18}O$ signature may involve re-melting of either low-$\delta^{18}O$ caldera collapse or seawater-hydrothermally altered oceanic lower crust (Zhang and Zheng, 2013). Increasing evidence from the Nanhua

107 Basin (Wang et al., 2011; Yang et al., 2015) and the Dabie-Sulu UHP metamorphic
108 rocks (Chen et al., 2003; Fu et al., 2013; Rumble et al., 2002; Zheng et al., 2004;
109 Zheng et al., 2003) shows that mid-Neoproterozoic low-$\delta^{18}O$ magmatism was
110 widespread around the Yangtze Block, making it the largest ^{18}O-depletion magmatic
111 province worldwide. Thus, the mechanism and spatial-temporal distribution of such
112 an ^{18}O-depleted magmatic province are important not only for understanding fluid
113 cycling between Earth's surface and its deep crust, but also for fluid-rock interaction
114 in UHP metamorphism. Mid-Neoproterozoic magmatic rocks from the northern
115 Yangtze Block are major protoliths of the Dabie-Sulu metamorphic rocks (e.g. Liu et
116 al., 2013; Rowley et al., 1997; Zheng et al., 2003). The primary oxygen isotopic
117 compositions of these mid-Neoproterozoic magmas therefore hold a key to
118 understanding origin of extremely ^{18}O-depletion in UP and UHP metamorphic rocks
119 in the Dabie-Sulu orogenic belt. However, due to younger geological processes, most
120 mid-Neoproterozoic igneous rocks might have been eroded (e.g. Bindeman, 2008).
121 Fortunately, detrital zircon grains within sedimentary rocks might have preserved the
122 primary depleted ^{18}O signature of the eroded igneous rocks (Bindeman, 2011; Wang
123 et al., 2011; Yang et al., 2015) due to their highly refractory property, extremely slow
124 rate of oxygen diffusion and high closure temperature (Cherniak and Watson, 2003;
125 Peck et al., 2003; Valley et al., 1994; Zheng and Fu, 1998). Therefore, an alternative
126 approach to constrain the timing and scale of the Neoproterozoic low-^{18}O magmas in
127 the South China Block is to conduct *in situ* O and U-Pb isotopic analyses on zircon
128 grains from unmetamorphosed or weakly metamorphosed sedimentary rocks.

In this paper, we report the U-Pb ages and Hf-O isotopes of zircon grains from sedimentary and volcanic rocks along the northern margin of the Yangtze Block. The integrated results provide important constraint on the temporal and spatial distribution of the Neoproterozoic low-$\delta^{18}O$ magmas in the Yangtze Block and offer insights into the genesis of the low-$\delta^{18}O$ Dabie-Sulu UHP metamorphic rocks. This also allows us to evaluate the proposed mechanism producing the worldwide largest low-$\delta^{18}O$ magmatic province, which is crucial for understanding deep-Earth fluid cycling.

2 Geological setting and sampling

The South China Block (SCB) is separated from North China Craton by the Qinling-Tongbai-Dabie-Sulu orogen in the north, from the Songpan-Ganzi terrane by the Longmengshan Fault to the northwest, from the Indochina Block by the Ailaoshan-Songma suture zone in the southwest, and is bounded by the Pacific Ocean to the southeast (Fig. 1a). The SCB consists of the Yangtze Block in the northwest and the Cathaysia Block in the southeast, which amalgamated together during the early Neoproterozoic (e.g. Li et al., 2009; Li et al., 2007; Li et al., 2008; Ye et al., 2007).

The Yangtze Block consists mainly of Proterozoic rocks with sporadic outcrops of Archean rocks. Archean and Paleoproterozoic basement rocks have only been reported from the northern and southwestern parts of the Yangtze Block, e.g. 3.4-3.2 Ga and 3.0-2.9 Ga tonalite-trondjemite-granodiorite (TTG) rocks from Kongling terrane (Chen et al., 2013; Gao et al., 2011; Guo et al., 2014; Jiao et al., 2009; Qiu et al., 2000), 2.65 Ga Huji high-K granite (Zhou et al., 2015), 2.5 Ga TTG rock from

Douling complex (Wu et al., 2014), 2.08 Ga gray gneiss from Houhe complex (Wu et al., 2012), and Dahongshan Group with 1.68 Ga tuffaceous schist unit (Greentree and Li, 2008). Voluminous Neoproterozoic magmatic rocks occurred in the Yangtze Block, with the main pulses of magmatic event during 860-750 Ma (Fig. 1a; Appendix S1). The Neoproterozoic strata can be classified into three tectonostratigraphic sequences: (I) the lower part of the Neoproterozoic strata consisting dominantly of clastic sedimentary rocks with minor volcanic rocks (850-820 Ma); (II) the most widely distributed Neoproterozoic volcanic sedimentary unit (820-720 Ma) that is usually overlying sequence (I) with an unconformity; (III) the glacial and interglacial deposits (720-635 Ma) (e.g., Lan et al., 2014; Lan et al., 2015; Wang and Li, 2003; Wang et al., 2012; Zhang et al., 2008).

The Tongbai area along the northern margin of the Yangtze Block is the middle segment of the Qinling-Tongbai-Dabie-Sulu orogen. It is separated from the western Dabie unit in the east by the Dawu fault and from the Qinling unit in the west by the Nanyang basin. The Tongbaishan unit from northeast to southwest consists of six collision-related lithotectonic units: (1) the Nanwan flysch, (2) the Balifan tectonic mélange, (3) the northern eclogite zone, (4) the Tongbai Complex, (5) the southern eclogite zone, and (6) the blueschist-greenschist zone (Liu et al., 2010; Liu et al., 2008). The blueschist-greenschist zone, equivalent to the Mulanshan unit of western Dabie, is composed mainly of metamorphic bimodal volcanics and some metasedimentary rocks (Liu et al., 2008). The studied Suixian Group is part of the blueschist-greenschist zone of the Tongbai unit. The studied area is bounded by the

173 Xiangfan-Guangji fault to the northeast and Xincheng-Huangpi fault to the southwest,
174 respectively (Fig. 1b). Although the original deposition sequences of the Suixian
175 Group had been disturbed during the Phanerozoic orogeny, reconstruction of the strata
176 divided the group into the Guijing, Liulin and Yuanziwan formations from bottom to
177 top (Fig. 2; HGB, 1982). The lower part of Gujing Formation consists of
178 sericite-albite-quartz schist, sericite-quartz-albite schist, and actinolite schist while the
179 upper part of the Gujing formation is characterized by sedimentary rocks mainly of
180 meta-feldspar quartz sandstone, sandstone, and siltstone. The Liulin Formation is
181 composed mainly of metasedimentary rocks such as pebbled sandstone and quartz
182 sandstone in the lower part and albite-quartz-sericite schist, sericite-albite-quartz
183 schist with metarhyolite and siltstone layers in the upper part. The Yuanziwan
184 Formation is made up mostly of albite-quartz-sericite schist, sericite-quartz-albite
185 schist and siltstone (HGB, 1982). Low-grade metamorphism at greenschist facies to
186 blueschist facies has been identified for the Suixian Group and equivalents (Liu et al.,
187 2011). The Gujing, Liulin, and Yuanziwan formations were all intruded by
188 mafic-ultramafic intrusions with U-Pb age of ca. 630 Ma (Xue et al., 2011) (Fig. 1).
189 The Suixian Group is conformably overlain by muddy slate from Chahe Formation
190 (Fig.2). The Chahe Formation is assumed to be correlated with Doushantuo
191 Formation (HGB, 1982).

192 Eleven samples were collected from the Suixian Group (Fig. 2) for secondary ion
193 mass spectrometry (SIMS) oxygen and U-Pb analyses and LA-MC-ICPMS hafnium
194 isotopic measurements. Three samples 12SZ20 (31°21'11.7"N, 113°42'41.5"E),

12SZ24 (31°28’26.7"N, 113°41’48.1"E) and 12SZ28 (31°30'55.3"N, 113°35'45.0"E) were collected from the Gujing Formation. Sample 12SZ20 is a siltstone composed of 90% quartz and 10% sericite and sericite shows preferential orientation. Both samples12SZ24 and 12SZ28 are sandstone made of irregular quartz and matrix of sericites with weak preferred orientation. Six specimens 12SZ06 (31°31'45.4"N, 113°14'11.9"E), 12SZ07 (31°34'26.4"N, 113°21'38.3"E), 12SZ14 (31°49'10.1"N, 113°22'22.2"E), 12SZ17 (31°39'45.8"N, 113°34'43.8"E), 13SZ14 (31°34'59.1"N, 113°21'52.3"E) and 13SZ19 (31°35'19.8"N, 113°12'02.2"E) were collected from the Liulin Formation. Both samples 12SZ06 and 12SZ07 are sandstone composed of poorly sorted quartz. The main difference between sample 12SZ06 and sample 12SZ07 is that in the former the matrix mainly consists of calcite while in the latter the matrix is made of fine-grained quartz and sericite. Samples 13SZ14 and 13SZ19 are also sandstone with irregular quartz clastic similar to sample 12SZ07. Sample 12SZ14 is a metarhyolite with quartz as phenocryst. The matrix of metarhyolite 12SZ14 reveals weak preferred orientation and was variably altered to fine sericite. Sample 12SZ17 is a tuffaceous siltstone consisting mainly of orientated quartz and sericite. Siltstone 12SZ10 (31°39'17.2"N, 113°21'44.9"E) and sandstone 13SZ17 (31°39'45.2"N, 113°15'03.3"E) were collected from the Yuanziwan Formation. Sample 12SZ10 is a siltstone composed of quartz aligned with preferentially orientated sericites. Sandstone 13SZ17 consists mainly of irregular quartz with fine sericites as matrix. No mineral grains show preferred orientation in this sample. Representative micrographs can be found in Appendix S2.

3 Analytical techniques

Zircon concentrates were separated from ca. 2 kilograms of rock samples using standard density and magnetic separation techniques. All zircon grains were purified under binocular microscope for U-Pb dating, O and Hf isotope analysis. Zircon grains, together with zircon standards Plešovice (Sláma et al., 2008), Penglai (Li X. H. et al., 2010), and Qinghu (Li X. H. et al., 2013), were mounted in epoxy mounts which were then polished to section the crystals in half for analysis. All zircon grains were documented with transmitted and reflected light micrographs as well as cathodoluminescence (CL) images to reveal their internal structures, and the mount was vacuum-coated with high-purity gold prior to SIMS analyses.

3.1 SIMS zircon oxygen isotope measurements

The oxygen isotopic compositions of zircon grains were measured using the CAMECA IMS 1280 SIMS at the Institute of Geology and Geophysics, Chinese Academy of Sciences (IGGCAS). Analytical procedures are similar to those described by Li X.H. et al. (2010). The Cs^+ primary ion beam was accelerated at 10 kV, with an intensity of ca. 2 nA. The spot size is about 20 μm in diameter. The normal incidence electron flood gun was used to compensate for sample charging during analysis. Oxygen isotopes were measured using multi-collection mode on two off-axis Faraday cups with mass revolution of ~2500 (#slit 2). The intensity of ^{16}O was typically no less than 1×10^9 counts per second (cps). The nuclear magnetic resonance (NMR)

239 probe was used for magnetic field control. Each analysis takes less than 4 minutes
240 consisting of pre-sputtering (ca. 60 s), automatic beam centering (ca. 60 s) and
241 integration of oxygen isotopes (20 cycles × 4 s). Uncertainty on individual analysis is
242 usually better than 0.2‰ - 0.3‰ (2σ).

243 Measured $^{18}O/^{16}O$ ratios are reported as $\delta^{18}O$ per mil (‰) values, calculated
244 relative to oxygen isotopic composition of Vienna Standard Mean Ocean Water
245 $(^{18}O/^{16}O)_{VSMOW} = 0.0020052$ (Baertschi, 1976). The instrumental mass fractionation
246 factor (IMF) is corrected using zircon standard Penglai with a $\delta^{18}O$ value of 5.3 ±
247 0.1‰ (2σ) (Li X.H. et al., 2010). The standard data were collected regularly
248 throughout the analytical session as the IMF drifted with time. Qinghu zircon was
249 measured as an unknown to yield a standard deviation of 0.4 per mil (2σ), which is
250 used for least uncertainty for individual analysis. Low-$\delta^{18}O$ zircon grains in this study
251 are defined as those whose $\delta^{18}O$ values are no greater than those of mantle zircon (5.3
252 ± 0.6, 2SD; Valley et al., 1998; Valley et al., 2005). Statistically, a variable x with
253 uncertainty of α is significantly different from another variable y with uncertainty of β
254 if $|x - y| > \sqrt{\alpha^2 + \beta^2}$. Following this philosophy, zircon SIMS $\delta^{18}O$ value < 4.6‰
255 is distinctively lower than 5.3 ± 0.6‰ at significance level of 0.05, considering
256 analytical uncertainty of 0.4. Therefore, zircon grains with $\delta^{18}O$ values < 4.6‰ are
257 categorized as low-$\delta^{18}O$ zircon crystals in this study.

258

259 **3.2 SIMS U-Pb zircon dating**

260 Measurements of U, Th, and Pb isotopes were carried out by the CAMECA IMS

1280 SIMS at the IGGCAS. Analytical procedures are referred to those described by Li X.H.et al. (2009). The O_2^- primary bean with an intensity of ca. 10 nA was accelerated at - 13 kV. The ellipsoidal spot is about 20 μm × 30 μm in size. Oxygen flooding was used to increase the O_2 pressure to ca. 5×10^{-6} torr in the sample chamber, enhancing Pb^+ sensitivity by a factor of >2 to a value of ca. 25-28 cps/nA/ppm for zircon (Li X. H. et al., 2009). A single electron multiplier with a mass resolution of ca. 5400 (defined at 10% peak height) was used on ion-counting mode to measure secondary ion beam intensities by peak jumping sequences.

Measured Pb/U ratios were calibrated with power law relationship between Pb^+/U^+ and UO_2^+/U^+ relative to the standard zircon Plešovice dated at 337 Ma (Sláma et al., 2008). A long-term uncertainty of 1.5% (1 RSD) for $^{206}Pb/^{238}U$ measurements of the Plešovice standard was propagated to the unknowns, despite that the measured $^{206}Pb/^{238}U$ error in a specific session is generally around 1% (1 RSD) or less (Li Q. L. et al., 2010; Yang et al., 2014). The measured Pb isotopic compositions were corrected for common Pb using non-radiogenic ^{204}Pb. An average present-day crustal Pb composition (Stacey and Kramers, 1975) was used for the common Pb assuming that the common Pb was largely due to surface contamination introduced during sample preparation. Uncertainties in the isotopic ratios and ages in the tables are reported at 1σ level, but unless otherwise stated, whereas the final weighted mean ages are reported at 95% confidence level. The data were reduced with the Isoplot 3.75 program Ludwig (2012). Fifty-five analyses of the Qinghu U-Pb working reference zircon give a weighted mean $^{206}Pb/^{238}U$ age of 159.9 ± 0.7 Ma (MSWD =

283 1.2, n = 55), which agrees well with the recommended $^{206}Pb/^{238}U$ age of 159.5 ± 0.2
284 Ma (2SE) (Li X. H. et al., 2009) within analytical errors.
285
286 **3.3 LA-MC-ICPMS zircon Lu-Hf isotope analysis**
287 Zircon Hf isotopic analysis was carried out on a Neptune multi-collector ICP-MS
288 equipped with a Geolas-193 laser ablation system (LA-MC-ICPMS) at the IGGCAS.
289 Lu-Hf isotopic measurements were made on the same zircon grains previously
290 analyzed for O and U-Pb isotopes, with repetition rate of 8-10 Hz, laser beam energy
291 density of 10 J/cm^2, and ablation time of 26 s. The detailed analytical procedures were
292 similar to those described by Wu et al. (2006). Data were routinely acquired by
293 ablating 60μm diameter laser spots, but 44μm diameter laser spots were adopted
294 occasionally in case of small zircon grains. Contribution of isobaric interferences by
295 ^{176}Lu and ^{176}Yb on the ^{176}Hf signal was subtracted by monitoring the intensity of
296 ^{175}Lu and ^{172}Yb signals, using $^{176}Lu/^{175}Lu = 0.02655$ and $^{176}Yb/^{172}Yb = 0.5886$ (Chu
297 et al., 2002). The measured $^{176}Hf/^{177}Hf$ ratios for zircon standards Mud Tank, GJ-1,
298 and Qinghu are 0.282505 ± 28 (2SD), 0.282014 ± 37 (2SD), and 0.282994 ± 39 (2SD),
299 respectively, which are consistent with reference $^{176}Hf/^{177}Hf$ values of 0.282507 ±
300 0.000006, 0.282000 ± 0.000005, and 0.283002 ± 0.000004, respectively (Li X. H. et
301 al., 2013; Morel et al., 2008; Woodhead and Hergt, 2005).
302 Initial Hf isotope composition were calculated with the reference to the chondritic
303 ratios of $^{176}Hf/^{177}Hf = 0.282772$ and $^{176}Lu/^{177}Hf = 0.0332$ (Blichert-Toft and Albarède,
304 1997) and the U-Pb ages of the dated zircon crystals. A decay constant for ^{176}Lu of

305 1.867×10^{-11} yr^{-1} (Söderlund et al., 2004) was adopted. The results were donated as
306 the conventional $\varepsilon_{Hf}(t)$ values that represent the 0.1‰ difference between the sample
307 and the chondritic reservoir at the time of crystallization.
308
309 **4 Results**
310 **4.1 SIMS Zircon U-Pb ages**
311 Two hundred and ninety-five zircon grains from eleven samples of the Suixian
312 Group were collected for SIMS U-Pb dating (Fig. 2; Appendix S3). $^{206}Pb/^{238}U$ age and
313 its uncertainty are taken as the final U-Pb age if $^{206}Pb/^{238}U$ age is less than 1000 Ma
314 for single analysis; otherwise, $^{207}Pb/^{206}Pb$ age and accompanying uncertainty are
315 adopted. Age discordance is defined as percent deviation of $^{206}Pb/^{238}U$ age from
316 $^{207}Pb/^{206}Pb$ age.
317
318 **4.1.1 Gujing Formation, lower part of the Suixian Group**
319 Forty-eight zircon grains from three samples of upper part of the Gujing
320 Formation (siltstone 12SZ20, sandstone 12SZ24, and sandstone 12SZ28, Fig. 2) were
321 selected for SIMS U-Pb isotope analyses. Zircon grains in these samples are mostly
322 euhedral and range in length from 30 to 150 μm with aspect ratios of 1:1 to 3:1.
323 Cathodoluminescence (CL) images reveal clear oscillatory zoning or homogenous
324 illuminating, which together with Th/U ratios varying from 0.6 to 3.9 suggest
325 magmatic origin (Appendix S4). Of the forty-eight analyses on 48 zircon grains, 45
326 analyses are concordant within uncertainties (Appendix S3). The measured U-Pb ages

are between 718 and 1740 Ma, and the main age population peaks at 739 ± 4 Ma (Fig. 3a). In addition, two minor peaks at 830 Ma and 1840 Ma are also present. The youngest population age of 740 Ma provides a maximum constraint on the deposition time of the Gujing Formation (Fig. 2).

4.1.2 Liulin Formation, middle part of the Suixian Group

Four sandstone samples (12SZ06, 12SZ07, 13SZ14, and 13SZ19) were collected from the lower part of the Liulin Formation and one metarhyolite (12SZ14) and tuffaceous siltstone (12SZ17) from the upper part of the Liulin Formation (Fig. 2) for SIMS zircon U-Pb dating.

Zircon grains from the four sandstone samples (12SZ06, 12SZ07, 13SZ14, and 13SZ19) are represented by subrounded to rounded grains in addition to some being euhedral and prismatic in shape (Appendix S4). They range in length from 50 to 260 μm, with aspect ratios of 1:1 to 4:1. Their CL images reveal that most of them show clear oscillatory zoning, indicating provenance of igneous rocks (Corfu et al., 2003). One hundred and forty-four U-Pb analyses were conducted on 144 zircon grains for these sandstones. The results show relative large variations of U contents (26 to 1919 ppm) and Th contents (7 to 1486 ppm). This gives Th/U ratios 0.1 to 2.0 which is typical of magmatic zircon. One hundred and thirty-six out of the 144 analyses are concordant within uncertainties. The U-Pb ages vary from 709 to 2739 Ma, and the main population ranges from 742 to 878 Ma (accounting for 74% of the total analyzed grains) with a peak of 789 ± 5 Ma (Fig. 3b). There is one obvious subordinate age

group peaking at about 2.02 Ga. Minor peaks at 1.0 Ga and 1.6 Ga are also revealed.

Most zircon grains recovered from metarhyolite 12SZ14 are euhedral and prismatic (Appendix S4). They range in length from 50 to 200 μm, and have length to width ratios of 1:1 to 3:1. In CL images, most of them exhibit clear fine or broad oscillatory zoning, a typical characteristic of magmatic zircon (Corfu et al., 2003). Twenty-four analyses were carried out on 24 grains. The results exhibit U and Th contents of 31 to 205 ppm and 46 to 279 ppm, respectively. They give U/Th ratios of 0.4 to 2.0, consistent with their igneous origin. Except for one zircon core with $^{207}Pb/^{206}Pb$ age of 999 ± 19 Ma (12SZ14@21), the remaining analyses form a coherent group with a weighted mean $^{206}Pb/^{238}U$ age of 742 ± 6 Ma (MSWD = 1.7, n = 22) (Fig. 4a and 4a'). This was interpreted to represent the crystallization age of this metarhyolite.

Zircon grains from tuffaceous siltstone 12SZ17 are euhedral, prismatic and translucent. Their lengths range from 50 to 250 μm, with aspect ratios of 1:1 to 3.5:1. Their CL images reveal that most of them show relatively broad oscillatory zoning (Appendix S4). Twenty-seven analyses were conducted on 27 grains. The results show variable contents of U and Th of 84 to 670 ppm and 27 to 757 ppm, respectively. They yield relatively high Th/U ratios of 0.3 to 1.1, consistent with their igneous origin. Except for one older grain having a $^{206}Pb/^{238}U$ age of 831 ± 12 Ma, the other analyses yield a weighted mean $^{206}Pb/^{238}U$ age of 727 ± 5 Ma (MSWD = 1.16, n = 26) (Fig. 4b and 4b'), representing the maximum deposition age of the tuffaceous siltstone.

371

372 #### 4.1.3 Yuanziwan Formation, upper part of the Suixian Group

373 Zircon grains of siltstone 12SZ10 and sandstone 13SZ17 from the upper part of
374 Yuanziwan Formation (Fig. 2) are euhedral and prismatic. Their CL images are
375 characterized by relative broad oscillatory zoning, typical of magmatic zircon grains
376 (Appendix S4). Fifty-two analyses were done on 52 zircon grains for these two
377 samples. The result reveals U and Th contents of 30 to 626 ppm and 36 to 1258 ppm,
378 respectively. This gives Th/U ratios of 0.4 to 3.1, which is consistent with magmatic
379 origin. The U-Pb ages range from 709 to 799 Ma and form one single population with
380 the peak age at ca. 730 Ma. Since siltstone 12SZ10 and sandstone 13SZ17 are located
381 to the uppermost part of the Yuanziwan Group (Fig. 2), the peak age of 734 ± 3 Ma
382 provides a maximum timing constraint on the end of the deposition of the Suixian
383 Group (Fig. 3c).

384

385 ### 4.2 *In situ* zircon oxygen and hafnium isotopes

386 All the zircon grains dated were selected for *in situ* oxygen and hafnium isotopic
387 analyses. A total of 295 O-isotope measurements had been conducted on 295 zircon
388 grains (Appendix S3). With the exception of fifteen O-isotope analyses that have
389 discordant ages, the remaining data are adopted in the following discussion. Among
390 them, two hundred and seventy isotopic compositions were obtained on 270 zircon
391 grains (Appendix S3).

392 Zircon $\delta^{18}O$ values from the Gujing Formation (lower part of the Suixian Group)

393 vary from 1.4‰ to 7.6‰ with ca. 64% of low-$\delta^{18}O$ zircon grains (Fig. 5). Zircon
394 grains from the Liulin Formation (middle part of the Suixian Group) reveal highly
395 variable $\delta^{18}O$ values from 10.5‰ to 1.4‰. Pre-1.5 Ga zircon crystals from the Liulin
396 group show $\delta^{18}O$ values of 7.5‰ to 5.9‰ while maximum $\delta^{18}O$ values of the post-1.0
397 Ga zircon grains climbed from 5.3‰ at ca. 930 Ma up to highest $\delta^{18}O$ value of 10.5‰
398 at ca. 820 Ma (Fig. 5b). Also noteworthy is the abrupt occurrence of low-$\delta^{18}O$ zircon
399 grains at ca. 780 Ma (Fig. 5b). The zircon $\delta^{18}O$ values from the Yuanziwan Formation
400 range from 8.6‰ to 1.3‰. Sandstone 13SZ17 from the Yuanziwan Formation is
401 characterized by large amount of low-$\delta^{18}O$ zircon grains (19 out of 24 grains).

402 The zircon $\varepsilon_{Hf}(t)$ values from the Gujing Formation range from 9.7 to -16.0, and
403 36 out of 43 zircon grains bear negative $\varepsilon_{Hf}(t)$ values peaking at ca. -6.8 (Fig. 6a). The
404 $\varepsilon_{Hf}(t)$ values of zircon grains from the Liulin Formation vary from 12.4 to -18.1, and
405 59% of the zircon $\varepsilon_{Hf}(t)$ values are positive (Fig. 6b). The Hf isotopic compositions
406 form two major populations with $\varepsilon_{Hf}(t)$ peaks at ca. 5.9 and -9.2. Besides, zircon
407 grains older than 1.5 Ga from the Liulin Formation are dominated by negative $\varepsilon_{Hf}(t)$
408 values from -1.1 to -12.2 (Fig. 7a). The zircon grains from the Yuanziwan Formation
409 reveal $\varepsilon_{Hf}(t)$ values from 6.3 to -15.5 (Fig. 6c). Ninety-three percent of zircon grains
410 give negative $\varepsilon_{Hf}(t)$ values with the dominant group peaking at about -5.9. Two minor
411 peaks at ca. -12.5 and 6.3 are also present.

412 To sum up, oxygen isotopes of Neoproterozoic magmatic zircon grains from the
413 Tongbai low-grade sedimentary and meta-volcanic rocks along the northern margin of
414 the South China Block display the following characteristics. First, their $\delta^{18}O$ values

show a large variation from 1.3‰ to 10.5‰, but no negative $\delta^{18}O$ values are identified in this study (Fig.5a). Second, low-$\delta^{18}O$ zircon grains started sporadically since ca. 840 Ma, and culminated at ca. 780-700 Ma (Fig.5b). These zircon grains reveal a wide range of $\varepsilon_{Hf}(t)$ values from -18.1 to 12.4. Particularly, Neoproterozoic positive-$\varepsilon_{Hf}(t)$ zircon grains make up 38% of total analyses (Fig. 7b). The pre-1.0 Ga zircon grains are dominated by negative-$\varepsilon_{Hf}(t)$ values (Fig. 7a).

5 Discussion

5.1 Timing and provenance of the Suixian Group sedimentary rocks

The youngest group of ages from detrital zircon grains could be used to constrain the maximum depositional age of sedimentary rocks (e.g. Dickinson and Gehrels, 2009; Gehrels, 2014). Detrital zircon U-Pb ages from the upper part of the Gujing Formation (siltstone 12SZ20, sandstone 12SZ24, and sandstone 12SZ28, Fig. 2) display one dominant group with a weighted mean $^{206}Pb/^{238}U$ age of 739 ± 4 Ma, providing a maximum depositional timing of the upper part of the Gujing Formation and onset age for the Liulin Formation. Zircon grains from the metarhyolite 12SZ14 and tuffaceous siltstone 12SZ17 (Fig. 2) from the upper part of the Liulin Formation give weighted mean $^{206}Pb/^{238}U$ ages of 742 ± 6 Ma and 727 ± 5 Ma (Fig. 3c), respectively, pinning the ending of the deposition of the Liulin Formation and initiating of the Yuanziwan Formation at ca. 740-720 Ma. Zircon U-Pb measurements for siltstone 12SZ10 and sandstone 13SZ17 from the upper part of Yuanziwan Formation (Fig.2) yield a consistent Neoproterozoic population peaking at 734 ± 3

437 Ma, which constrains the ending of Yuanziwan Formation deposition < 734 ± 3 Ma.
438 Therefore, the onset deposition of the Suixian Group is approximately 739 ± 4 Ma
439 constrained by zircon U-Pb dating results from the Gujing Formation, consistent with
440 the SHRIMP U-Pb zircon age of 741 ± 7 Ma for a meta-trachandesite from the Gujing
441 Formation (Xue et al., 2011). The 632 ± 6 Ma troctolite (Xue et al., 2011) that
442 intruded the Suixian Group (Fig.1 b) serves as a minimum age for the deposition for
443 this group (Fig. 2). Considering the lack of glacial deposits similar to diamictite of
444 either Nantuo Formation (650-635 Ma; Liu et al., 2015) or Jiangkou glaciation (<715
445 Ma; Lan et al. 2014; Zhang et al., 2008), the Suixian Group is supposed to be
446 correlated with the Liantuo Formation (780-714 Ma; Lan et al., 2015) in the Yangtze
447 Block. Thus, we tentatively set the ending deposition of the Suixian Group at ca. 720
448 Ma, which is in accordance with the deposition time of the Yuanziwan Formation less
449 than 734 ± 3 Ma (Figs. 2, 3). In conclusion, the deposition age of the Suixian Group is
450 constrained between 740 and 720 Ma. If the stratigraphic reconstruction (HGB, 1982)
451 is valid, the short duration of the deposition and at least one kilometer of sediments
452 (Fig. 2) might indicate a high rate of deposition.

453 Detrital zircon grains from the Suixian Group display a U-Pb age pattern with
454 multiple peaks at ca. 0.73-0.74 Ga, 0.79 Ga, and 2.0 Ga (Fig. 3). The zircon grains of
455 the 0.73-0.74 Ga population are mainly from the Gujing and Yuanziwan formations
456 (Fig. 3a and 3c). These zircon grains have similar oxygen and hafnium isotopic
457 compositions, with dominantly negative $\varepsilon_{Hf}(t)$ values and ca. 67% of low-$\delta^{18}O$ zircon
458 grains (Fig. 8). Such zircon Hf and O isotopic characteristics are consistent with those

459 of 742 ± 6 Ma metarhyolite and 727 ± 5 Ma tuffaceous siltstone from the Liulin
460 Formation (Fig. 8). This, together with their euhedral and subhedral morphology
461 (Appendix S4) and widespread coeval magmatic events along the northern margin of
462 the Yangtze Block (Fig.1a), indicate that the ca. 0.73-0.74 Ga detrital zircon grains
463 from the Gujing and Yuanziwan formations most likely derived from locally exposed
464 Neoproterozoic rocks in this region. Zircon grains with a peak at 0.79 Ga mainly
465 come from the 4 sandstone samples (12SZ06, 12SZ07, 13SZ14 and 13SZ19) of the
466 Liulin Formation (Fig. 3b). These zircon grains show large variation of $\varepsilon_{Hf}(t)$ values
467 from 11.1 to -17.5 (Fig. 6b) and $\delta^{18}O$ values between 7.6‰ and 3.0‰ (Fig. 5b).
468 Neoproterozoic 730-820 Ma magmatic rocks are widely occurred along the northern
469 margin of the Yangtze Block (Fig. 1a), which are likely sources for those
470 mid-Neoproterozoic zircon grains.

471 Seventeen zircon grains with $^{207}Pb/^{206}Pb$ age ranging from 1960 to 2050 Ma from
472 the Liulin Formation (Fig. 3b) form a consistent population with a weighted mean age
473 of 2005 ± 10 Ma (MSWD = 0.97). These grains have a limited variation of $\varepsilon_{Hf}(t)$
474 between -12.2 and -8.1 and a narrow range of $\delta^{18}O$ values from 7.5‰ to 6.4‰.
475 Paleoproterozoic magmatic rocks dated at ca. 2.0 Ga in the Yangtze Block is only
476 reported for gray gneisses from the Houhe complex (Wu et al., 2012) and a felsic
477 gneiss at Huangtuling from the northern Dabie unit (Wu et al., 2008). However, the
478 age of gray gneiss from the Houhe complex is constrained by LA-ICPMS zircon U-Pb
479 analyses at 2081 ± 9 Ma (Wu et al., 2012), which is older than the ca. 2.0 Ga zircon
480 grains from the Liulin Formation. In addition, the $\varepsilon_{Hf}(t)$ values (-5.9 to 0.7) for the

481 zircon grains from the Houhe gneiss (Wu et al., 2012) are consistently higher than
482 those for ca. 2.0 Ga zircon grains from this study. Thus the gneiss from the Houhe
483 complex is precluded as the source of the ca. 2.0 Ga zircon grains from the Suixian
484 Group. As no Hf or O isotopic composition was reported for the 1984 ± 14 Ma
485 Huangtuling gneiss (Wu et al., 2008), we assume it as one possible candidate from
486 which the ca. 2.0 Ga zircon grains of the Suixian Group were derived. The 2.08 Ga
487 Houhe complex, 1.98 Ga Huanglingling gneiss together with ca. 2.0 Ga
488 metamorphism as confirmed by the Huangtuling granulite (Sun et al., 2008; Wu et al.,
489 2008) and metasedimentary rocks, amphibolites and migmatites from the Kongling
490 terrane (Wu et al., 2009; Zhang et al., 2006a; Zhang et al., 2006b) suggested that the
491 Yangtze Block experienced a Paleoproterozoic high-grade metamorphic event at ca.
492 2.0 Ga during the assembly of the supercontinent Columbia. Magmatic rocks
493 generated during this process likely served as the source for the zircon grains with age
494 of 1960 to 2050 Ma. This is supported by the 2.02 Ga zircon xenocrysts with $\varepsilon_{Hf}(t)$
495 values between -22.5 to -6.1 (recalculated using the ^{176}Lu decay constant value of
496 1.867×10^{-11} yr^{-1}; Söderlund et al., 2004) separated from lamproite at Jingshan
497 (Zheng et al., 2006), 30 km south to the study area in this research (Fig.1b). Therefore,
498 Paleoproterozoic rocks (ca. 2.0 Ga) along the northern margin of the South China
499 Block might serve as an important provenance contributor to the Suixian Group.
500
501 **5.2 Origin of Neoproterozoic low-$\delta^{18}O$ magmas**
502 Unusually ^{18}O-depletion in HP and UHP metamorphic rocks in the Dabie-Sulu

503 orogenic belt have been reported to cover an overall area of more than 20,000 km^2
504 and volume of likely 60,000 km^3 (Zheng et al., 2004). The low to negative $\delta^{18}O$
505 values are proposed to be inherited from their protoliths (700 to 880 Ma) through
506 high-T hydrothermal alteration with near surface meteoric water (Yui et al., 1995;
507 Zheng et al., 1996). It is significant that the UHP metamorphic rocks still retain
508 pre-metamorphic oxygen isotopic composition after subduction to at least 120 km
509 deep and subsequent exhumation to the upper crustal level (Okay et al., 1989; Wang
510 et al., 1989; Xu et al., 1992; Ye et al., 2000). This is of importance to enlighten the
511 geodynamics of continental crust subduction and provides critical evidence for the
512 proposed fast in, very short stay and fast out of subducted continental crust into the
513 upper mantle (i.e. ice cream-frying model) (Zheng et al., 1997; Zheng et al., 2003).
514 Thus the occurrence of 870-700 Ma low-$\delta^{18}O$ zircon grains around the Yangtze Block
515 provides us the chance to constrain the primary oxygen isotopic compositions of the
516 protoliths for the HP-UHP metamorphic rocks and explore the origin of such
517 large-scale low-$\delta^{18}O$ magmas.

518 Non-metamict zircon grains can preserve their initial $\delta^{18}O$ values from the time
519 of crystallization, even after going through subsequent high-grade metamorphism,
520 subsolidus hydrothermal alteration, and likely magmatic assimilation or anataxis
521 (Gilliam and Valley, 1997; Valley, 2003; Zheng et al., 2004), while zircon grains with
522 high U contents are usually associated with ^{18}O depletion (Booth et al., 2005; Gao et
523 al., 2014; Wang et al., 2015). The majority of zircon grains from this study exhibit
524 euhedral morphology and zoned textures (Appendix S4) with Th/U ratios no less than

525 0.1 (Fig. 9a), which is typical of magmatic origin (e.g., Corfu et al., 2003). The fresh,
526 crack-free crystalline zircon grains from the Suixian Group do not display any
527 correlation between zircon $\delta^{18}O$ values and their U contents (Fig. 9b). This suggests
528 that these grains retain their primary oxygen isotopic composition after crystallization
529 from magmas. Therefore, occurrence of low-$\delta^{18}O$ zircon grains from the Suixian
530 Group points to Neoproterozoic low-$\delta^{18}O$ magmas in the South China Block.

531 Zircon oxygen and U-Pb isotopic data from this study reveal that abundant
532 occurrence of low-$\delta^{18}O$ zircon grains started at ≥780 Ma, which is at least 60 Ma prior
533 to the earliest known glacigenic diamictites in South China (i.e. Jiangkou glaciation of
534 <715 Ma; Lan et al., 2014; Zhang et al., 2008) (Fig. 10). Such observation is
535 supported by SIMS oxygen isotope and U-Pb dating analyses from coeval
536 sedimentary and igneous rocks across the Yangtze Block (Fig. 10). Low-$\delta^{18}O$ zircon
537 grains sprung along northwestern Yangtze Block at ca. 800 Ma and started
538 sporadically at the northern Yangtze at as early as ca. 840 Ma (Fig. 11; Liu and Zhang,
539 2013; Liu et al., 2013; Fu et al., 2013). Along the southeastern Yangtze Block,
540 low-$\delta^{18}O$ zircon grains from the Neoproterozoic sedimentary rocks can be traced back
541 to ca. 870 Ma (Fig. 11; Lan et al., 2015; Wang et al., 2011; Yang et al., 2015), even
542 earlier than the proposed first episode of climate cooling during 815-710 Ma (Huang
543 et al., 2014). Thus formation of low-$\delta^{18}O$ magmatic zircon grains was not necessarily
544 attributed to glacial events (Bindeman, 2011; Liu and Zhang, 2013; Wang et al.,
545 2011). In contrast, we propose that earlier initiation of Neoproterozoic low-$\delta^{18}O$
546 magmas along southeastern Yangtze than those along the northern and western

547 Yangtze Block might be due to diachronous onset of postorogenic extension and
548 rifting of Rodinia supercontinent.

549 Negative-$\delta^{18}O$ magmatic zircon should be distinguished from low-$\delta^{18}O$ grains
550 because of their different origins. Rocks with negative-$\delta^{18}O$ values can only be
551 generated through high-T meteoric-hydrothermal alteration, while high-T
552 hydrothermal alteration by sea water merely lowers the $\delta^{18}O$ values of rocks yet not
553 likely lower than 0‰ (Zhang and Zheng, 2013). Whether negative-$\delta^{18}O$ values
554 demand contribution from continental deglacial meltwater or could be used as the
555 proxy for cold paleoclimate depends on the degree of ^{18}O depletion (e.g. Bindeman,
556 2011). Significantly ^{18}O-depleted metamorphic mineral assemblages and zircon rims
557 (-25‰ to -27.3‰) of Paleoproterozoic rocks of the Belomorian Belt, Russia
558 (Bindeman and Serebryakov, 2011) and extremely negative $\delta^{18}O$ values between
559 -18.12‰ and -13.19‰ for hydrothermal zircon from an A-type granite at Baerzhe in
560 northeastern China were attributed to meteoric water under glaciation (Yang et al.,
561 2013). In contrast, estimated $\delta^{18}O$ value of -11‰ for altering water of the
562 ^{18}O-depleted Dabie-Sulu HP and UHP metamorphic rocks and -4‰ for garnet from
563 Kokchetav eclogite do not necessarily require glaciation meltwater or cold climates
564 (Bindeman, 2011). The cut-off point of $\delta^{18}O$ value between meteoric water under cold
565 climate and precipitation under non-glaciation condition is around -13‰ based on the
566 $\delta^{18}O$ in precipitation for the modern distribution of land masses (Bindeman, 2011;
567 www.waterisotopes.org). Almost all the Neoproterozoic zircon O isotope
568 microanalyses reveal positive $\delta^{18}O$ values, except for three zircon grains displaying

569 negative $\delta^{18}O$ values of -5.3‰, -4.1‰ and -0.9‰ (Fig. 10b), which is still higher than
570 the $\delta^{18}O$ value that has to call for meteoric water under cold climate. The exact origin
571 for the garnet with $\delta^{18}O$ values between -14.4% and -10.0% from Wozicun granite,
572 Beihuaiyang zone, Dabie orogen (Zheng et al., 2007) warrants further investigation to
573 determine whether glacier meltwater or precipitation under cold climate was required.

574 Origin of low-$\delta^{18}O$ magmas has been proposed to require partial melting or
575 assimilation of ^{18}O-depleted rocks, which could be either high-T hydrothermally
576 altered upper continental crust in shallow extensional environments (Larson and
577 Taylor, 1986) or subducted oceanic lower crust (Wei et al., 2002). Evidence from
578 adakite, high-Mg andesite and other arc lavas that were proposed to contain high
579 proportional slab melts show that these arc magmas have no oxygen anomalies
580 (Bindeman et al., 2005). The low-$\delta^{18}O$ magmas produced by partial melting of altered
581 oceanic gabbro should have MORB-like Hf isotopes. However, as shown in Fig. 8,
582 low-$\delta^{18}O$ magmatic zircon grains in this study display diverse $\varepsilon_{Hf}(t)$ values from 10.7
583 to -15.5, concentrating on negative $\varepsilon_{Hf}(t)$values, in contrast with those for the
584 low-$\delta^{18}O$ magmas mainly derived from oceanic lower crust. This implies that partial
585 melting of oceanic lower crust cannot be a dominant mechanism to produce the
586 largest low-$\delta^{18}O$ magmatic province in the Yangtze Block. In contrast, hafnium
587 isotopic diversity in low-$\delta^{18}O$ zircon grains possibly indicates multiple origins for the
588 low-$\delta^{18}O$ magmas. Therefore, the predominant negative $\varepsilon_{Hf}(t)$ values for the low-$\delta^{18}O$
589 zircon grains suggest that the Neoproterozoic low-$\delta^{18}O$ magmas in the South China
590 Block most likely originated from remelting of high-T hydrothermally altered upper

591 continental crust in shallow extensional environments.

592 Such a large and long-lived (800-700 Ma) low-$\delta^{18}O$ magma province (Fig. 11)
593 may require multiple cycles of high-T hydrothermal alteration to deplete ^{18}O of the
594 protoliths and remelting of ^{18}O depleted rocks. The prominent feature of low-$\delta^{18}O$
595 felsic volcanic rocks from the Snake River Plain, Iceland, Kamchatka Peninsula, and
596 other environments is their isotopically diverse minerals (Bindeman et al., 2014).
597 Diverse zircon $\delta^{18}O$ values of the low-$\delta^{18}O$ magmas indicate that magma generation
598 happens by remelting of variably hydrothermally altered protoliths. The generation of
599 zircon Hf-O isotope diversity was proposed to happen at shallow depths of a few
600 kilometers, where meteoric water can circulate at large water/rock ratios to imprint
601 low $\delta^{18}O$ values on the protolith (Bindeman et al., 2014; Watts et al., 2011). Evidence
602 from long-lived large-volume silicic centers in the Snake River Plain and elsewhere
603 showed that low-$\delta^{18}O$ zircon grains mainly occurred at the end of the magmatic
604 evolution (Bindeman et al., 2014; Watts et al., 2011). This evidence indicates that the
605 generation of low-$\delta^{18}O$ rhyolites by recycling hydrothermally altered subsolidus
606 predecessors may be a common evolutionary trend for many rhyolites worldwide,
607 especially in hotspot and rift environments with high magma and heat fluxes
608 (Bindeman and Simakin, 2014). The time gap between initial high-T water–rock
609 interaction and occurrence of major phase of low-$\delta^{18}O$ zircon grains in long-lived
610 large-volume silicic centers from the Snake River Plain can be up to 30-40 m.y. (e.g.
611 Boroughs et al., 2005). This implies that the occurrence of major low-$\delta^{18}O$ zircon
612 grains in long-lived felsic magma provinces might be much younger than formation of

613 their hydrothermally altered subsolidus predecessors. The important application of the
614 study from the Yellowstone low-$\delta^{18}O$ magmas is that the timing of occurrence of
615 major phase of ca. 800-700 Ma low-$\delta^{18}O$ magmatic zircon grains cannot be simply
616 linked to the time of formation of low-$\delta^{18}O$ predecessors in the Yangtze Block. Thus,
617 we propose that early occurrence of low-$\delta^{18}O$ zircon grains at 850-870 Ma (Wang et
618 al., 2011; Yang et al., 2015) in the South China Block implies that early recycled
619 hydrothermally altered subsolidus predecessors should be formed at ≥870 Ma.
620 Therefore, formation of long-lasting low-$\delta^{18}O$ magmas from 870 to 700 Ma requires
621 persistent supply of high magma, heat, and water fluxes.

622 Permeable hydrogeological conditions near magma chambers in shallow
623 extensional environments, such as rifts and calderas, favor the generation of low-$\delta^{18}O$
624 magmas (Bindeman and Valley, 2001; Larson and Taylor, 1986; Wang et al., 2011;
625 Watts et al., 2011; Watts et al., 2010; Zhang and Zheng, 2011). The tectonic setting
626 along the western and northern margin of the Yangtze Block from 850 to 730 Ma is
627 highly debatable and two main schools of thoughts have been proposed. On one hand,
628 an active continental margin between 950 Ma and 700 Ma (i.e. the Panxi-Hanan arc
629 system) was suggested mainly on basis of the intrusive bodies bearing arc-like
630 geochemical features (e.g. Dong et al., 2012; Xiang et al., 2015; Zhao and Zhou, 2007;
631 Zhao and Zhou, 2008; Zhao and Zhou, 2009; Zhao et al., 2011; Zhou et al., 2002;
632 Zhou et al., 2006; Zhou et al., 2002; Zhu et al., 2014). Although low-$\delta^{18}O$ magmas
633 might be generated in a highly-extensional back-arc regime (Li Y. et al., 2015), they
634 rarely occur along subduction zones. Moreover, this model predicts linear distribution

635 low-$\delta^{18}O$ magma along the subduction zone, which contradicts the spatial-temporal
636 distribution of Neoproterozoic low-$\delta^{18}O$ magmas across the Yangtze Block (Fig.1a).
637 Therefore, subduction-related environments are not favorable for generation of
638 large-scale, voluminous low-$\delta^{18}O$ magmas. On the other hand, there exists evidence
639 that suggest a continental rifting setting, exemplified by the 857 ± 13 Ma anorogenic
640 Guandaoshan pluton (Li et al., 2003), rifting-related 820-800 Ma Gaojiacun and
641 Lengshuiqing mafic-ultramafic intrusions (Li et al., 2006) and stratigraphic and facies
642 analysis in the north-south trending Kangdian basin (Wang and Li, 2003), the
643 well-developed 800 Ma Suxiong bimodal volcanic successions (Li et al., 2002) in the
644 western Yangtze Block, and the 820-810 Ma Bikou Group basalt with anomalously
645 high potential temperature along the northern Yangtze Block (Wang et al., 2008).
646 Thus, the high magma production rate and heat flux along with long-lived
647 intra-continental rifting offer the ideal prerequisite to produce widespread low-$\delta^{18}O$
648 magmas across the Yangtze Block.

649 In detail, the oxygen isotopic characteristics of Neoproterozoic zircon grains from
650 the Yangtze Block could be attributed to following processes. (1) From 870 Ma on,
651 the maximum $\delta^{18}O$ value increased and peaked with 10.5‰ at ca. 820 Ma (Fi.g 5b).
652 This coincided with the onset of a major rifting on the impingement of ca. 825 Ma
653 mantle plume upon the South China Block (Li et al., 2003; Li et al., 2002; Li et al.,
654 2008; Li et al., 1999; Wang et al., 2009). Zircon grains formed during this episode are
655 dominated by positive $\varepsilon_{Hf}(t)$ from 12.4 to 0.5 paired with $\delta^{18}O$ values similar to or
656 higher than those of mantle zircon. While the mantle-like $\delta^{18}O$ values may indicate

657 the addition of juvenile materials to the crust, the high-$\delta^{18}O$ values possibly suggest
658 melting of juvenile material that had suffered oxygen isotope exchange near crust
659 surface. Two zircon grains with $\delta^{18}O$ values of 4.1‰ indicate that high-T water-rock
660 interaction was possibly rare. (2) Abrupt decrease of zircon $\delta^{18}O$ from mantle-like
661 values to less than 4.6‰ occurred at around 780 Ma for Suixian Group along the
662 northern margin of the Yangtze Block (Fig. 5b). This corresponded to transition from
663 the first phase of rifting to the main stage of rifting with large-scale extension in the
664 South China Block. The brittle fractures and coeval large quantities of magma
665 eruption and intrusion provided feasible conditions that allowed generation of the
666 low-$\delta^{18}O$ magmas in the crust via remelting or assimilation of hydrothermally altered
667 rocks (Bindeman and Valley, 2000; Bindeman and Valley, 2001; Bindeman et al.,
668 2010; Watts et al., 2011).
669
670 **6 Conclusions**
671 Integrated U-Pb, O and Hf isotopic analyses on zircon grains from the Suixian
672 Group along the northern margin of the South China Block offer new constraints on
673 the deposition timing of Neoproterozoic strata, and shed insights on the
674 temporal-spatial distribution and origin of the Neoproterozoic low-$\delta^{18}O$ magmas.
675 Zircon SIMS U-Pb ages for the volcanic and sedimentary rocks reveal that the
676 Suixian Group was deposited during 740-720 Ma, coeval with the second
677 tectonostratigraphic sequence of the Neoproterozoic deposition in the South China
678 Block. The zircon U-Pb age spectrum, Hf-O and morphological features indicated

679 these zircon grains were likely derived from proximal igneous rocks and possible
680 Paleoproterozoic rocks along the northern margin of the South China Block.

681 Zircon $\delta^{18}O$ values started to drop abruptly to less than 4.6‰ at ~ 800 Ma, which
682 is ca. 80 Ma earlier than the first episode of mid-Neoproterozoic Jiangkou (or
683 Chang'an) glaciation in the South China Block, thus rendering the involvement of
684 water under cold climate unnecessary. Neoproterozoic low-$\delta^{18}O$ magmas in the
685 Yangtze Block developed diachronously. Initiation of low-$\delta^{18}O$ magmas in the
686 southeastern Yangtze was at ca. 870 Ma, while in northern and northwestern Yangtze,
687 low-$\delta^{18}O$ magmas did not start until ca. 840 Ma and 800 Ma, respectively. Around the
688 Yangtze Block, low-$\delta^{18}O$ magmas persisted until at ca. 700 Ma, which was most
689 likely due to remelting of high-T altered rocks under the long-lasting rifting
690 environments in the South China Block during the breakup of Rodinia supercontinent.

691

692 **Acknowledgements**

693 We thank Dr. Han-Wen Zhou, Dr. Zhong-Wu Lan, and Mr. Zao-Xue Liu for their
694 assistance during field excursion. We are grateful to Ms. Hong-Xia Ma for making
695 SIMS mounts, Mr.Yu Liu and Mr. Guo-Qiang Tang for SIMS zircon U-Pb and O
696 isotope analyses, Dr. Yue-Heng Yang for zircon Hf isotope analyses, and Ms.
697 Sai-Hong Yang for assistance with cathodeluminescence (CL) characterization of
698 zircon grains. We are indebted to Editor Guochun Zhao and two anonymous reviewers
699 for their constructive comments. This research was supported by the National Basic
700 Research Program of China (973 Program) to Xian-Hua Li (Grant No.

2013CB835005), Natural Science Foundation of China to Qiu-Li Li (Grant No. 41222023), and the Australian Research Council (ARC) Future Fellowship (FT140100826) to Xuan-Ce Wang.

706 **References**

707

708 Baertschi, P., 1976. Absolute ^{18}O content of standard mean ocean water. Earth and
709 Planetary Science Letters, 31(3): 341-344.

710 Bindeman, I., 2008. Oxygen isotopes in mantle and crustal magmas as revealed by
711 single crystal analysis. Reviews in Mineralogy and Geochemistry, 69: 445 -478.

712 Bindeman, I., 2011. When do we need pan-global freeze to explain ^{18}O-depleted
713 zircons and rocks? Geology, 39(8): 799 -800.

714 Bindeman, I.N., Eiler, J.M.,Yogodzinski, G.M., Tatsumi, Y., Stern, C.R., Grove, T.L.,
715 Portnyagin, M., Hoernle, K. and Danyushevsky, L.V., 2005. Oxygen isotope
716 evidence for slab melting in modern and ancient subduction zones. Earth and
717 Planetary Science Letters, 235(3 -4): 480-496.

718 Bindeman, I.N., Serebryakov, N.S., Schmitt, A.K., Vazquez, J.A., Guan, Y., Azimov,
719 P.Ya.,Astafiev, B.Yu., Palandri, J. and Dobrzhinetskaya, L., 2014. Field and
720 microanalytical isotopic investigation of ultradepleted in ^{18}O Paleoproterozoic
721 "Slushball Earth" rocks from Karelia, Russia. Geosphere, 10(2): 308 -339.

722 Bindeman, I.N. and Serebryakov, N. S., 2011. Geology, petrology and O and H
723 isotope geochemistry of remarkably 18O depleted Paleoproterozoic rocks of the
724 Belomorian Belt, Karelia, Russia, attributed to global glaciation 2.4 Ga. Earth
725 and Planetary Science Letters, 306: 163-174.

726 Bindeman, I.N. and Simakin, A.G., 2014. Rhyolites—Hard to produce, but easy to
727 recycle and sequester: Integrating microgeochemical observations and numerical
728 models. Geosphere, 10(5): 930 -957.

729 Bindeman, I.N. and Valley, J.W., 2000. Formation of low-$\delta^{18}O$ rhyolites after caldera
730 collapse at Yellowstone, Wyoming, USA. Geology, 28(8): 719-722.

731 Bindeman, I.N. and Valley, J.W., 2001. Low-$\delta^{18}O$ rhyolites from Yellowstone:
732 magmatic evolution based on analyses of zircons and individual phenocrysts.
733 Journal of Petrology, 42(8): 1491 -1517.

734 Bindeman, I.N., Schmitt, A.K. and Evans, D.A.D., 2010. Limits of
735 hydrosphere-lithosphere interaction: Origin of the lowest-known $\delta^{18}O$ silicate

736 rock on Earth in the Paleoproterozoic Karelian rift. Geology, 38(7): 631 -634.
737 Blichert-Toft, J. and Albarède, F., 1997. The Lu-Hf isotope geochemistry of
738 chondrites and the evolution of the mantle-crust system. Earth and Planetary
739 Science Letters, 148(1 -2): 243-258.
740 Booth, A.L., Kolodny, Y., Chamberlain, C. P., McWilliams, M., Schmitt, A.K. and
741 Wooden, J., 2005. Oxygen isotopic composition and U-Pb discordance in zircon.
742 Geochimica et Cosmochimica Acta, 69(20): 4895-4905.
743 Boroughs, S., Wolff, J., Bonnichsen, B., Godchaux,. M., Larson, P., 2005.
744 Large-volume, low $\delta^{18}O$ rhyolites of the central Snake River Plain, Idaho, USA.
745 Geology, 33(10): 821-824.
746 Cavosie, A., Kita, N. T. and Valley, J. W., 2009. Primitive oxygen-isotope recorded in
747 magmatic zircon from the Mid-Atlantic Ridge. American Mineralogist, 94:
748 926-934.
749 Chen, D. G., Deloule, E., Cheng, H., Xia, Q. K. and Wu, Y. B., 2003. Preliminary
750 study of microscale zircon oxygen isotopes for Dabie-Sulu metamorphic rocks:
751 Ion probe in situ analyses. Chinese Science Bulletin, 48(16): 1670-1678.
752 Chen, K., Gao, S., Wu, Y.B., Guo, J.L., Hu, Z.C., Liu, L.S., Zong, K.Q., Liang, Z.W.
753 and Geng, X.L., 2013. 2.6–2.7 Ga crustal growth in Yangtze craton, South
754 China. Precambrian Research, 224: 472-490.
755 Cherniak, D.J. and Watson, E.B., 2003. Diffusion in Zircon. Reviews in Mineralogy
756 and Geochemistry, 53: 113 -143.
757 Chu, N. C., Taylor, R.N., Chavagnac, V., Nesbitt, R.W., Boella, R.M., Milton, J.A.,
758 German, C.R., Bayon, G. and Burton, K., 2002. Hf isotope ratio analysis using
759 multi-collector inductively coupled plasma mass spectrometry: an evaluation of
760 isobaric interference corrections. Journal of Analytical Atomic Spectrometry,
761 17(12): 1567-1574.
762 Corfu, F., Hanchar, J.M., Hoskin, P.W.O. and Kinny, P., 2003. Atlas of Zircon
763 Textures. Reviews in Mineralogy and Geochemistry, 53: 469 -500.
764 Dickinson, W.R. and Gehrels, G.E., 2009. Use of U–Pb ages of detrital zircons to
765 infer maximum depositional ages of strata: A test against a Colorado Plateau

766 Mesozoic database. Earth and Planetary Science Letters, 288(1-2): 115-125.
767 Dong, Y. P., Liu, X.M., Santosh, M., Chen, Q., Zhang, X.N., Li, W., He, D.F. and
768 Zhang, G.W., 2012. Neoproterozoic accretionary tectonics along the
769 northwestern margin of the Yangtze Block, China: Constraints from zircon U-Pb
770 geochronology and geochemistry. Precambrian Research, 196-197: 247-274.
771 Fu, B., Kita, N.T., Wilde, S.A., Liu, X.C., Cliff, J. and Greig, A., 2013. Origin of the
772 Tongbai-Dabie-Sulu Neoproterozoic low-$\delta^{18}O$ igneous province, east-central
773 China. Contributions to Mineralogy and Petrology, 165: 641-662.
774 Gao, S., Yang, J., Zhou, L., Li, M., Hu, Z.C., Guo, J.L., Yuan, H.L., Gong, H.J., Xiao,
775 G.Q. and Wei, J.Q., 2011. Age and growth of the Archean Kongling terrain,
776 South China, with emphasis on 3.3 Ga granitoid gneisses. American Journal of
777 Science, 311(2): 153 -182.
778 Gao, Y. Y., Li, X. H., Griffin, W.L., O'Reilly, S.Y. and Wang, Y. F., 2014. Screening
779 criteria for reliable U-Pb geochronology and oxygen isotope analysis in
780 uranium-rich zircons: A case study from the Suzhou A-type granites, SE China.
781 Lithos, 192-195: 180-191.
782 Gehrels, G., 2014. Detrital Zircon U-Pb Geochronology Applied to Tectonics. Annual
783 Review of Earth and Planetary Sciences, 42: 127-149.
784 Gilliam, C.E. and Valley, J.W., 1997. Low $\delta^{18}O$ magma, Isle of Skye, Scotland:
785 Evidence from zircons. Geochimica et Cosmochimica Acta, 61(23): 4975-4981.
786 Greentree, M.R. and Li, Z. X., 2008. The oldest known rocks in south‐western
787 China: SHRIMP U-Pb magmatic crystallisation age and detrital provenance
788 analysis of the Paleoproterozoic Dahongshan Group. Journal of Asian Earth
789 Sciences, 33(5-6): 289-302.
790 Grimes, C. B., Ushikubo, T., John, B. E., Valley, J. W., 2011. Uniformly mantle-like
791 $\delta^{18}O$ in zircons from oceanic plagiogranites and gabbros. Contributions to
792 Mineralogy and Petrology, 161: 13-33.
793 Guo, J. L., Guo, S., Wu, Y.B., Li, M., Chen, K., Hu, Z.C., Liang, Z.W., Zhou., L.,
794 Zong, K.Q., Zhang, W. and Chen, H.H., 2014. 3.45 Ga granitic gneisses from the
795 Yangtze Craton, South China: Implications for Early Archean crustal growth.

796 Precambrian Research, 242: 82-95.
797 Huang, J., Feng, L.J., Lu, D.B., Zhang, Q.R., Sun, T. and Chu, X.L., 2014. Multiple
798 climate cooling prior to Sturtian glaciations: Evidence from chemical index of
799 alteration of sediments in South China. Scientific Report, 4, 6868; DOI:
800 10.1038/srep06868.
801 HGB (Hubei Geological Bureau), 1982. 1:200,000 Regional Geological Investigation
802 Report for the Suixian area, Hubei Province, the People's Republic of China. 294
803 pp (in Chinese).
804 Jiao, W. F., Wu, Y. B., Peng, M., Wang, J. and Yang, S. H., 2009. The oldest
805 basement rock in the Yangtze Craton revealed by zircon U-Pb age and Hf
806 isotope composition. Science in China Series D-Earth Sciences, 52(9):
807 1393-1399 (in Chinese).
808 Lackey, J.S., Valley, J.W., Chen, J.H. and Stockli, D.F., 2008. Dynamic magma
809 systems, crustal recycling, and alteration in the Central Sierra Nevada Batholith:
810 the oxygen isotope record. Journal of Petrology, 49(7): 1397 -1426.
811 Lan, Z. W., Li, X.H., Zhu, M.Y., Chen, Z.Q., Zhang, Q.R., Li, Q.L., Lu, D.B., Liu, Y.
812 and Tang, G.Q., 2014. A rapid and synchronous initiation of the wide spread
813 Neoproterozoic glaciations. Precambrian Research, 255: 401-411.
814 Lan, Z. W., Li, X. H., Zhu, M. Y., Zhang, Q. R. and Li, Q. L., 2015. Revisiting the
815 Liantuo Formation in Yangtze Block, South China: SIMS U-Pb zircon age
816 constraints and regional and global significance. Precambrian Research, 263:
817 123-141.
818 Larson, P. and Taylor, H.P., 1986. $^{18}O/^{16}O$ ratios in ash-flow tuffs and lavas erupted
819 from the central Nevada caldera complex and the central San Juan caldera
820 complex, Colorado. Contributions to Mineralogy and Petrology, 92(2): 146-156.
821 Li, X. H., Li, Z. X., Sinclair, J.A., Li, W. X. and Carter, G., 2006. Revisiting the
822 "Yanbian Terrane": Implications for Neoproterozoic tectonic evolution of the
823 western Yangtze Block, South China. Precambrian Research, 151(1-2): 14-30.
824 Li, F. L., Li, Y.L., Zhou, G.H., Xu, S.Y., Li, Z.G. and Zhou, H.W., 2010. LA-ICPMS
825 zircon U-Pb dating of schist from the Dalangshan Group in Suizhou City, Hubei

826 Province, and its implications. Acta Petrologica Et Mineralogica, 29(5): 488-496
827 (in Chinese with English abstract).
828 Li, Q. L., Li, X.H., Liu, Y., Tang, G.,Q., Yang, J.H. and Zhu, W.G., 2010. Precise
829 U-Pb and Pb-Pb dating of Phanerozoic baddeleyite by SIMS with oxygen
830 flooding technique. Journal of Analytical Atomic Spectrometry, 25(7):
831 1107-1113.
832 Li, X. H., Li, Z.X., Ge, W.C., Zhou, H.W., Li, W.X., Liu, Y. and Wingate, M.T.D.,
833 2003. Neoproterozoic granitoids in South China: crustal melting above a mantle
834 plume at ca. 825 Ma? Precambrian Research, 122(1-4): 45-83.
835 Li, X. H., Li. Z.X., Zhou, H.W., Liu, Y., Liang, X.R. and Li, W.X., 2003. SHRIMP
836 U-Pb zircon age, geochemistry and Nd isotope of the Guandaoshan pluton in SW
837 Sichuan: Petrogenesis and tectonic significance. Science in China Series D:
838 Earth Sciences, 46 supp.: 73-83.
839 Li, X. H., Li, W.X., Li, Z.X., Lo, C.H., Wang, J., Ye, M.F. and Yang, Y.H., 2009.
840 Amalgamation between the Yangtze and Cathaysia Blocks in South China:
841 Constraints from SHRIMP U-Pb zircon ages, geochemistry and Nd-Hf isotopes
842 of the Shuangxiwu volcanic rocks. Precambrian Research, 174(1-2): 117-128.
843 Li, X. H., Long, W.G., Li, Q.L., Liu, Y., Zheng, Y.F., Yang, Y.H., Chamberlain, K.R.,
844 Wan, D.F., Guo, C.H., Wang, X.C. and Tao, H., 2010. Penglai Zircon
845 Megacrysts: A Potential New Working Reference Material for Microbeam
846 Determination of Hf-O Isotopes and U-Pb Age. Geostandards and Geoanalytical
847 Research, 34(2): 117-134.
848 Li, X. H., Li, Z. X., Zhou, H. W., Liu, Y. and Kinny, P.D., 2002. U-Pb zircon
849 geochronology, geochemistry and Nd isotopic study of Neoproterozoic bimodal
850 volcanic rocks in the Kangdian Rift of South China: implications for the initial
851 rifting of Rodinia. Precambrian Research, 113(1-2): 135-154.
852 Li, X. H., Liu, Y., Li, Q. L., Guo, C. H. and Chamberlain, K.R., 2009. Precise
853 determination of Phanerozoic zircon Pb/Pb age by multicollector SIMS without
854 external standardization. Geochemistry, Geophysics, Geosystems, 10(4):
855 Q04010.

856 Li, X. H., Wang, X. C., Li, W. X. and Li, Z. X., 2008. Petrogenesis and tectonic
857 significance of Neoproteorozoic basaltic rokcs in South China: From orogenesis
858 to introcontiental rifting. Geochimica, 37(4): 382-398 (in Chinese with English
859 abstract).
860 Li, X. H., Tang, G.Q., Gong, B., Yang, Y.H., Hong, K.J., Hu, Z.C., Li, Q.L., Liu, Y.
861 and Li, W.X., 2013. Qinghu zircon: a working reference for microbeam analysis
862 of U-Pb age and Hf and O isotopes. Chinese Science Bulletin, 58: 4647-4654.
863 Li, Y., Ma, C.Q., Xing, G.F., Zhou, H.W., Zhang, H. and Brouwer, F.M., 2015.
864 Origin of a Cretaceous low-^{18}O granitoid complex in the active continental
865 margin of SE China. Lithos, 216–217: 136-147.
866 Li, Z. X., Wartho, J.A., Occhipinti, S., Zhang, C.L., Li, X.H., Wang, J. and Bao, C.M.,
867 2007. Early history of the eastern Sibao Orogen (South China) during the
868 assembly of Rodinia: New mica $^{40}Ar/^{39}Ar$ dating and SHRIMP U-Pb detrital
869 zircon provenance constraints. Precambrian Research, 159(1-2): 79-94.
870 Li, Z.X., Bogdanova, S.V., Collins, A.S., Davidson, A., De Waele, B., Ernst, R.E.,
871 Fitzsimons, I.C.W., Fuck, R.A., Gladkochub, D.P., Jacobs, J., Karlstrom, K.E.,
872 Lu, S., Natapov, L.M., Pease, V., Pisarevsky, S.A., Thrane, K. and Vernikovsky,
873 V., 2008. Assembly, configuration, and break-up history of Rodinia: A synthesis.
874 Precambrian Research, 160(1-2): 179-210.
875 Li, Z.X., Li, X.H., Kinny, P.D. and Wang, J., 1999. The breakup of Rodinia: did it
876 start with a mantle plume beneath South China? Earth and Planetary Science
877 Letters, 173(3): 171-181.
878 Liu, J. B. and Zhang, L. M., 2013. Neoproterozoic low to negative $\delta^{18}O$ volcanic and
879 intrusive rocks in the Qinling Mountains and their geological significance.
880 Precambrian Research, 230: 138-167.
881 Liu, J. B., Zhang, L.M., Ye K., Su, W. and Chen, N.F., 2013. Oxygen isotopes of
882 whole rock and zircon and zircon U-Pb ages of meta-rhyolite from the
883 Luzhenguan Group and associated meta-granite in the northern Dabie Mountains.

884 Acta Petrologica Sinica, 29(5): 1511-1524 (in Chinese with English abstract).
885 Liu P. J., Li, X.H., Chen, S.M., Lan, Z.W., Yang, B., Shang, X.D. and Yin, C.Y.,
886 2015. New SIMS U-Pb zircon age and its constraint on the beginning of the
887 Nantuo glaciation. Science Bulletin, 60(10): 958-963,
888 Liu, X. C., Jahn, B.M., Cui, J.J., Li, S.Z., Wu, Y.B. and Li, X.H., 2010. Triassic
889 retrograded eclogites and Cretaceous gneissic granites in the Tongbai Complex,
890 central China: Implications for the architecture of the HP/UHP
891 Tongbai-Dabie-Sulu collision zone. Lithos, 119(3-4): 211-237.
892 Liu, X. C., Jahn, B.M., Li, S.Z., Cui, J.J., Liu, X., Lou, Y.X. and Qu. W., 2011. The
893 Tongbai HP metamorphic terrane: Constraints on the architecture and
894 subduction/exhumation of the Tongbai-Dabie-Sulu HP/UHP metamorphic belt.
895 Acta Petrologica Sinica, 27(4): 1151-1162 (in Chinese with English abstract).
896 Liu, X. C., Jahn, B., Dong, S., Lou, Y. and Cui, J., 2008. High-pressure metamorphic
897 rocks from Tongbaishan, central China: U－Pb and 40Ar/39Ar age constraints
898 on the provenance of protoliths and timing of metamorphism. Lithos, 105(3-4):
899 301-318.
900 Liu, Y. C., Li, Y., Liu, L.X., Gu, X.F., Deng, L.P. and Liu, J., 2013. Triassic
901 low-grade metamorphosed Neoproterozoic igneous rocks in Dabie orogen: slices
902 detached and exhumed from subducted continental crust. Chinese Science
903 Bulletin, 58(23): 2330-2337 (in Chinese).
904 Ludwig, K.R., 2012. User's manual for Isoplot 3.75: a geochronological toolkit for
905 Microsoft Excel. Berkeley Geochonology Centre Special Publication No.5, pp.
906 75.
907 Monani, S. and Valley, J.W., 2001. Oxygen isotope ratios of zircon: magma genesis
908 of low $\delta^{18}O$ granites from the British Tertiary Igneous Province, western
909 Scotland. Earth and Planetary Science Letters, 184(2): 377-392.
910 Morel, M.L.A., Nebel, O., Nebel-Jacobsen, Y.J., Miller, J.S. and Vroon, P.Z., 2008.
911 Hafnium isotope characterization of the GJ-1 zircon reference material by
912 solution and laser-ablation MC-ICPMS. Chemical Geology, 255(1－2): 231-235.

913 Muñoz, M., Charrier, R., Fanning, C. M., Deckart, K., 2012. Zircon trace element and
914 O-Hf isotope analyses of mineralized intrusions from El Teniente ore deposit,
915 Chilean Andes: constraints on the source and magmatic evolution of porphyry
916 Cu-Mu related magmas. Journal of Petrology, 53(6): 1091-1122.
917 Okay, A.I., Xu, S. and Sengor, A.M.C., 1989. Coesite from the Dabie Shan eclogites,
918 central China. European Journal of Mineralogy, 1(4): 595 -598.
919 Peck, W.H., Valley, J.W. and Graham, C.M., 2003. Slow oxygen diffusion rates in
920 igneous zircons from metamorphic rocks. American Mineralogist, 88(7): 1003
921 -1014.
922 Qiu, Y.M., Gao, S., McNaughton, N.J., Groves, D.I. and Ling, W., 2000. First
923 evidence of >3.2 Ga continental crust in the Yangtze craton of south China and
924 its implications for Archean crustal evolution and Phanerozoic tectonics.
925 Geology, 28: 11 -14.
926 Rowley, D.B., Xue, F., Tucker, R.D., Peng, Z.X., Baker, J. and Davis, A., 1997. Ages
927 of ultrahigh pressure metamorphism and protolith orthogneisses from the eastern
928 Dabie Shan: U/Pb zircon geochronology. Earth and Planetary Science Letters,
929 151(3-4): 191-203.
930 Rumble, D., Giorgis, D., Ireland, T., Zhang, Z.M., Xu, H.F, Yui, T.F., Yang, J.S., xu,
931 Z.Q. and Liou, J.G., 2002. Low $\delta^{18}O$ zircons, U-Pb dating, and the age of the
932 Qinglongshan oxygen and hydrogen isotope anomaly near Donghai in Jiangsu
933 Province, China. Geochimica et Cosmochimica Acta, 66(12): 2299-2306.
934 Sláma, J., Košler, J., Condon, D.J., Crowley, J.L., Gerdes, A., Hanchar, J.M.,
935 Horstwood, M.S.A., Morris, G.A., Nasdala, L., Norberg, N., Schaltegger, U.,
936 Schoene, B., Tubrett, M.N. and Whitehouse, M.J., 2008. Plešovice zircon - A
937 new natural reference material for U-Pb and Hf isotopic microanalysis. Chemical
938 Geology, 249(1-2): 1-35.
939 Söderlund, U., Patchett, P.J., Vervoort, J.D. and Isachsen, C.E., 2004. The 176Lu
940 decay constant determined by Lu – Hf and U – Pb isotope systematics of
941 Precambrian mafic intrusions. Earth and Planetary Science Letters, 219(3-4):
942 311-324.

943 Stacey, J.S. and Kramers, J.D., 1975. Approximation of terrestrial lead isotope
944 evolution by a two-stage model. Earth and Planetary Science Letters, 26(2):
945 207-221.
946 Sun, M., Chen, N.S., Zhao, G.C., Wilde, S.A., Ye, K., Guo, J.H., Chen, Y. and Yuan,
947 C., 2008. U-Pb Zircon and Sm-Nd isotopic study of the huangtuling granulite,
948 dabie-sulu belt, China: Implication for the paleoproterozoic tectonic history of
949 the yangtze craton. American Journal of Science, 308(4): 469 -483.
950 Tang, J., Zheng, Y.F., Gong, B., Wu, Y.B., Gao, T.S., Yuan, H.L. and Wu, F.Y., 2008.
951 Extreme oxygen isotope signature of meteoric water in magmatic zircon from
952 metagranite in the Sulu orogen, China: Implications for Neoproterozoic rift
953 magmatism. Geochimica et Cosmochimica Acta, 72(13): 3139-3169.
954 Valley, J.W., 2003. Oxygen Isotopes in Zircon. Reviews in Mineralogy and
955 Geochemistry, 53(1): 343 -385.
956 Valley, J.W., Chiarenzelli, J.R. and McLelland, J.M., 1994. Oxygen isotope
957 geochemistry of zircon. Earth and Planetary Science Letters, 126(4): 187-206.
958 Valley, J.W., Kinny, P.D., Schulze, D.J. and Spicuzza, M.J., 1998. Zircon megacrysts
959 from kimberlite: oxygen isotope variability among mantle melts. Contributions
960 to Mineralogy and Petrology, 133: 1-11.
961 Valley, J.W., Lackey, J.S., Cavosie, A.J., Clechenko, C.C., Spicuzza, M.J., Basei,
962 A.S., Bindeman, I.N., Ferreira, V.P., Sial., A.N., King, E.M., Peck, W.H., Sinha,
963 A.K. and Wei, C.S., 2005. 4.4 billion years of crustal maturation: oxygen isotope
964 ratios of magmatic zircon. Contributions ot Mineralogy and Petrology, 150:
965 561-580.
966 Wang, J. and Li, Z., 2003. History of Neoproterozoic rift basins in South China:
967 implications for Rodinia break-up. Precambrian Research, 122(1-4): 141-158.
968 Wang, X. C., Li, X.H., Li, W.X., Li, Z.X., Liu, Y., Yang, Y.H., Liang, X.R. and Tu,
969 X.L., 2008. The Bikou basalts in the northwestern Yangtze block, South China:
970 Remnants of 820-810 Ma continental flood basalts? Geological Society of
971 America Bulletin, 120(11-12): 1478 -1492.
972 Wang, X. C., Li, X.H., Li, Z.X., Li, Q.L., Tang, G.Q., Gao, Y.Y., Zhang, Q.R. and

973 Liu, Y., 2012. Episodic Precambrian crust growth: Evidence from U-Pb ages and
974 Hf-O isotopes of zircon in the Nanhua Basin, central South China. Precambrian
975 Research, 222-223: 386-403.
976 Wang, X. C., Li, X. H., Li, W. X. and Li, Z. X., 2009. Variable involvements of
977 mantle plumes in the genesis of mid-Neoproterozoic basaltic rocks in South
978 China: A review. Gondwana Research, 15(3-4): 381-395.
979 Wang, X. M., Liou, J.G. and Mao, H.K., 1989. Coesite-bearing eclogite from the
980 Dabie Mountains in central China. Geology, 17(12): 1085 -1088.
981 Wang, X.C., Li, Z.X., Li, X.H., Li, Q.L., Tang, G.Q., Zhang, Q.R. and Liu, Y., 2011.
982 Nonglacial origin for low-$\delta^{18}O$ Neoproterozoic magmas in the South China
983 Block: Evidence from new in-situ oxygen isotope analyses using SIMS. Geology,
984 39(8): 735-738.
985 Wang, X. L., Zhou, J.C., Wan, Y.S., Kitajima, K., Wang, D., Bonamici, C., Qiu, J.S.
986 and Sun, Tao., 2013. Magmatic evolution and crustal recycling for
987 Neoproterozoic strongly peraluminous granitoids from south China: Hf and O
988 isotopes in zircon. Earth and Planetary Science Letters, 366: 71-82.
989 Wang, Y.F., Li, X.H., Jin, W., Zhang, J.H., 2015. Eoarchean ultra-depleted mantle
990 domains inferred from ca. 3.81 Ga Anshan trondhjemitic gneisses, North China
991 Craton. Precambrian Research 263, 88-107.
992 Watts, K.E., Bindeman, I.N. and Schmitt, A.K., 2011. Large-volume Rhyolite Genesis
993 in Caldera Complexes of the Snake River Plain: Insights from the Kilgore Tuff
994 of the Heise Volcanic Field, Idaho, with Comparison to Yellowstone and
995 Bruneau-Jarbidge Rhyolites. Journal of Petrology, 52(5): 857 -890.
996 Watts, K.E., Leeman, W.P., Bindeman, I.N. and Larson, P.B., 2010. Supereruptions
997 of the Snake River Plain: Two-stage derivation of low- $\delta^{18}O$ rhyolites from
998 normal-$\delta^{18}O$ crust as constrained by Archean xenoliths. Geology, 38(6): 503
999 -506.
1000 Wei, C. S., Zhao, Z. F. and Spicuzza, M.J., 2008. Zircon oxygen isotopic constraint
1001 on the sources of late Mesozoic A-type granites in eastern China. Chemical
1002 Geology, 250(1-4): 1-15.

1003 Wei, C. S., Zheng, Y. F., Zhao, Z. F. and Valley, J.W., 2002. Oxygen and neodymium
1004 isotope evidence for recycling of juvenile crust in northeast China. Geology,
1005 30(4): 375 -378.
1006 Woodhead, J.D. and Hergt, J.M., 2005. A preliminary appraisal of seven natural
1007 zircon reference materials for in situ Hf isotope determination. Geostandards and
1008 Geoanalytical Research, 29(2): 183-195.
1009 Wu, F. Y., Yang, Y. H., Xie, L. W., Yang, J. H. and Xu, P., 2006. Hf isotopic
1010 compositions of the standard zircons and baddeleyites used in U－Pb
1011 geochronology. Chemical Geology, 234(1-2): 105-126.
1012 Wu, Y. B., Gao, S., Zhang, H.F., Zheng, J.P., Liu, X.C., Wang, H., Gong, H.J., Zhou,
1013 L. and Yuan, H.L., 2012. Geochemistry and zircon U-Pb geochronology of
1014 Paleoproterozoic arc related granitoid in the Northwestern Yangtze Block and its
1015 geological implications. Precambrian Research, 200-203: 26-37.
1016 Wu, Y. B., Zhou, G.Y., Gao, S., Liu, X.C., Qin, Z.W., Wang, H., Yang, J.Z. and Yang,
1017 S.H., 2014. Petrogenesis of Neoarchean TTG rocks in the Yangtze Craton and its
1018 implication for the formation of Archean TTGs. Precambrian Research, 254:
1019 73-86.
1020 Wu, Y. B., Zheng, Y. F., Gao, S., Jiao, W. F. and Liu, Y. S., 2008. Zircon U-Pb age
1021 and trace element evidence for Paleoproterozoic granulite-facies metamorphism
1022 and Archean crustal rocks in the Dabie Orogen. Lithos, 101(3-4): 308-322.
1023 Wu, Y.B., Gao, S., Gong, H.J., Xiang, H., Jiao, W.F., Yang, S.H., Liu, Y.S. and Yuan,
1024 H.L., 2009. Zircon U-Pb age, trace element and Hf isotope composition of
1025 Kongling terrane in the Yangtze Craton: refining the timing of Palaeoproterozoic
1026 high-grade metamorphism. Journal of Metamorphic Geology, 27(6): 461-477.
1027 Xiang, Z. J., Yan, Q. R., White, J.D.L., Song, B. and Wang, Z. Q., 2015. Geochemical
1028 constraints on the provenance and depositional setting of Neoproterozoic
1029 volcaniclastic rocks on the northern margin of the Yangtze Block, China:
1030 Implications for the tectonic evolution of the northern margin of the Yangtze
1031 Block. Precambrian Research, 264: 140-155.
1032 Xu, S. T. Su, W., Liu, Y.C., Jiang, L.X., Ji, S.Y., Okay, A.I. and Sengör, A.M.C.,

1033 1992. Diamond from the Dabie Shan Metamorphic Rocks and Its Implication for
1034 Tectonic Setting. Science, 256(5053): 80 -82.
1035 Xue, H. M. and Ma, F., 2013. Detrital-zircon geochronology from the
1036 metasedimentary rocks of the Suizhou Group in the southern foot of the
1037 Tongbaishan Orogen and their geological significance. Acta Petrologica Sinica,
1038 29(2): 564-580 (in Chinese with English abstract).
1039 Xue, H. M., Ma, F. and Song, Y. Q., 2011. Geochemistry and SHRIMP zircon U-Pb
1040 data of Neoproterozoic meta-magamtic rocks in the Suizhou-Zaoyang area,
1041 northern margin of the Yangtze Craton, Cental China. Acta Petrologica Sinica,
1042 27(4): 1116-1130 (in Chinese with English abstract).
1043 Yang, C., Li, X. H., Wang, X. C. and Lan, Z. W., 2015. Mid-Neoproterozoic angular
1044 unconformity in the Yangtze Block revisited: Insights from detrital zircon U-Pb
1045 age and Hf-O isotopes. Precambrian Research, 266: 165-178.
1046 Yang, Y.N., Li, Q.L., Liu, Y., Tang, G.Q., Ling, X.X. and Li, X.H., 2014. Zircon
1047 U-Pb dating by secondary ion mass spectrometry (in Chinese with English
1048 abstract). Earth Science Frontiers, 21(2): 81-92.
1049 Yang W. B., Niu, H.C., Sun, W.D., Shan, Q., Zheng, Y.F., Li, N.B., Li, C.Y., Arndt,
1050 N.T., Xu, X., Jiang, Y.H. and Yu, X.Y., 2013. Isotopic evidence for continental
1051 ice sheet in mid-latitude region in the supergreenhouse Early Cretaceous.
1052 Scientific Report, 3, 2732; DOI: 10.1038/ srep02732.
1053 Ye, K., Cong, B. L. and Ye, D. N., 2000. The possible subduction of continental
1054 material to depths greater than 200[thinsp]km., 407(6805): 734-736.
1055 Ye, M. F., Li, X. H., Li, W. X., Liu, Y. and Li, Z. X., 2007. SHRIMP zircon U－Pb
1056 geochronological and whole-rock geochemical evidence for an early
1057 Neoproterozoic Sibaoan magmatic arc along the southeastern margin of the
1058 Yangtze Block. Gondwana Research, 12(1-2): 144-156.
1059 Yui, T., Rumble III, D. and Lo, C., 1995. Unusually low $\delta^{18}O$ ultra-high-pressure
1060 metamorphic rocks from the Sulu Terrain, eastern China. Geochimica et
1061 Cosmochimica Acta, 59(13): 2859-2864.
1062 Zhang, Q. R., Li, X. H., Feng, L. J., Huang, J. and Song, B., 2008. A new age

1063 constraint on the onset of the Neoproterozoic glaciations in the Yangtze Platform,
1064 South China. The Journal of Geology, 116(4): 423-429.
1065 Zhang, S. B., Zheng, Y.F., Wu, Y.B., Zhao, Z.F., Gao, S. and Wu. F.Y., 2006a.
1066 Zircon U-Pb age and Hf-O isotope evidence for Paleoproterozoic metamorphic
1067 event in South China. Precambrian Research, 151(3-4): 265-288.
1068 Zhang, S. B., Zheng, Y.F., Wu, Y.B., Zhao, Z.F., Gao, S. and Wu. F.Y., 2006b.
1069 Zircon isotope evidence for ≥3.5 Ga continental crust in the Yangtze craton of
1070 China. Precambrian Research, 146(1-2): 16-34.
1071 Zhang, S.B. and Zheng, Y. F., 2011. On the genesis of low-$\delta^{18}O$ magmatic rocks.
1072 Acta Petrologica Sinica, 27(2): 520-530 (in Chinese with English abstract).
1073 Zhang, S. B. and Zheng, Y. F., 2013. Spatial and temporal distribution of
1074 Neoproterozoic low-$\delta^{18}O$ magmas in the South China Block. Chinese Science
1075 Bulletin, 58(23): 2344-2350 (in Chinese).
1076 Zhao, J. H. and Zhou, M. F., 2007. Neoproterozoic Adakitic Plutons and Arc
1077 Magmatism along the western margin of Yangtze Block, South China. The
1078 Journal of Geology, 115: 675-689.
1079 Zhao, J. H. and Zhou, M. F., 2008. Neoproterozoic adakitic plutons in the northern
1080 margin of the Yangtze Block, China: Partial melting of a thickened lower crust
1081 and implications for secular crustal evolution. Lithos, 104(1-4): 231-248.
1082 Zhao, J. H. and Zhou, M. F., 2009. Secular evolution of the Neoproterozoic
1083 lithospheric mantle underneath the northern margin of the Yangtze Block, South
1084 China. Lithos, 107(3-4): 152-168.
1085 Zhao, J. H., Zhou, M. F., Yan, D. P., Zheng, J. P. and Li, J. W., 2011. Reappraisal of
1086 the ages of Neoproterozoic strata in South China: No connection with the
1087 Grenvillian orogeny. Geology, 39(4): 299 -302.
1088 Zhao, J. H., Zhou, M. F., Zheng, J.P., 2013. Constraints from zircon U-Pb ages, O and
1089 Hf isotopic compositions on the origin of Neoproterozoic peraluminous
1090 granitoids from the Jiangnan Fold Belt, South China. Contributions to
1091 Mineralogy and Petrology, 166(5): 1505-1519.
1092 Zheng, J. P., Griffin, W.L., O'Reilly, S.Y., Zhang, M. Pearson, N. and Pan, Y.M.,

2006. Widespread Archean basement beneath the Yangtze craton. Geology, 34(6): 417 -420.

Zheng, Y. F., Fu, B., Xiao, Y.L., Gong, B., Ge, N.J. and Li, S.G., 1997. Hydrogen and oxygen isotopic composition of the Dabie eclogites and their geodynamic significance. Science In China (Series D), 27(2): 121-126 (in Chinese).

Zheng, Y.F., Wu. Y.B., Chen, F.K., Gong, B., Li, L. and Zhao, Z.F., 2004. Zircon U-Pb and oxygen isotope evidence for a large-scale ^{18}O depletion event in igneous rocks during the Neoproterozoic. Geochimica et Cosmochimica Acta, 68(20): 4145-4165.

Zheng, Y. F., Wu, Y.B., Gong, B., Chen, R.X., Tang, J. and Zhao, Z.F., 2007. Tectonic driving of Neoproterozoic glaciations: Evidence from extreme oxygen isotope signature of meteoric water in granite. Earth and Planetary Science Letters, 256(1-2): 196-210.

Zheng, Y. F. and Fu, B., 1998. Estimation of oxygen diffusivity from anion porosity in minerals. Geochemical Journal, 32(2): 71-89.

Zheng, Y. F., Fu, B., Gong, B. and Li, L., 2003. Stable isotope geochemistry of ultrahigh pressure metamorphic rocks from the Dabie-Sulu orogen in China: implications for geodynamics and fluid regime. Earth-Science Reviews, 62(1-2): 105-161.

Zheng, Y. F., Fu, B., Gong, B. and Li, S. G., 1996. Extreme ^{18}O depletion in eclogite from the Su-Lu terrane in East China. European Journal of Mineralogy, 8(2): 317-324.

Zhou, G. Y., Wu, Y.B, Gao, S., Yang, J.Z., Zheng, J.P., Qin, Z.W., Wang., H. and Yang, S.H., 2015. The 2.65 Ga A-type granite in the northeastern Yangtze craton: Petrogenesis and geological implications. Precambrian Research, 258: 247-259.

Zhou, M. F., Yan, D. P., Kennedy, A.K., Li, Y. Q. and Ding, J., 2002. SHRIMP U－Pb zircon geochronological and geochemical evidence for Neoproterozoic arc-magmatism along the western margin of the Yangtze Block, South China. Earth and Planetary Science Letters, 196(1-2): 51-67.

Zhou, M. F., Yan, D. P., Wang, C. L, Qi, L. and Kennedy, A., 2006.

1123 Subduction-related origin of the 750 Ma Xuelongbao adakitic complex (Sichuan
1124 Province, China): Implications for the tectonic setting of the giant
1125 Neoproterozoic magmatic event in South China. Earth and Planetary Science
1126 Letters, 248(1-2): 286-300.
1127 Zhou, M.F., Kennedy, A.K., Sun, M., Malpas, J. and Lesher, C.M., 2002.
1128 Neoproterozoic arc‐related mafic intrusions along the northern margin of South
1129 China: implications for the accretion of rodinia. The Journal of geology, 110(5):
1130 611-618.
1131 Zhu, X. Y., Chen, F.K., Nie, H. Siebel, W., Yang, Y.Z., Xue, Y.Y. and Zhai, M.G.,
1132 2014. Neoproterozoic tectonic evolution of South Qinling, China: Evidence from
1133 zircon ages and geochemistry of the Yaolinghe volcanic rocks. Precambrian
1134 Research, 245: 115-130.

Figure Captions

Fig.1. (a) Distribution of Neoproterozoic igneous rocks and mid-Neoproterozoic strata with geochronological results for key outcrops (modified after Wang et al., 2012; Li et al., 2014; Yang et al., 2015). The inset shows a tectonic sketch of China. Please refer to Appendix S1 for references for cited ages. Filled hexagons show the sample positions of low-$\delta^{18}O$ zircon grains identified by SIMS analyses. (b) A simplified geological map showing of the studied area. Filled stars represent the locations of dated samples in this study. F1 and F2 represent Xiangfan-Guangji fault and Xincheng-Huangpin fault, respectively. Ages shown near the sample site indicate either the crystallization age of rhyolite (i.e. 12SZ14) or the youngest group of ages of detrital zircon grains for sedimentary rocks (all samples except sample 12SZ14).

Fig.2. Generalized stratigraphic column and sampling site in the Suixian Group. The lithologic column is modified after the 1: 200,000 geological map of the Suixian area by the HGB (1982). Source for the quoted ages: A1, A2, and A3 - Xue et al., 2011. Relative positions of samples in this study and quoted ages within each formation are based on dating results as no detailed strata correlation is available to allow for precisely locating each sample along the stratigraphic column.

Fig.3. Relative probability diagram of U-Pb ages for zircon grains from Suixian Group. (a) Detrital zircon crystals from Gujing Formation (siltstone 12SZ20, sandstone 12SZ24 and sandstone 12SZ28); (b) Detrital zircon crystals from lower part of Liulin Formation (sandstone 12SZ06, sandstone 12SZ07, sandstone 13SZ14 and sandstone 13SZ19); (c) Detrital zircon grains from Yuanziwan Formation (12SZ10 siltstone and 13SZ17 sandstone). Fm represents Formation. Relative probability diagrams were constructed using Isoplot 3.75 (Ludwig, 2012). Bin width was set at 10 Ma approximate to the 1σ U-Pb age uncertainty.

Fig.4. U-Pb concordia diagrams showing SIMS U-Pb dating results for zircon grains from metarhyolite 12SZ14 (a) and tuffaceous siltstone 12SZ17 (b), respectively. (a')

and (b') are weighted mean of $^{206}Pb/^{238}U$ ages for the consistent population of zircon U-Pb analyses for metarhyolite 12SZ14 and tuffaceous siltstone 12SZ17, respectively. Data-point error symbols in U-Pb concordia diagrams (a) and (b) are 2σ. Error bars in (a') and (b') are 2σ. Fm stands for Formation.

Fig.5. $\delta^{18}O$ value versus U-Pb age for zircon grains from the Suixian Group. (a) For all analyzed grains; (b) For 950-650 Ma grains. The reference $\delta^{18}O$ value for mantle zircon is from the recommended value of 5.3 ± 0.6‰ (2 SD) by Valley et al. (1998) and Valley et al. (2005).

Fig.6. Relative probability diagram for zircon $\varepsilon_{Hf}(t)$ values from the Gujing (a), Liulin (b) and Yuanziwan (c) formations, Suixian Group. Bar width was set as 2.

Fig.7. $\varepsilon_{Hf}(t)$ value versus U-Pb age for zircon grains from the Suixian Group. (a) For all analyzed grains; (b) For 950-650 Ma grains. The depleted mantle evolution curve was based on the average modern-day values of $^{176}Hf/^{177}Hf$ of 0.28325 and $^{176}Lu/^{177}Hf$ of 0.0384 (Griffin et al., 2002). CHUR refers to **CH**ondritic **U**niform **R**eservoir.

Fig.8.$\varepsilon_{Hf}(t)$ value versus $\delta^{18}O$ value for 700-800 Ma zircon grains with U-Pb ages peaking at ca. 0.73 Ga (a) and 0.79 Ga (b). $\varepsilon_{Hf}(t)$ and $\delta^{18}O$ values for magmatic zircon grains from metarhyolite 12SZ14 and tuffaceous siltstone 12SZ17 are shown for comparison in (a). Gray field in (a) and (b) represents range of low-$\delta^{18}O$ zircon grains (<4.6‰) from this study. Rectangle field filled with dotted line in (a) indicates estimated Hf and O isotopic range of zircon grains crystalized from magmas supposed to be partial melts of subducted oceanic crust. O isotopic composition for the field filled with dotted lines is taken as 5.3 ± 0.8‰ (2SD) (Valley et al., 1998; Valley et al., 2005).

Fig.9. $\delta^{18}O$ value versus Th/U ratio (a) and U content for zircon grains from the

1195 Suixian Group.

1196

1197 **Fig.10.** Compilation of SIMS O isotope data for Neoproterozoic zircon grains from(a)
1198 the Suixian Group from this study, northern Yangtze, (b) the tuff and granitoid from
1199 the Beihuaiyang unit of Dabie orogen (Liu et al., 2013) and south Qinling (Fu et al.,
1200 2013; Liu and Zhang, 2013), northern Yangtze Block, (c) the diorite from Hannan
1201 massif and granitoids from the Baoxing complex, northwestern Yangtze Block (Fu et
1202 al., 2013), and (d) the Neoproterozoic sedimentary rocks (Lan et al., 2015; Wang et al.,
1203 2011; Yang et al., 2015) and granitoids (Wang et al., 2013; Zhao et al., 2013),
1204 southeastern Yangtze Block. Vertical gray fields with age range of 715-670 Ma (e.g.
1205 Lan et al., 2015; Zhang et al., 2008) and 650-635 Ma (e.g. Liu et al., 2015) indicate
1206 time interval of Jiangkou glaciation and Nantuo glaciation in the South China Block.
1207 Dash line infers the upper limit $\delta^{18}O$ value for low-$\delta^{18}O$ zircon (i.e. < 4.6‰). Only
1208 concordant age are adopted here. "Concordant" here is defined as discordance
1209 (percent deviation of $^{206}Pb/^{238}U$ age from $^{207}Pb/^{206}Pb$ age) less than 12% referring to
1210 Wang et al. (2011).

1211

1212 **Fig.11.** Zircon U-Pb age histogram for the Neoproterozoic low-$\delta^{18}O$ zircon grains in
1213 the Yangtze Block. Data source: Granitoids and sedimentary rocks, southeastern
1214 Yangtze: Wang et al., 2013; Lan et al., 2015; Wang et al., 2011; Yang et al., 2015;
1215 Zhao et al., 2013. Igneous intrusions, northwestern Yangtze: Fu et al., 2013. Tuff and
1216 grantoids, northern Yangtze: Liu and Zhang, 2013; Liu et al., 2013. Suixian Group,
1217 norther Yangtze: this study. Bin width was set at 10 Ma approximate to the 1σ U-Pb
1218 age uncertainty.

Fig.1

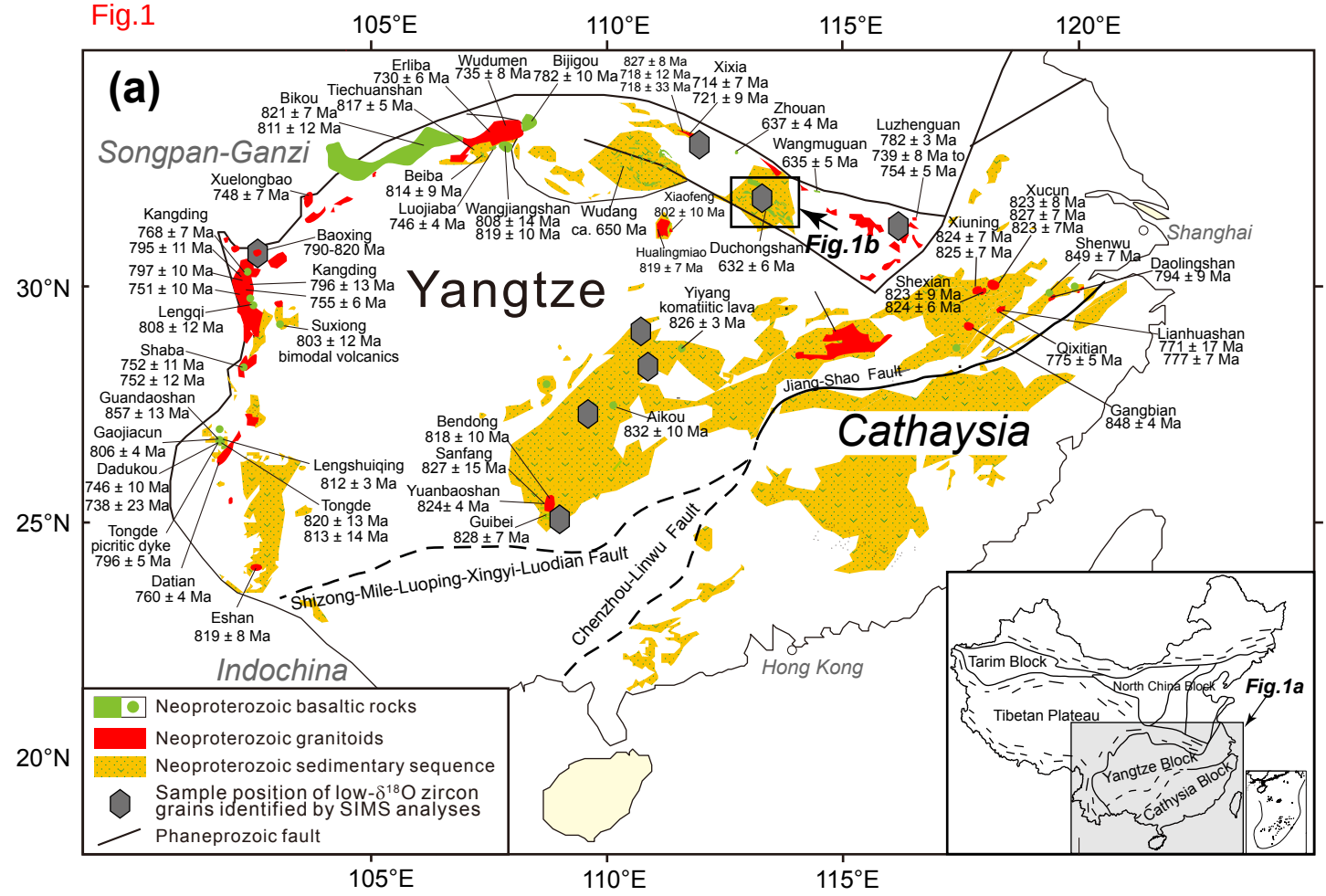
(a)
Songpan-Ganzi
Yangtze
Cathaysia
Indochina
Hong Kong
Shanghai
Erliba 730 ± 6 Ma
Wudumen 735 ± 8 Ma
Bijigou 782 ± 10 Ma
827 ± 8 Ma
718 ± 12 Ma
718 ± 33 Ma
Xixia 714 ± 7 Ma
721 ± 9 Ma
Bikou 821 ± 7 Ma
811 ± 12 Ma
Tiechuanshan 817 ± 5 Ma
Zhouan 637 ± 4 Ma
Wangmuguan 635 ± 5 Ma
Luzhenguan 782 ± 3 Ma
739 ± 8 Ma to 754 ± 5 Ma
Xuelongbao 748 ± 7 Ma
Beiba 814 ± 9 Ma
Luojiaba 746 ± 4 Ma
Wangjiangshan 808 ± 14 Ma
819 ± 10 Ma
Wudang ca. 650 Ma
Xiaofeng 802 ± 10 Ma
Huaiingmiao 819 ± 7 Ma
Duchongshan 632 ± 6 Ma
Fig.1b
Xucun 823 ± 8 Ma
827 ± 7 Ma
823 ± 7Ma
Xiuning 824 ± 7 Ma
825 ± 7 Ma
Shenwu 849 ± 7 Ma
Daolingshan 794 ± 9 Ma
Kangding 768 ± 7 Ma
795 ± 11 Ma
Baoxing 790-820 Ma
797 ± 10 Ma
751 ± 10 Ma
Kangding 796 ± 13 Ma
755 ± 6 Ma
Lenggi 808 ± 12 Ma
Suxiong 803 ± 12 Ma
bimodal volcanics
Shaba 752 ± 11 Ma
752 ± 12 Ma
Guandaoshan 857 ± 13 Ma
Gaojiacun 806 ± 4 Ma
Dadukou 746 ± 10 Ma
738 ± 23 Ma
Tongde picritic dyke 796 ± 5 Ma
Datian 760 ± 4 Ma
Eshan 819 ± 8 Ma
Yiyang komatiitic lava 826 ± 3 Ma
Shexian 823 ± 9 Ma
824 ± 6 Ma
Qixitian 775 ± 5 Ma
Lianhuashan 771 ± 17 Ma
777 ± 7 Ma
Jiang-Shao Fault
Gangbian 848 ± 4 Ma
Aikou 832 ± 10 Ma
Bendong 818 ± 10 Ma
Sanfang 827 ± 15 Ma
Yuanbaoshan 824± 4 Ma
Guibei 828 ± 7 Ma
Lengshuiqing 812 ± 3 Ma
Tongde 820 ± 13 Ma
813 ± 14 Ma
Shizong-Mile-Luoping-Xingyi-Luodian Fault
Chenzhou-Linwu Fault
Neoproterozoic basaltic rocks
Neoproterozoic granitoids
Neoproterozoic sedimentary sequence
Sample position of low-δ18O zircon grains identified by SIMS analyses
Phaneprozoic fault
Tarim Block
North China Block
Tibetan Plateau
Yangtze Block
Cathysia Block
Fig.1a
105°E
110°E
115°E
120°E
30°N
25°N
20°N

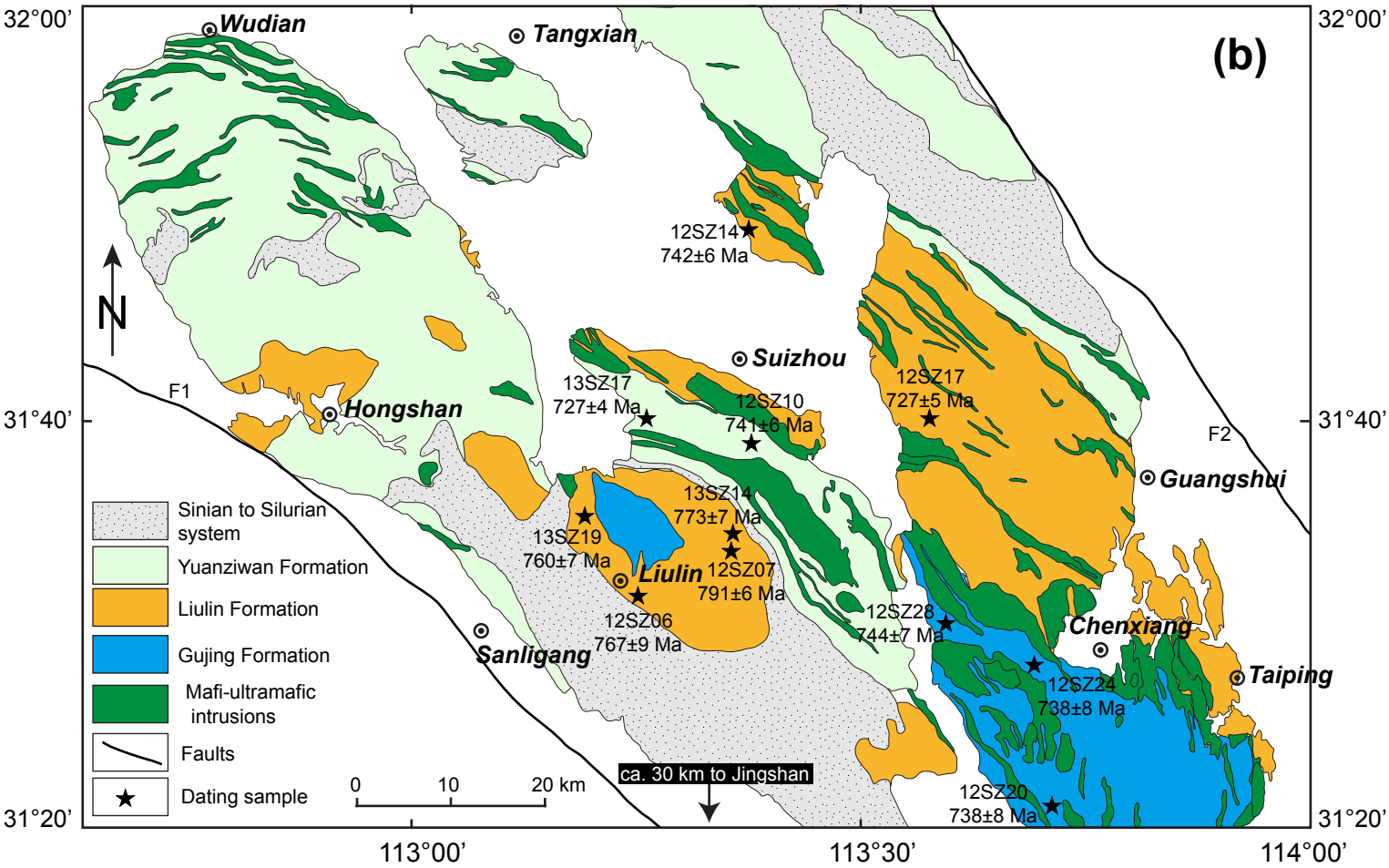
(b)
Wudian
Tangxian
Suizhou
Hongshan
Guangshui
Chenxiang
Taiping
Liulin
Sanligang
F1
F2
N
12SZ14 742±6 Ma
13SZ17 727±4 Ma
12SZ10 741±6 Ma
12SZ17 727±5 Ma
13SZ14 773±7 Ma
13SZ19 760±7 Ma
12SZ07 791±6 Ma
12SZ06 767±9 Ma
12SZ28 744±7 Ma
12SZ24 738±8 Ma
12SZ20 738±8 Ma
ca. 30 km to Jingshan
Sinian to Silurian system
Yuanziwan Formation
Liulin Formation
Gujing Formation
Mafi-ultramafic intrusions
Faults
Dating sample
0
10
20 km
32°00'
31°40'
31°20'
113°00'
113°30'
114°00'

Fig.2

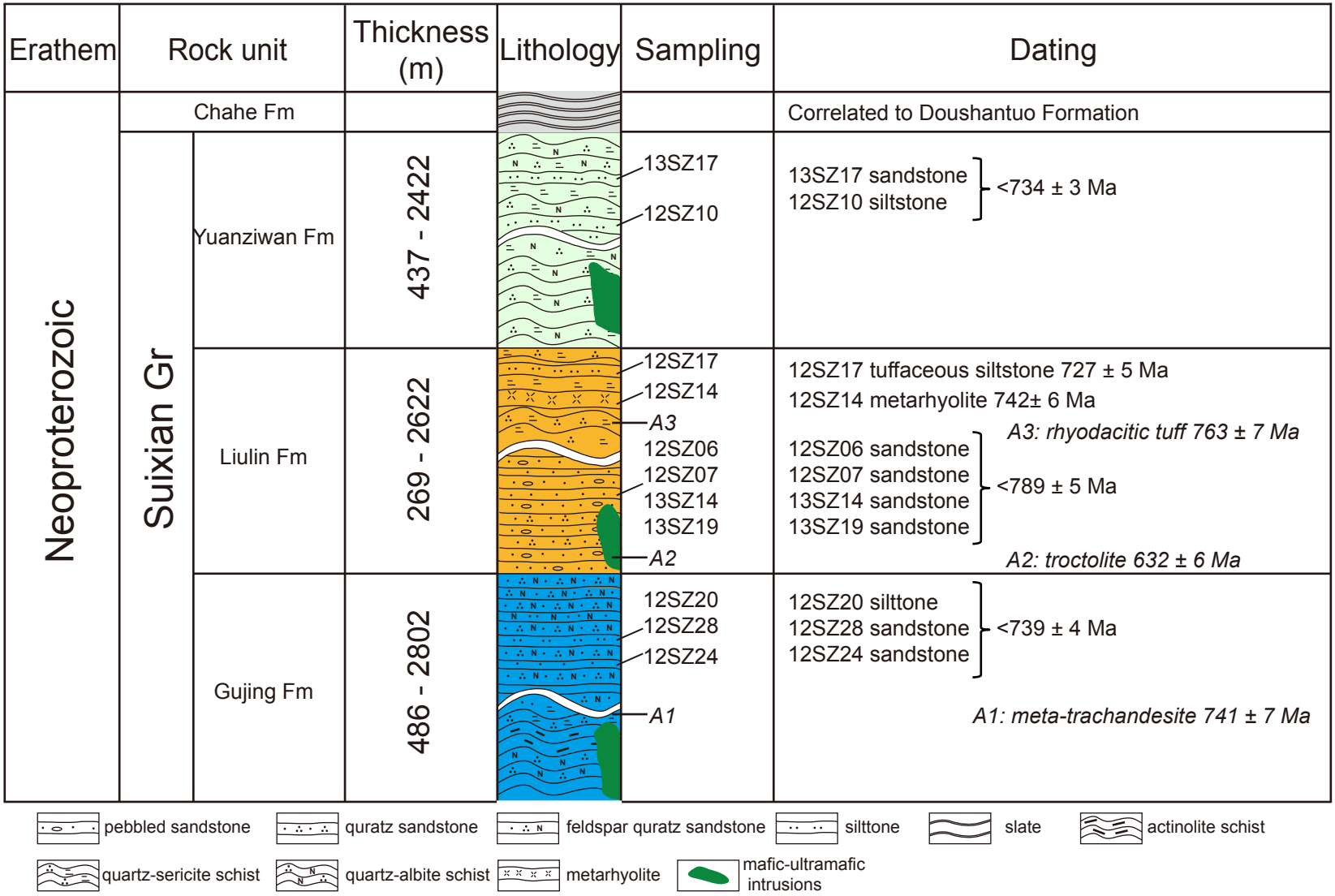
Erathem
Rock unit
Thickness (m)
Lithology
Sampling
Dating
Neoproterozoic
Suixian Gr
Chahe Fm
Correlated to Doushantuo Formation
Yuanziwan Fm
437 - 2422
13SZ17
12SZ10
13SZ17 sandstone
12SZ10 siltstone
<734 ± 3 Ma
Liulin Fm
269 - 2622
12SZ17
12SZ14
A3
12SZ06
12SZ07
13SZ14
13SZ19
A2
12SZ17 tuffaceous siltstone 727 ± 5 Ma
12SZ14 metarhyolite 742± 6 Ma
A3: rhyodacitic tuff 763 ± 7 Ma
12SZ06 sandstone
12SZ07 sandstone
13SZ14 sandstone
13SZ19 sandstone
<789 ± 5 Ma
A2: troctolite 632 ± 6 Ma
Gujing Fm
486 - 2802
12SZ20
12SZ28
12SZ24
A1
12SZ20 silttone
12SZ28 sandstone
12SZ24 sandstone
<739 ± 4 Ma
A1: meta-trachandesite 741 ± 7 Ma
pebbled sandstone
quratz sandstone
feldspar quratz sandstone
silttone
slate
actinolite schist
quartz-sericite schist
quartz-albite schist
metarhyolite
mafic-ultramafic intrusions

Fig.3

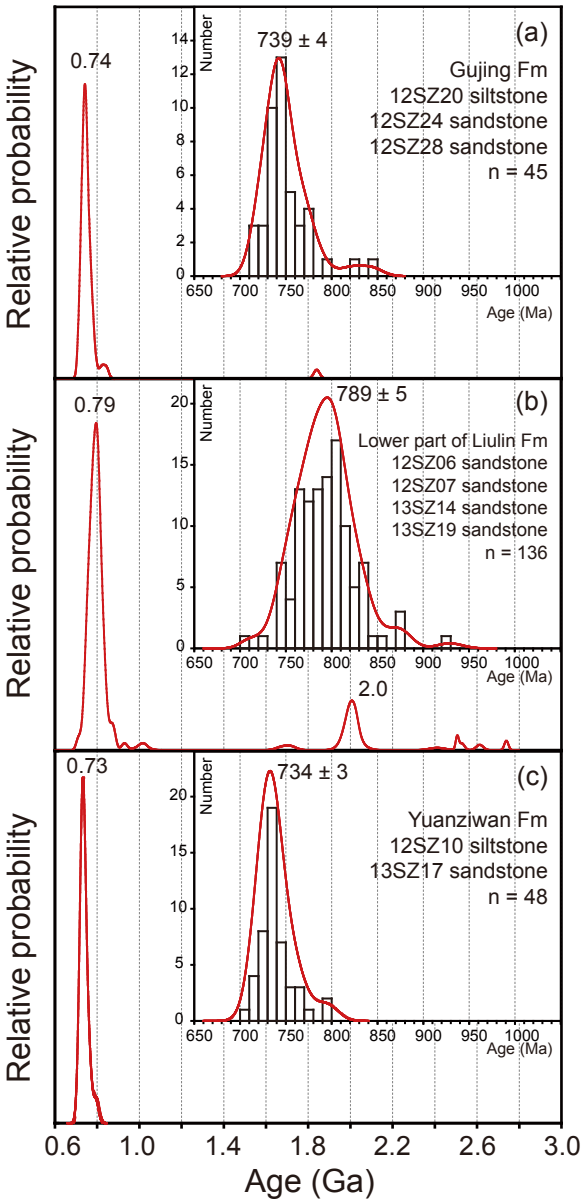
Relative probability
0.74
739 ± 4
(a)
Gujing Fm
12SZ20 siltstone
12SZ24 sandstone
12SZ28 sandstone
n = 45
Number
Age (Ma)
0.79
789 ± 5
(b)
Lower part of Liulin Fm
12SZ06 sandstone
12SZ07 sandstone
13SZ14 sandstone
13SZ19 sandstone
n = 136
2.0
0.73
734 ± 3
(c)
Yuanziwan Fm
12SZ10 siltstone
13SZ17 sandstone
n = 48
0.6
1.0
1.4
1.8
2.2
2.6
3.0
Age (Ga)

Fig.4

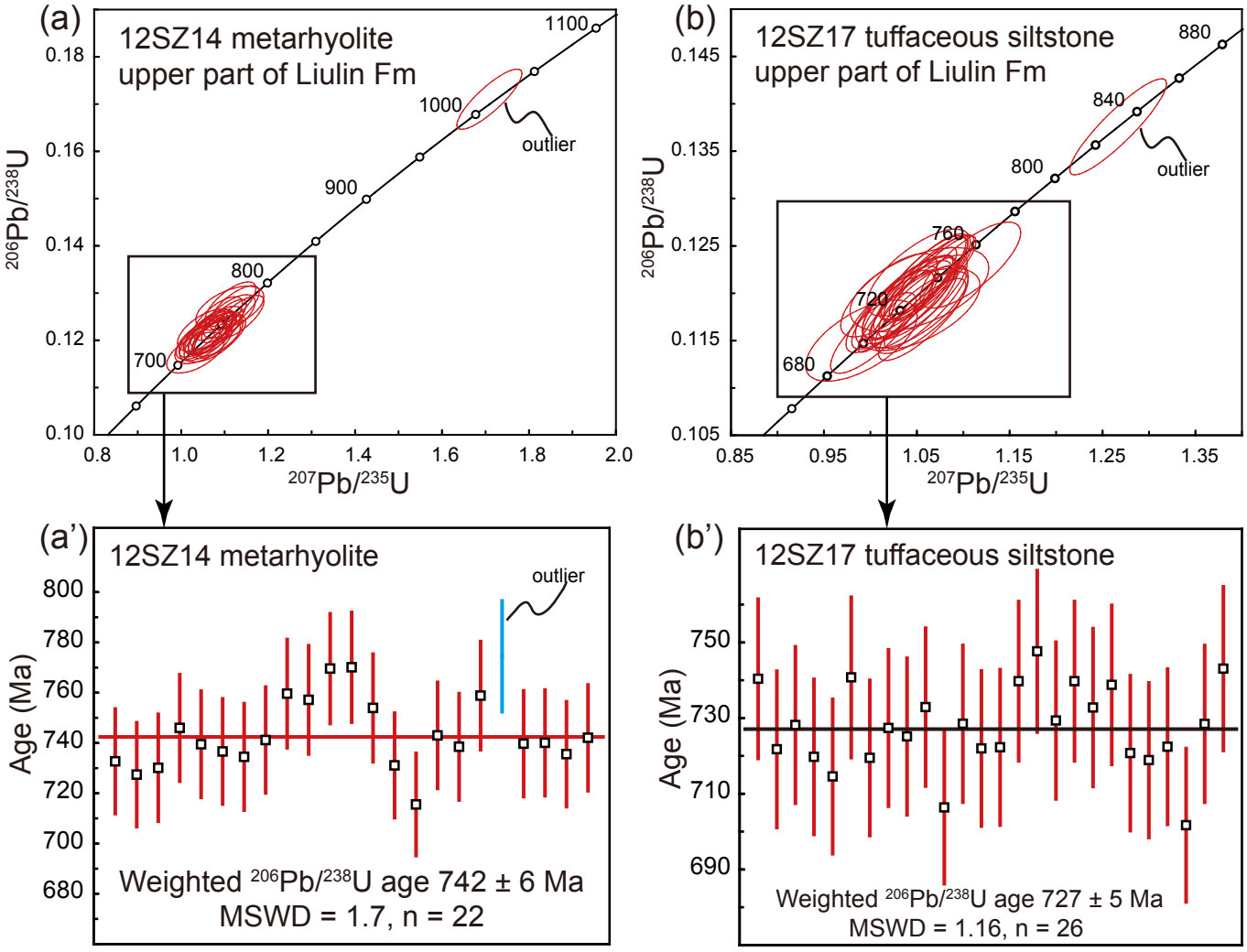
(a)
12SZ14 metarhyolite
upper part of Liulin Fm
1100
1000
900
800
700
outlier
0.18
0.16
0.14
0.12
0.10
0.8
1.0
1.2
1.4
1.6
1.8
2.0
206Pb/238U
207Pb/235U
(b)
12SZ17 tuffaceous siltstone
upper part of Liulin Fm
880
840
800
760
720
680
outlier
0.145
0.135
0.125
0.115
0.105
0.85
0.95
1.05
1.15
1.25
1.35
206Pb/238U
207Pb/235U
(a')
12SZ14 metarhyolite
outlier
800
780
760
740
720
700
680
Age (Ma)
Weighted 206Pb/238U age 742 ± 6 Ma
MSWD = 1.7, n = 22
(b')
12SZ17 tuffaceous siltstone
750
730
710
690
Age (Ma)
Weighted 206Pb/238U age 727 ± 5 Ma
MSWD = 1.16, n = 26

Fig.5

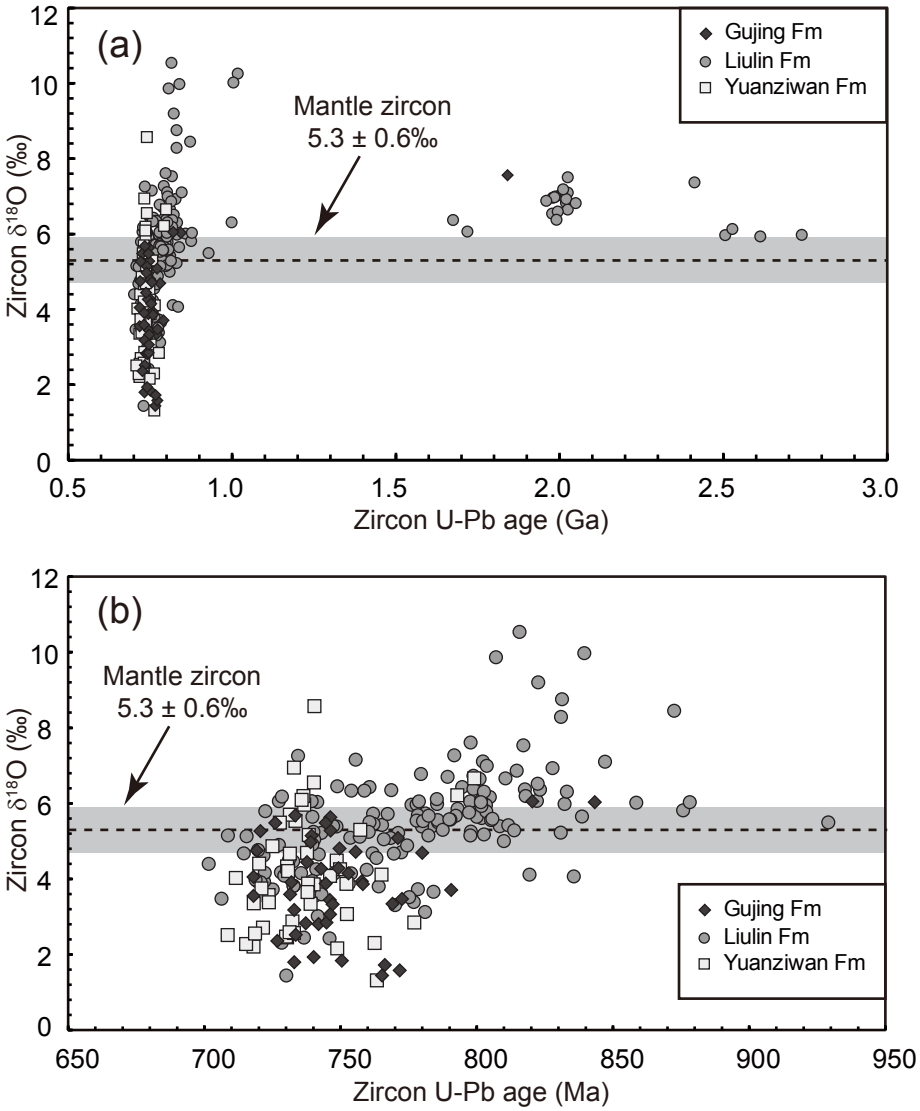
(a)
Mantle zircon
5.3 ± 0.6‰
Gujing Fm
Liulin Fm
Yuanziwan Fm
Zircon δ18O (‰)
Zircon U-Pb age (Ga)
0
2
4
6
8
10
12
0.5
1.0
1.5
2.0
2.5
3.0
(b)
Mantle zircon
5.3 ± 0.6‰
Gujing Fm
Liulin Fm
Yuanziwan Fm
Zircon δ18O (‰)
Zircon U-Pb age (Ma)
650
700
750
800
850
900
950

Fig. 6

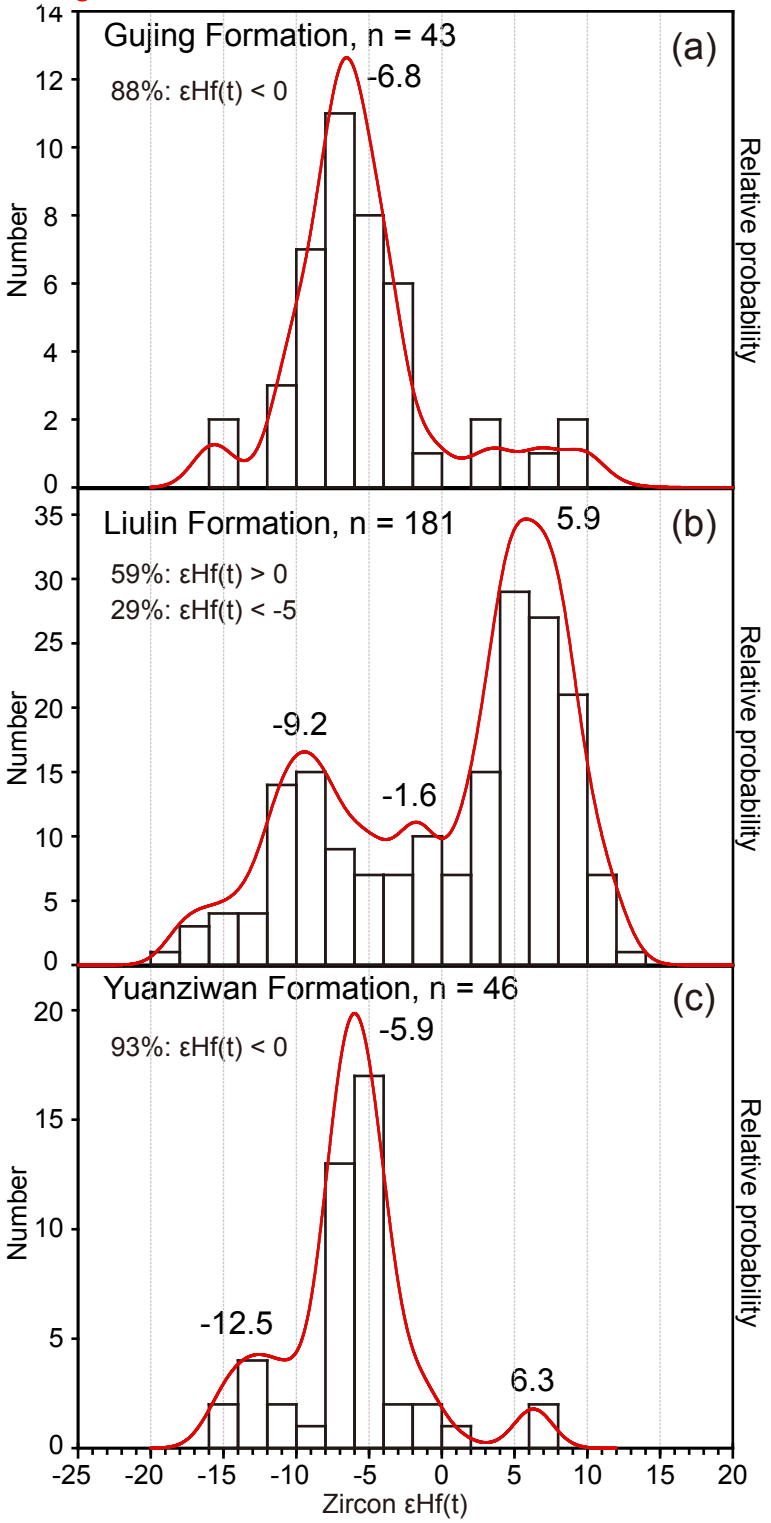
Gujing Formation, n = 43
(a)
88%: εHf(t) < 0
-6.8
Number
Relative probability
Liulin Formation, n = 181
(b)
59%: εHf(t) > 0
29%: εHf(t) < -5
5.9
-9.2
-1.6
Number
Relative probability
Yuanziwan Formation, n = 46
(c)
93%: εHf(t) < 0
-5.9
-12.5
6.3
Number
Relative probability
Zircon εHf(t)

Fig.7

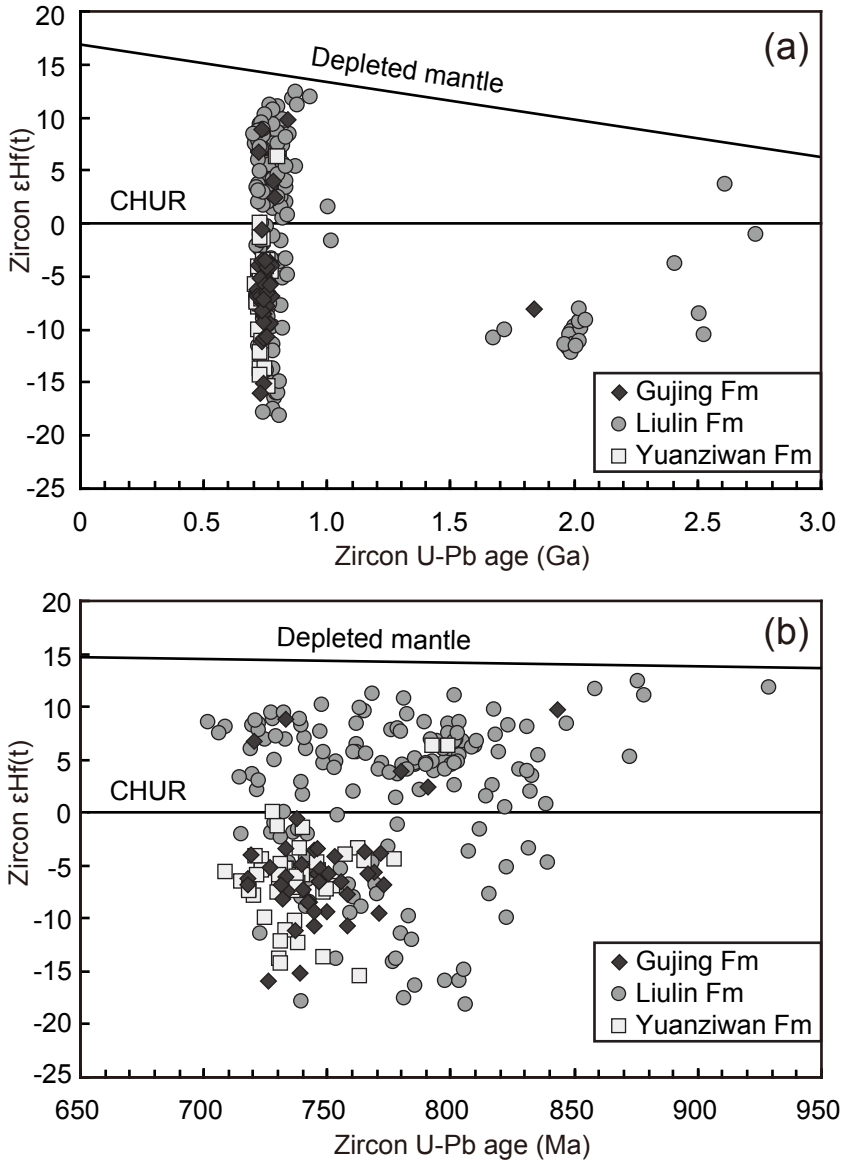
(a)
Depleted mantle
CHUR
Zircon εHf(t)
Zircon U-Pb age (Ga)
Gujing Fm
Liulin Fm
Yuanziwan Fm
(b)
Depleted mantle
CHUR
Zircon εHf(t)
Zircon U-Pb age (Ma)
Gujing Fm
Liulin Fm
Yuanziwan Fm

Fig. 8

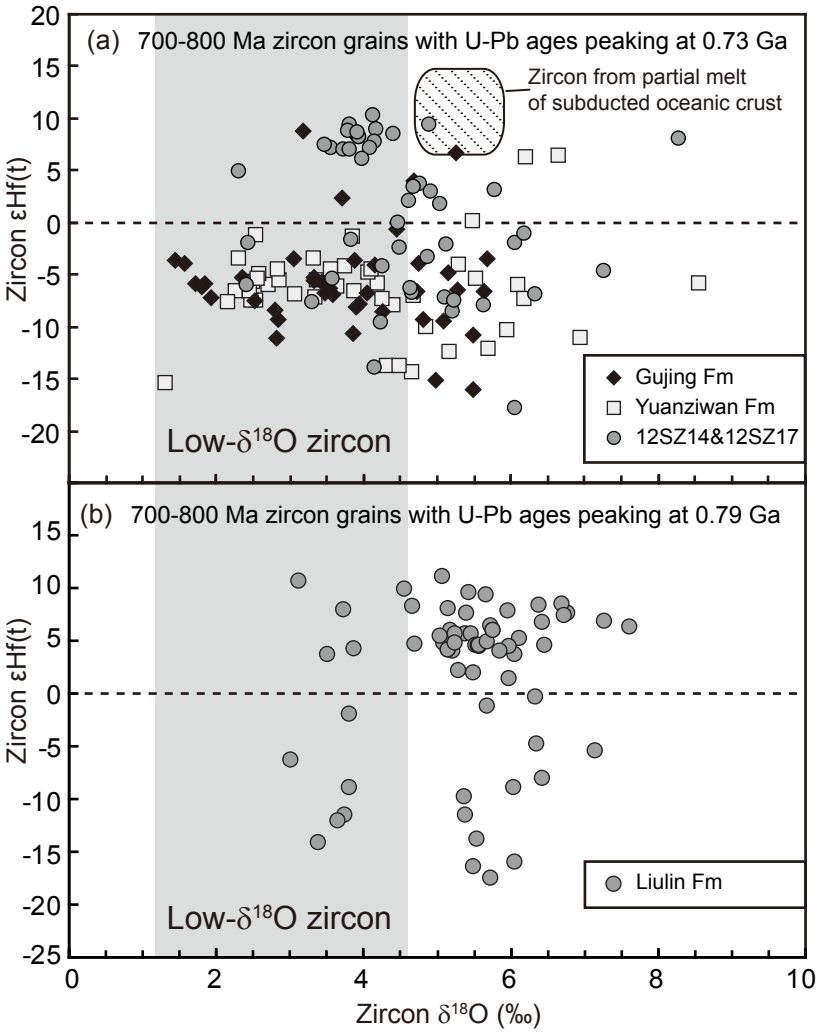
(a) 700-800 Ma zircon grains with U-Pb ages peaking at 0.73 Ga
Zircon from partial melt of subducted oceanic crust
Gujing Fm
Yuanziwan Fm
12SZ14&12SZ17
Low-δ18O zircon
(b) 700-800 Ma zircon grains with U-Pb ages peaking at 0.79 Ga
Liulin Fm
Low-δ18O zircon
Zircon εHf(t)
Zircon δ18O (‰)

Fig. 9

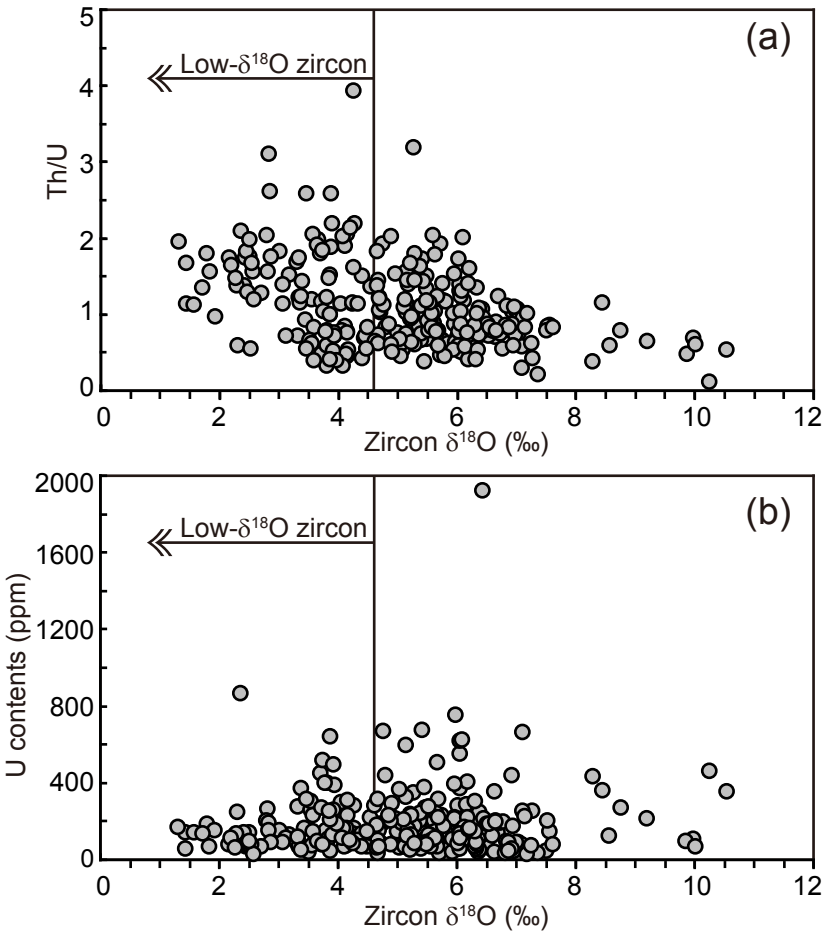
(a)
Low-δ18O zircon
Th/U
Zircon δ18O (‰)
(b)
Low-δ18O zircon
U contents (ppm)
Zircon δ18O (‰)

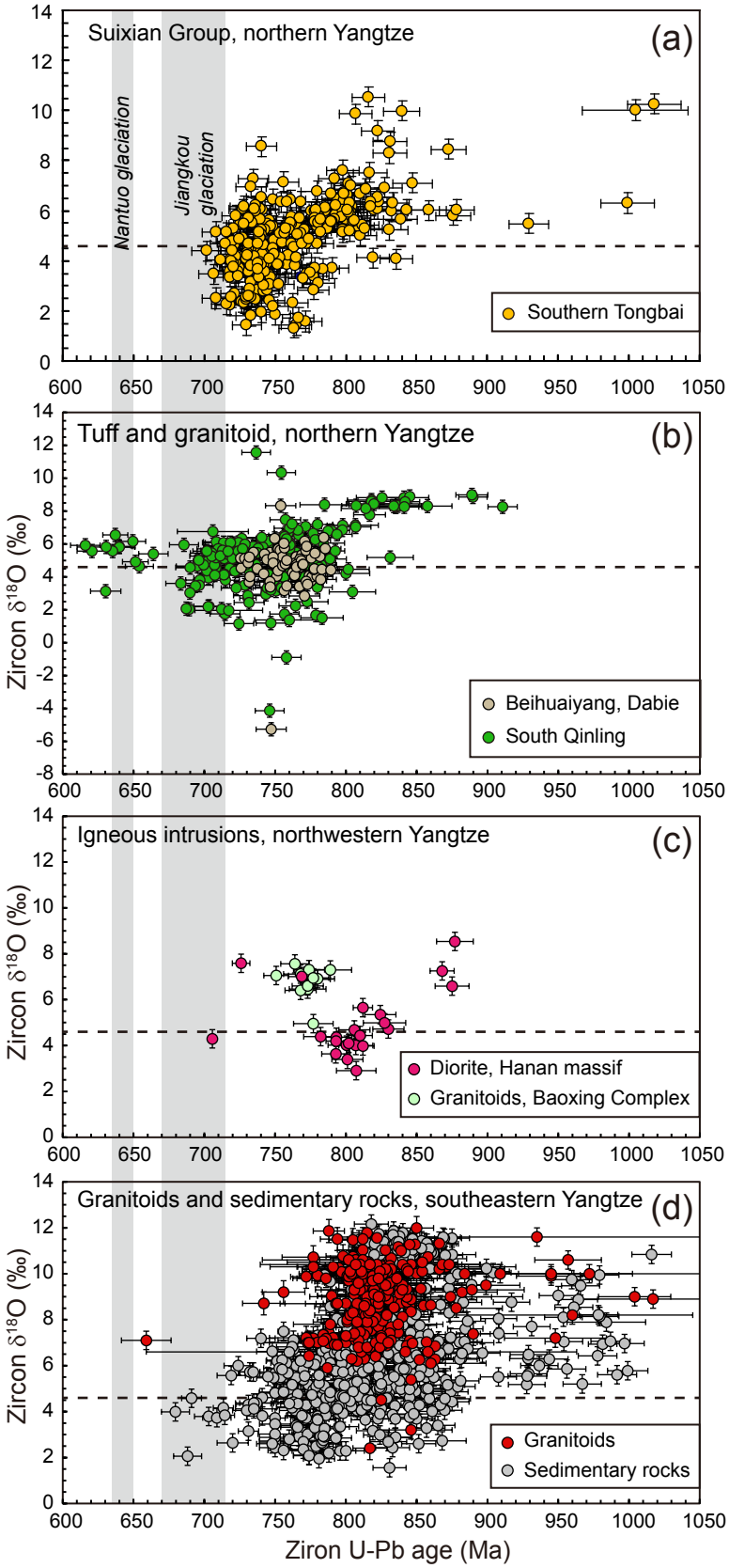
Suixian Group, northern Yangtze
(a)
Nantuo glaciation
Jiangkou glaciation
Southern Tongbai
Tuff and granitoid, northern Yangtze
(b)
Beihuaiyang, Dabie
South Qinling
Igneous intrusions, northwestern Yangtze
(c)
Diorite, Hanan massif
Granitoids, Baoxing Complex
Granitoids and sedimentary rocks, southeastern Yangtze
(d)
Granitoids
Sedimentary rocks
Zircon δ18O (‰)
Ziron U-Pb age (Ma)

Fig. 10

Fig.11

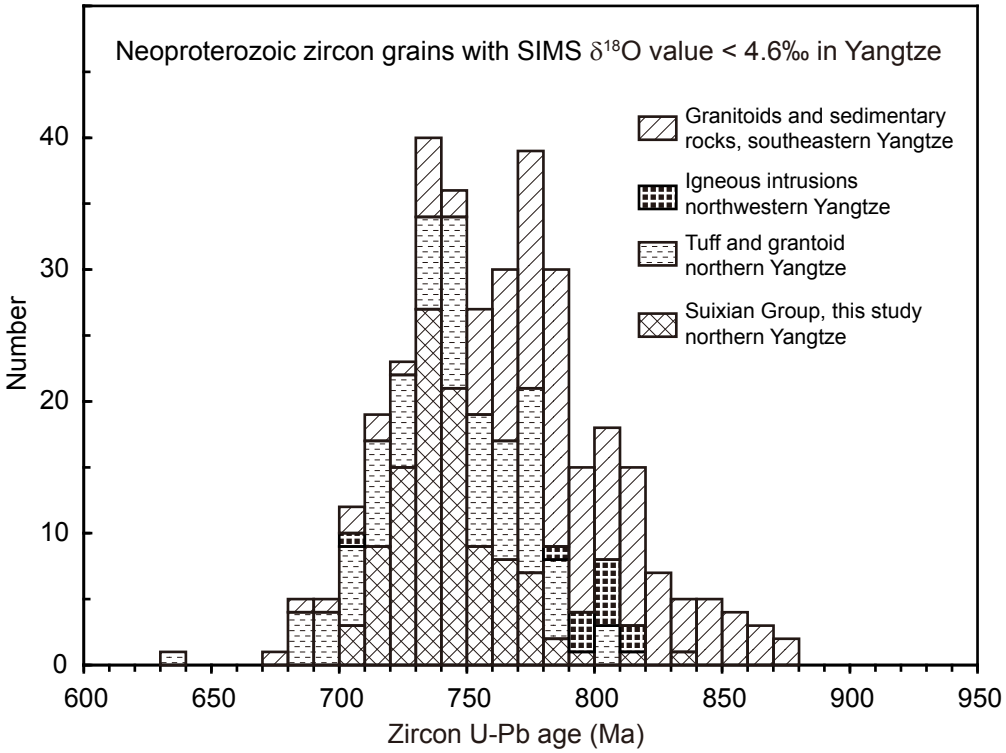
Neoproterozoic zircon grains with SIMS δ18O value < 4.6‰ in Yangtze
Granitoids and sedimentary rocks, southeastern Yangtze
Igneous intrusions northwestern Yangtze
Tuff and grantoid northern Yangtze
Suixian Group, this study northern Yangtze
Number
0
10
20
30
40
600
650
700
750
800
850
900
950
Zircon U-Pb age (Ma)

Appendix S1. References for U-Pb ages cited in Fig. 1(a)

Southeastern Margin of the Yangtze Craton

The Shengwu doleritic dyke (849 ± 7 Ma) and the Daolingshan granite-diabase (794 ± 9 Ma) (Li et al., 2008); Xucun granidiorite (823 ± 8 Ma) (Li et al., 2003) and (827 ± 7 Ma; 823 ± 7 Ma) (Wu et al., 2006); Xiuning granidiorite (824 ± 7 Ma; 825 ± 7 Ma) (Wu et al., 2006); Shexian granidiorite (823 ± 9 Ma; 824 ± 6 Ma) (Wu et al., 2006); Lianhuashan granite (771 ± 17 Ma; 777 ± 7 Ma) (Zheng et al., 2008); Qixitain granite (775 ± 5 Ma) (Zheng et al., 2008); Jiuling granodiorite (819 ± 9 Ma) (Li et al., 2003); Yiyang komatiitic lava (826 ± 3 Ma) (Wang et al., 2007); Bendong granodiorite (818 ± 10 Ma), Sanfang granite (827 ± 15 Ma), and Yuanbaoshan grantie (824 ± 4 Ma) (Li, 1999).

Western Margin of the Yangtze Craton

Eshan porphyritic granite (819 ± 8 Ma) (Li et al., 2003); Datian diorite (760 ± 4 Ma) (Zhao and Zhou, 2007) ; Dadukou olivine gabbro (746 ± 10 Ma; 738 ± 23 Ma) (Zhao and Zhou, 2007); Tongde picritic dyke (796 ± 5 Ma) (Zhu et al., 2010); Tongde gabbro (820 ± 13 Ma) and diorite (813 ± 14 Ma) (Sinclair, 2001); Lengshuiqing diorite (812 ± 3 Ma) and Gaojiacun (806 ± 4 Ma) (Zhou et al., 2006); Guandaoshan granite (857 ± 13 Ma) (Li et al., 2003); Shaba gabbroic rocks (752 ± 12 Ma; 752 ± 11 Ma) (Li et al., 2003);Suxiong bimodal volcanics (803 ± 12 Ma) (Li et al., 2002a); Lengqi gabbro (808 ± 12 Ma) (Li et al., 2002b); Kangting diorite (768 ± 7 Ma), granodiorite (755 ± 6 Ma), and granitic rock (751 ± 10 Ma) (Li et al., 2003) and Kangting ganitoids (797 ± 10 Ma;796 ± 13 Ma; 795 ± 11 Ma) (Zhou et al., 2002); Xuelongbao tonalite (748 ± 7 Ma) (Zhou et al., 2006); Baoxing complex (790-720 Ma) (Fu et al., 2013).

Northern Magrin of the Yangtze Craton

Bikou basalts (821 ± 7 Ma; 811 ± 12 Ma) (Wang et al., 2008); Xixiang dacite (950 ± 4 Ma), Xixiang rhyolite (897 ± 3 Ma), and Tiechuanshan rhyolite (817 ± 5 Ma) (Ling et al., 2003); Beiba gabbro (814 ± 9 Ma) and Luojiaba hornblende gabbro (746 ± 4 Ma) (Zhao and Zhou, 2009); Erliba granodiorite (730 ± 6 Ma) and Wudumen granodiorite (735 ± 8 Ma) (Zhao and Zhou, 2008); Wangjiangshan diorite (819 ± 10 Ma) and gabbro (808 ± 14 Ma), Bijigou gabbro (782 ± 10 Ma) (Zhou et al., 2002); Xixia granite (718 ± 12 Ma; 714 ± 7 Ma; 721 ± 9 Ma), granodiorite (718 ± 33 Ma) and diorite (827 ± 8 Ma) (Liu and Zhang, 2013); Wudang mafic dyke (651 ± 5 Ma) (Zhu et al., 2014); Zhouan lherzolite (637 ± 4 Ma) (Wang et al., 2013); Duchongshan troctolite (632 ± 6 Ma) (Xue et al., 2011); Hualingmiao trondhjemite-granodiorite suite (819 ± 7 Ma) (Ma et al., 1989); Xiaofeng dykes (802 ± 10 Ma) (Li et al., 2003); Wangmuguan olivine-gabbro (635 ± 5 Ma) (Liu et al., 2006); Luzhenguan granite (782 ± 3 Ma) (Zheng et al., 2007), granite (741 ± 7 Ma; 754 ± 5 Ma; 746 ± 6 Ma) (Wu et al., 2007), and gabbro-diorite (744 ± 13 Ma; 739 ± 8 Ma; 746 ± 6 Ma) (Wu et al., 2007).

References

Fu, B. et al., 2013. Origin of the Tongbai-Dabie-Sulu Neoproterozoic low-$\delta^{18}O$ igneous province, east-central China. Contributions to Mineralogy and Petrology, 165: 641-662.

Li, X., 1999. U－Pb zircon ages of granites from the southern margin of the Yangtze Block: timing of Neoproterozoic Jinning: Orogeny in SE China and implications for Rodinia Assembly. Precambrian Research, 97(1－2): 43-57.

Li, X. et al., 2003. Neoproterozoic granitoids in South China: crustal melting above a mantle plume at ca. 825 Ma? Precambrian Research, 122(1 – 4): 45-83.

Li, X. et al., 2003. SHRIMP U-Pb zircon age, geochemistry and Nd isotope of the Guandaoshan pluton in SW Sichuan: Petrogenesis and tectonic significance. Science in China Series D: Earth Sciences, 46 supp.: 73-83.

Li, X., Li, W., Li, Z. and Liu, Y., 2008. 850 – 790 Ma bimodal volcanic and intrusive rocks in northern Zhejiang, South China: A major episode of continental rift magmatism during the breakup of Rodinia. Lithos, 102(1 – 2): 341-357.

Li, X., Li, Z., Zhou, H., Liu, Y. and Kinny, P. D., 2002a. U–Pb zircon geochronology, geochemistry and Nd isotopic study of Neoproterozoic bimodal volcanic rocks in the Kangdian Rift of South China: implications for the initial rifting of Rodinia. Precambrian Research, 113: 135-154.

Li, X., Li, Z., Zhou, H., Liu, Y. and Liang, X., 2002b. U-Pb zircon geochronological, geochemical and Nd isotopic study of Neoproterozoic basaltic magmatism in western Sichuan: petrogenesis and geodynamic implications., 9(4): 329-338 (in Chinese with English abstract).

Li, Z.X. et al., 2003. Geochronology of Neoproterozoic syn-rift magmatism in the Yangtze Craton, South China and correlations with other continents: evidence for a mantle superplume that broke up Rodinia. Precambrian Research, 122(1 – 4): 85-109.

Ling, W. et al., 2003. Neoproterozoic tectonic evolution of the northwestern Yangtze craton, South China: implications for amalgamation and break-up of the Rodinia Supercontinent. Precambrian Research, 122(1 – 4): 111-140.

Liu, J. and Zhang, L., 2013. Neoproterozoic low to negative $\delta^{18}O$ volcanic and intrusive rocks in the Qinling Mountains and their geological significance. Precambrian Research, 230(0): 138-167.

Liu, Y., Li, S., Gu, X. and Hou, Z., 2006. Zircon SHRIMP U-Pb age of Wangmuguan olivine-gabbro in Beihuanyang unit of Dabie orogen and its significance. Chinese Science Bulletin, 51(18): 2175-2180 (in Chinese).

Ma, G., Zhang, Z., Li, H., Chen, P. and Huang, Z., 1989. A geochronological study of the Sinian System in Yangtze Platform. Bulletin of Yichang Institute of Geology and Mineral Resources, 14: 83-124 (in Chinese with English abstract).

Sinclair, J.A., 2001. Petrology, geochemistry, and geochronology of the Mesoproterozoic Yanbian "ophiolite", western Sichuan Province, South China. Honours Thesis, The University of Western Australia, Perth.

Wang, M., Wang, C. and Zhao, J., 2013. Zircon U/Pb dating and Hf-O isotopes of the Zhouan ultramafic intrusion in the northern margin of the Yangtze Block, SW China: Constraints on the nature of mantle source and timing of the supercontinent Rodinia breakup. Chinese Science Bulletin, 58(7): 777-787.

Wang, X. et al., 2008. The Bikou basalts in the northwestern Yangtze block, South China: Remnants of 820 – 810 Ma continental flood basalts? Geological Society of America Bulletin, 120(11-12): 1478 -1492.

Wang, X., Li, X., Li, W. and Li, Z., 2007. Ca. 825 Ma komatiitic basalts in South China: First evidence for >1500 °C mantle melts by a Rodinian mantle plume. Geology, 35(12): 1103 -1106.

Wu, R. et al., 2006. Reworking of juvenile crust: Element and isotope evidence from

Neoproterozoic granodiorite in South China. Precambrian Research, 146(3 – 4): 179-212.

Wu, Y. et al., 2007. Zircon U – Pb dating of water – rock interaction during Neoproterozoic rift magmatism in South China. Chemical Geology, 246(1 – 2): 65-86.

Xue, H., Ma, F. and Song, Y., 2011. Geochemistry and SHRIMP zircon U-Pb data of Neoproterozoic meta-magamtic rocks in the Suizhou-Zaoyang area, northern margin of the Yangtze Craton, Cental China. Acta Petrologica Sinica, 27(4): 1116-1130 (in Chinese with English abstract).

Zhao, J. and Zhou, M., 2007. Neoproterozoic Adakitic Plutons and Arc Magmatism along the western margin of Yangtze Block, South China. The Journal of Geology, 115: 675-689.

Zhao, J. and Zhou, M., 2008. Neoproterozoic adakitic plutons in the northern margin of the Yangtze Block, China: Partial melting of a thickened lower crust and implications for secular crustal evolution. Lithos, 104(1 – 4): 231-248.

Zhao, J. and Zhou, M., 2009. Secular evolution of the Neoproterozoic lithospheric mantle underneath the northern margin of the Yangtze Block, South China. Lithos, 107(3 – 4): 152-168.

Zheng, Y. et al., 2007. Tectonic driving of Neoproterozoic glaciations: Evidence from extreme oxygen isotope signature of meteoric water in granite. Earth and Planetary Science Letters, 256(1 – 2): 196-210.

Zheng, Y. et al., 2008. Rift melting of juvenile arc-derived crust: Geochemical evidence from Neoproterozoic volcanic and granitic rocks in the Jiangnan Orogen, South China. Precambrian Research, 163(3 – 4): 351-383.

Zhou, M. et al., 2006. The Yanbian Terrane (Southern Sichuan Province, SW China): A Neoproterozoic arc assemblage in the western margin of the Yangtze Block. Precambrian Research, 144(1 – 2): 19-38.

Zhou, M., Yan, D., Kennedy, A.K., Li, Y. and Ding, J., 2002. SHRIMP U – Pb zircon geochronological and geochemical evidence for Neoproterozoic arc-magmatism along the western margin of the Yangtze Block, South China. Earth and Planetary Science Letters, 196(1 – 2): 51-67.

Zhou, M., Yan, D., Wang, C., Qi, L. and Kennedy, A., 2006. Subduction-related origin of the 750 Ma Xuelongbao adakitic complex (Sichuan Province, China): Implications for the tectonic setting of the giant Neoproterozoic magmatic event in South China. Earth and Planetary Science Letters, 248(1 – 2): 286-300.

Zhou, M.F., Kennedy, A.K., Sun, M., Malpas, J. and Lesher, C.M., 2002. Neoproterozoic arc – related mafic intrusions along the northern margin of South China: implications for the accretion of rodinia. The Journal of geology, 110(5): 611-618.

Zhu, W. et al., 2010. The Tongde Picritic Dikes in the Western Yangtze Block: Evidence for Ca. 800-Ma Mantle Plume Magmatism in South China during the Breakup of Rodinia. The Journal of Geology, 118(5): 509-522.

Zhu, X., Chen, F., Liu, B., Zhang, H. and Zhai, M., 2014. Geochemistry and zircon ages of mafic dikes in the South Qinling, central China: evidence for late Neoproterozoic continental rifting in the northern Yangtze block. International Journal of Earth Sciences: 1-18.

Appendix S2 Micrographs for samples in this study

12SZ20 siltstone Gujing Formation, lower part of Suixian Group

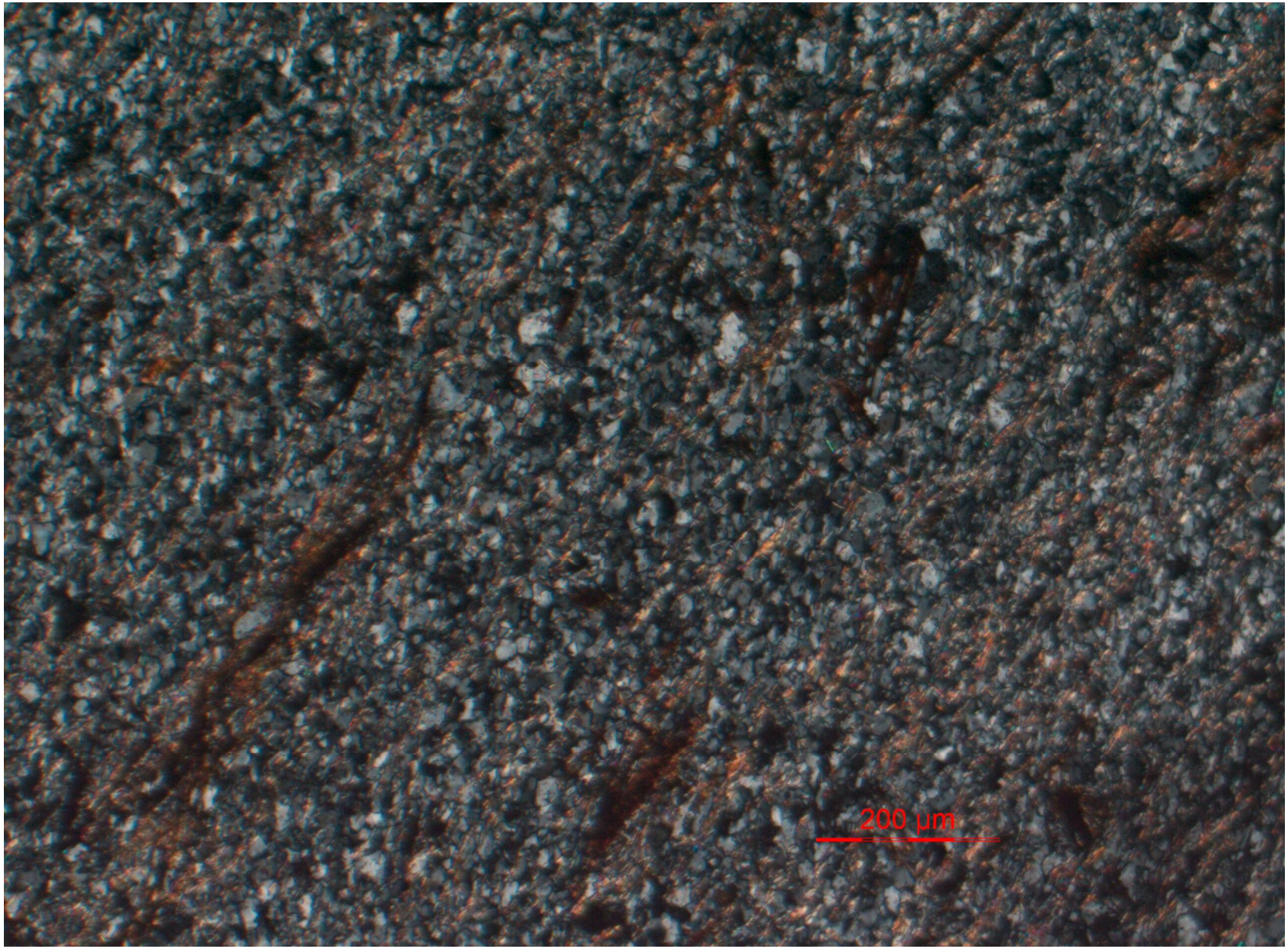

12SZ24 sandstone Gujing Formation, lower part of Suixian Group

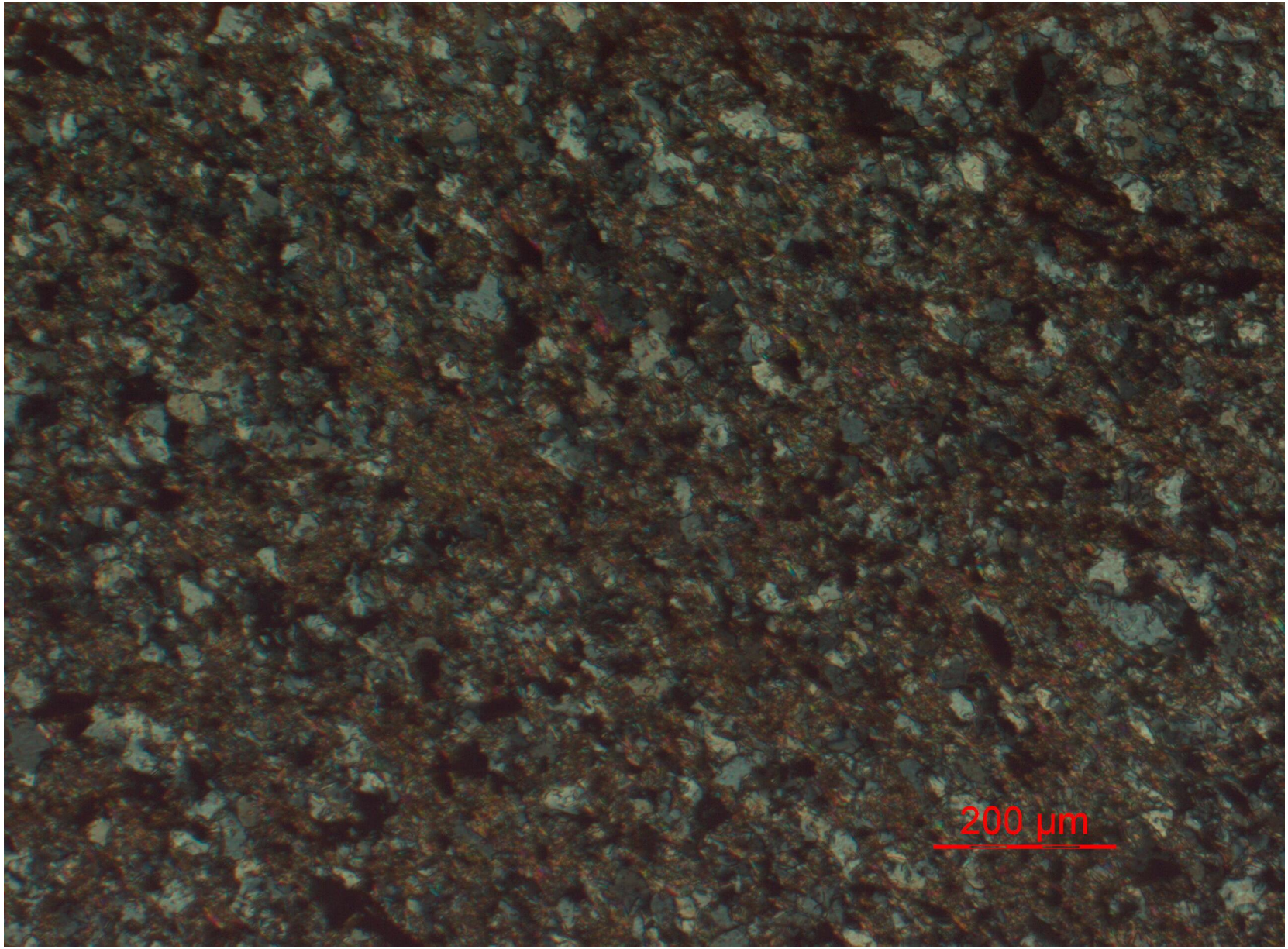

12SZ28 sandstone Gujing Formation, lower part of Suixian Group

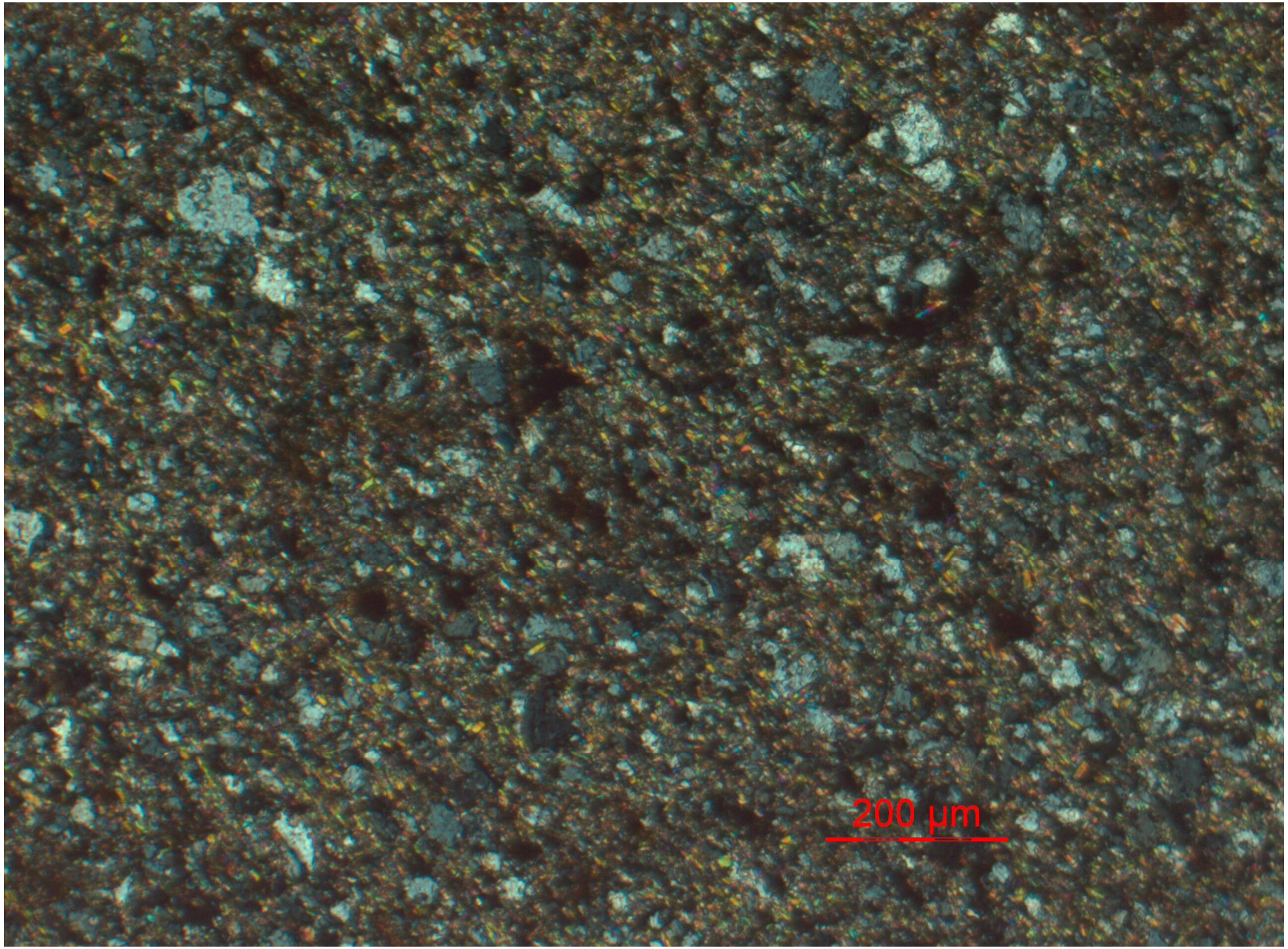

12SZ06 sandstone Liulin Formation, middle part of Suixian Group

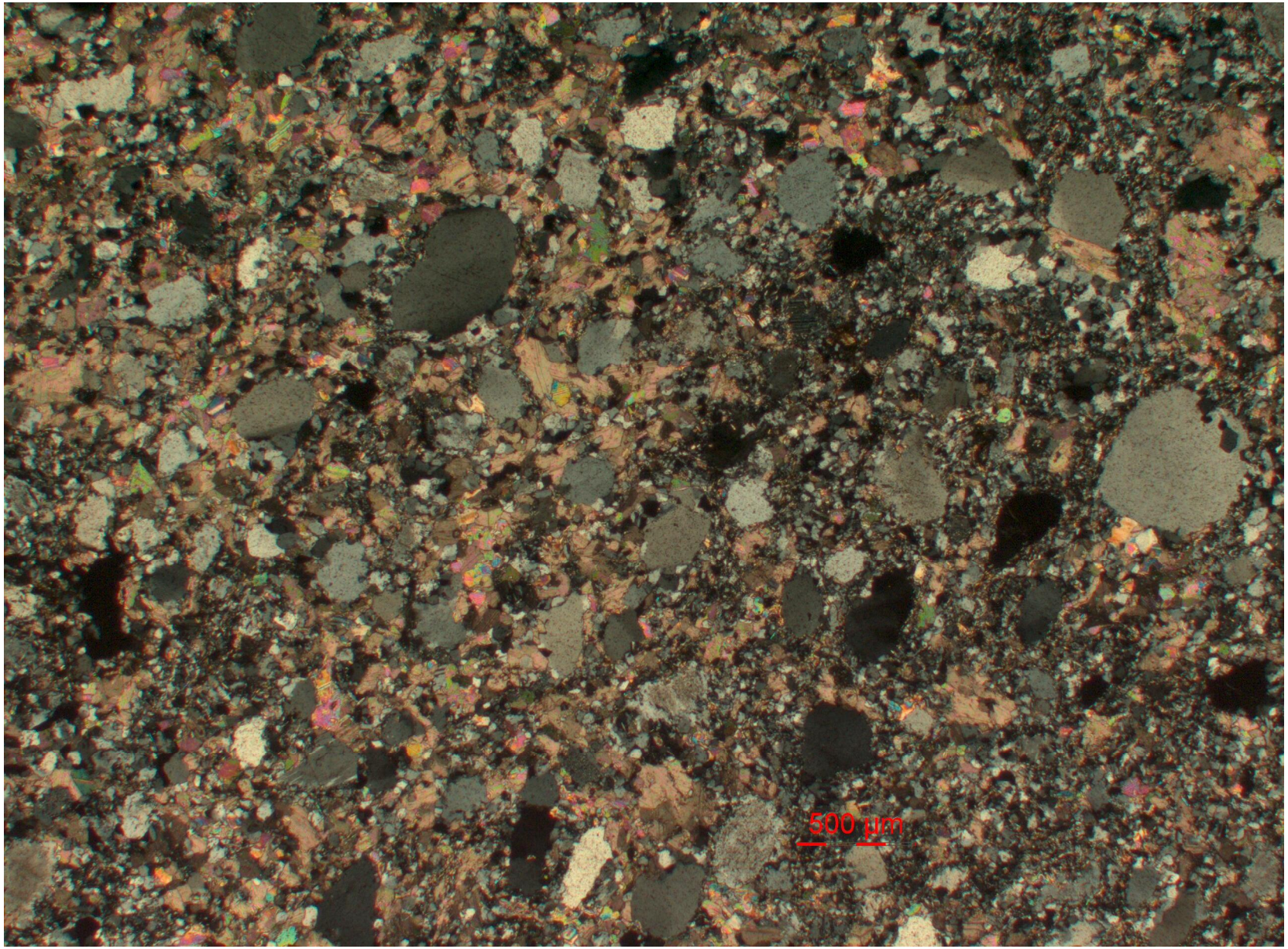

12SZ07 sandstone Liulin Formation, middle part of Suixian Group

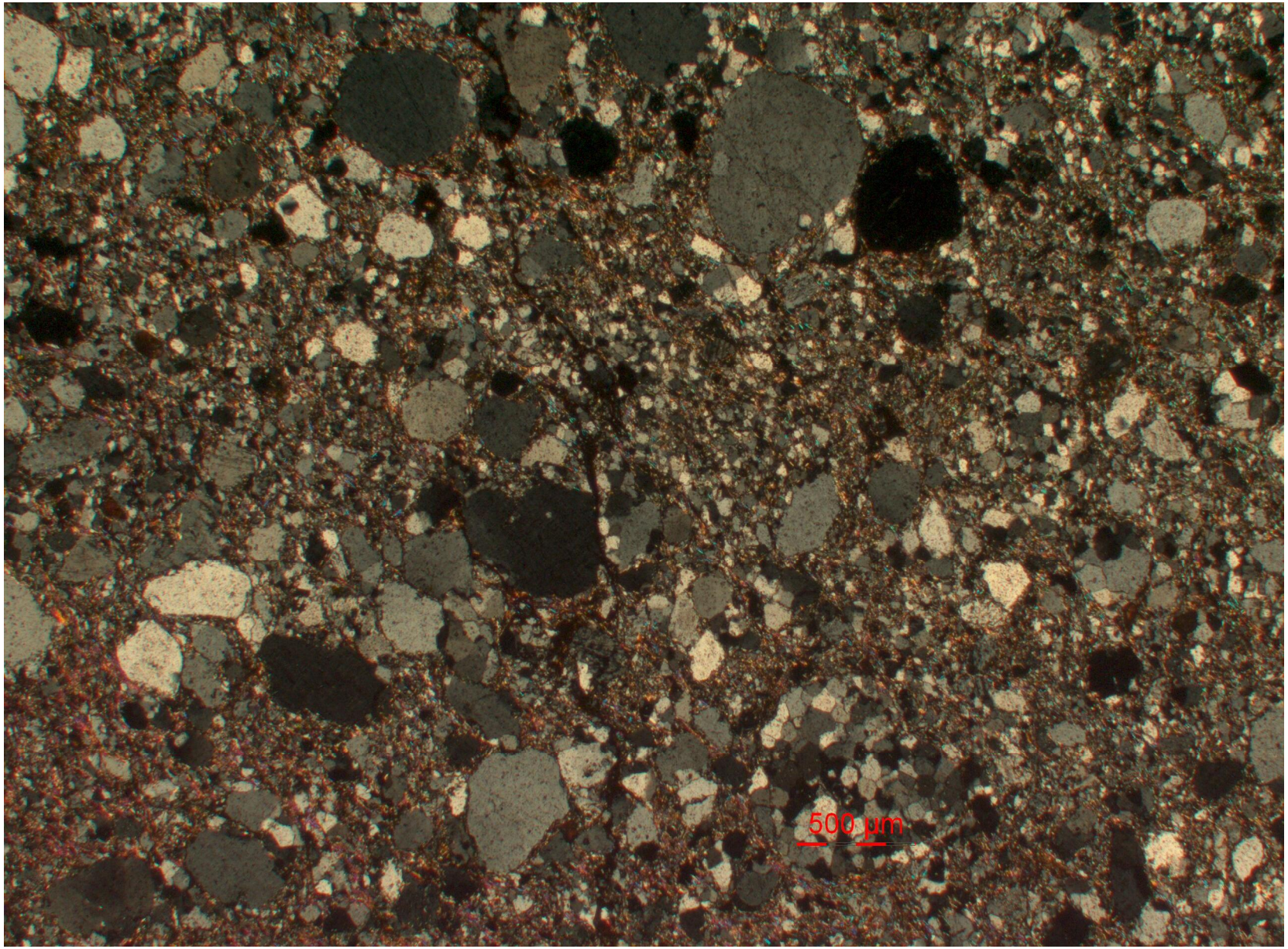

13SZ14 sandstone Liulin Formation, middle part of Suixian Group

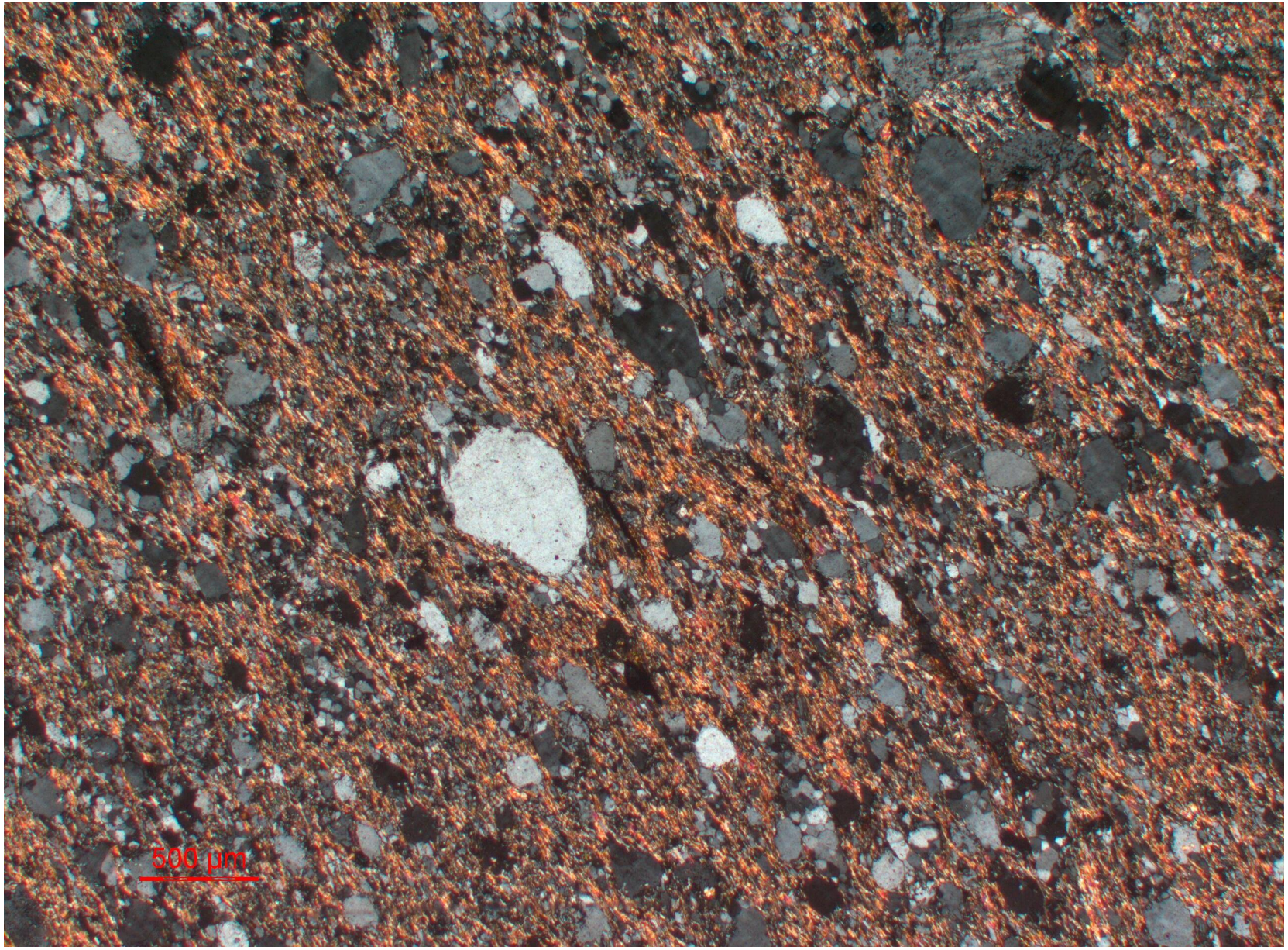

13SZ19 sandstone Liulin Formation, middle part of Suixian Group

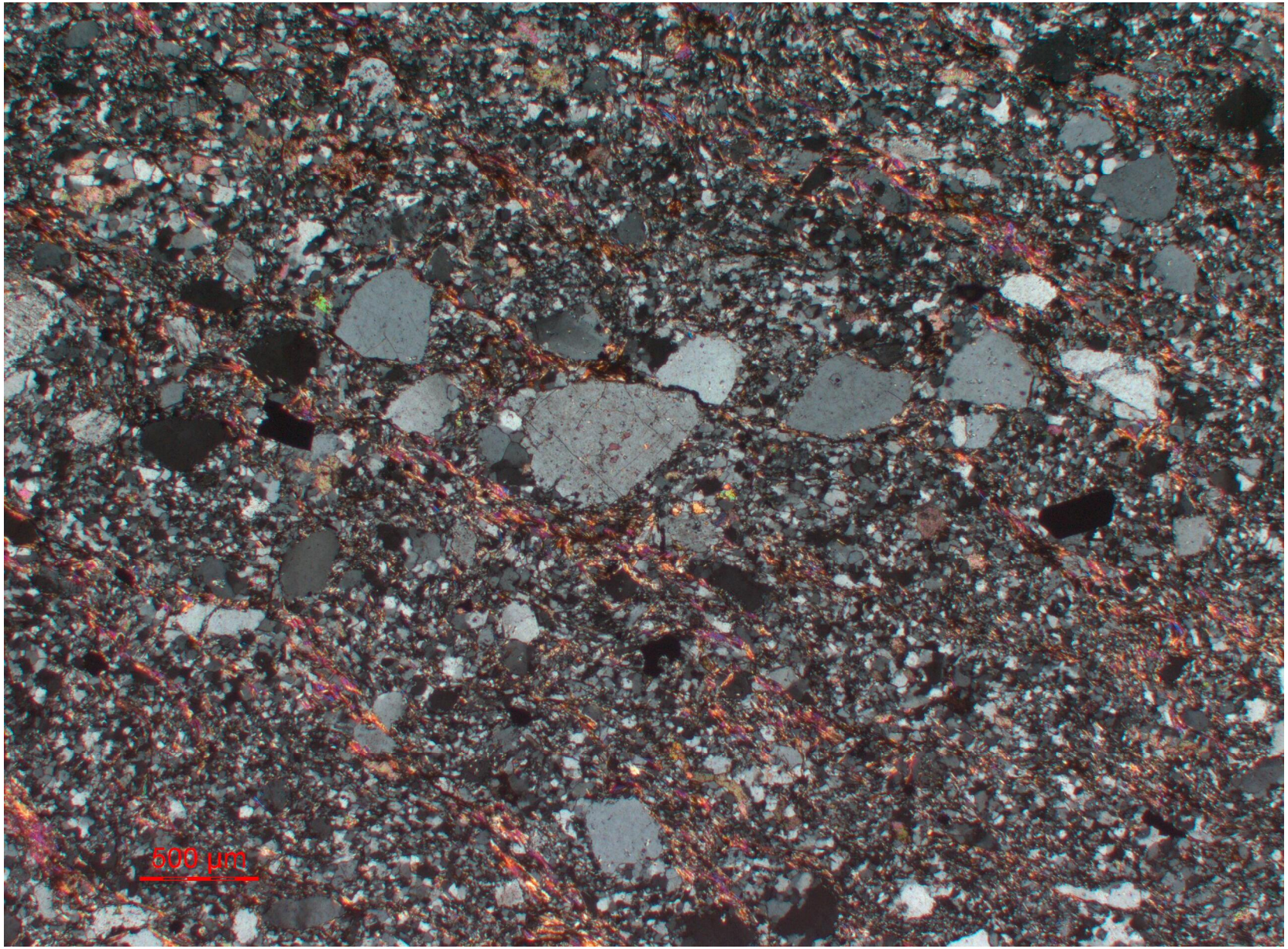

12SZ14 metarhyolite Liulin Formation, middle part of Suixian Group

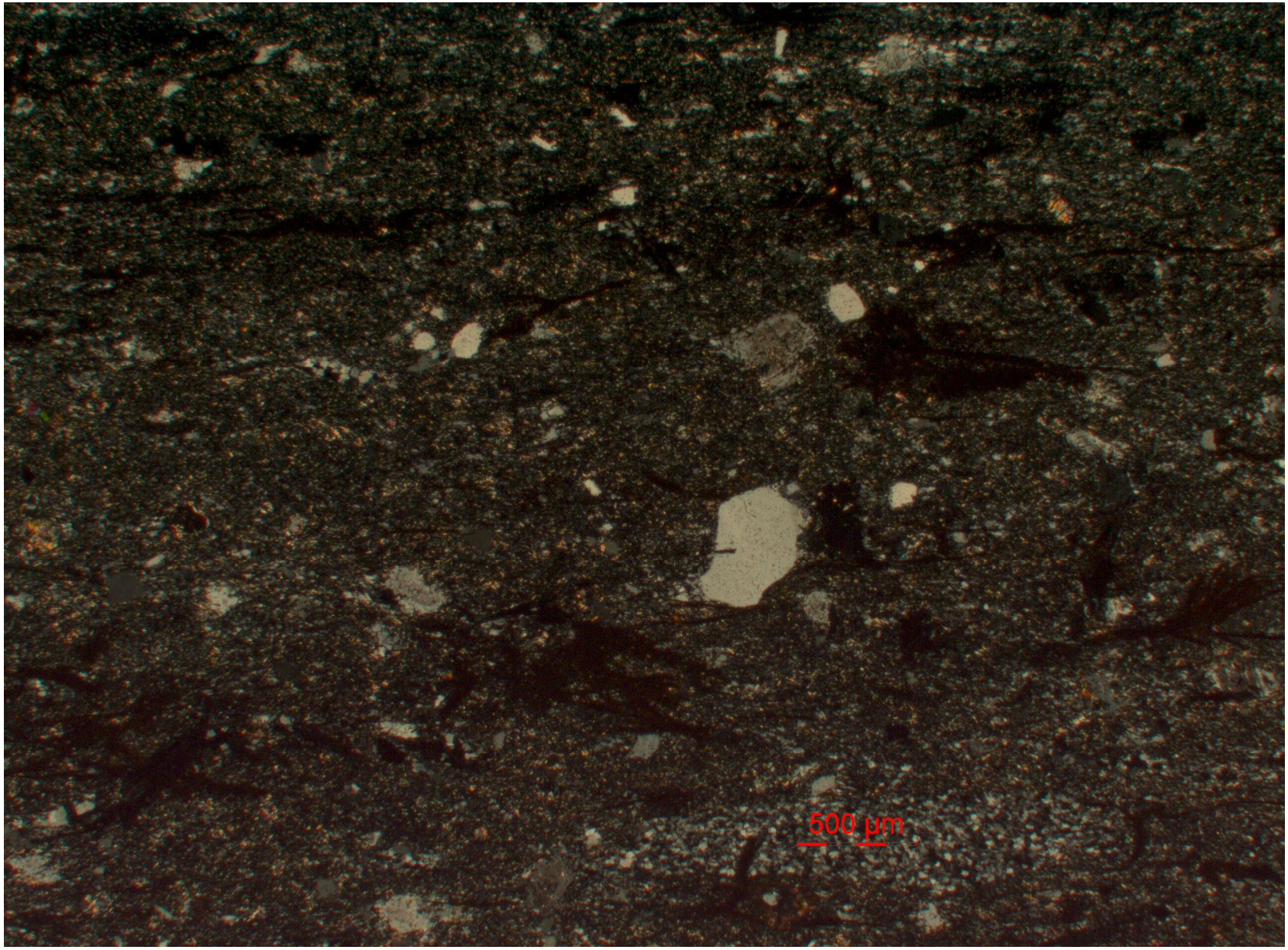

12SZ17 tuffaceous siltstone Liulin Formation, middle part of Suixian Group

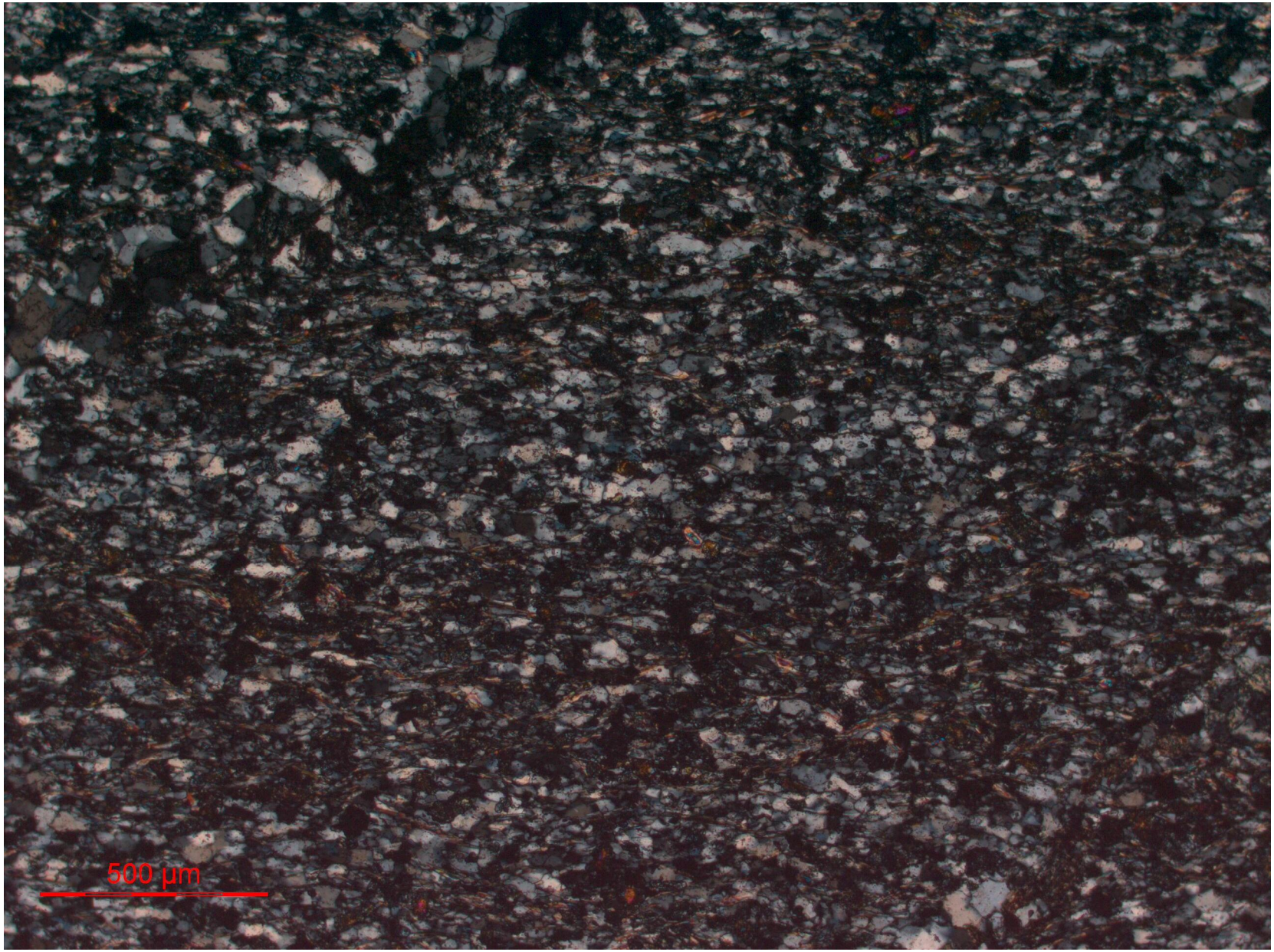

12SZ10 siltstone Yuanziwan Formation, upper part of Suixian Group

13SZ17 sandstone Yuanziwan Formation, upper part of Suixian Group

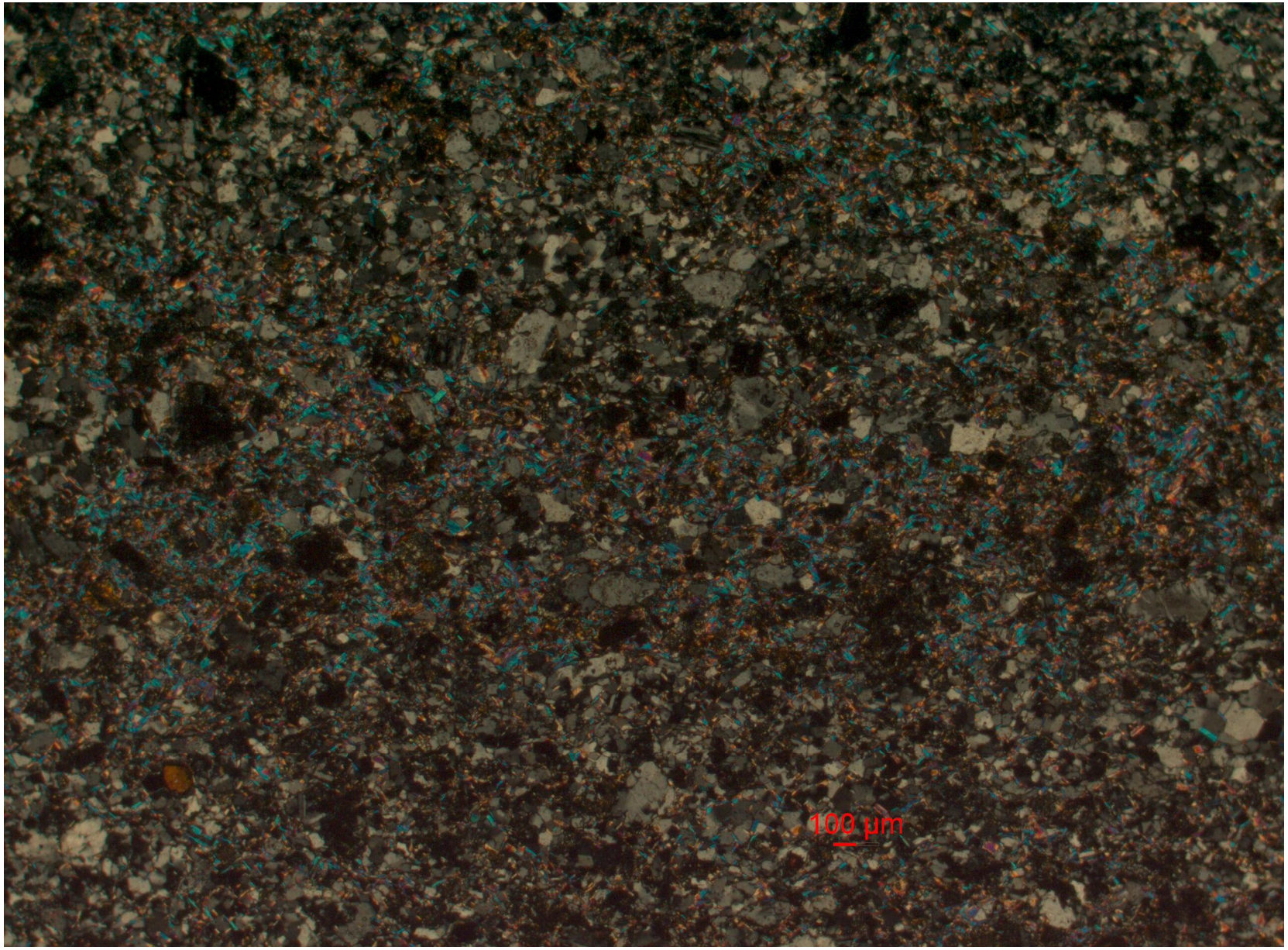

Appendix S3

Appendix S3 SIMS Zircon SIMS U-Pb dating results

Sample spot	U	Th	Th/U	^{204}Pb / ^{206}Pbm	f_{206} [b]	^{207}Pb / ^{206}Pb	±1σ (%)	^{207}Pb / ^{235}U	±1σ (%)	^{206}Pb / ^{238}U	±1σ (%)	ρ [c]	$t_{206/207}$ (Ma)	±1σ	$t_{207/235}$ (Ma)	±1σ	$t_{206/238}$ (Ma)	±1σ	Discordance [d] (%)
Gujing Formation, lower part of Suixian Group																			
12SZ20 (siltstone, 31°21'11.65"N, 113°42'41.54"E)																			
12SZ20@01	273	334	1.2	0	0	0.0642	1.29	1.1222	2.04	0.1267	1.58	0.77	749	27	764	11	769	11	-2.7
12SZ20@02	283	622	2.2	1.95E-05	0.04	0.0643	1.28	1.0923	1.98	0.1233	1.51	0.76	751	27	750	11	749	11	0.2
12SZ20@03	349	1114	3.2	0	0	0.0655	1.15	1.1087	1.90	0.1228	1.51	0.79	790	24	758	10	746	11	5.6
12SZ20@04	140	245	1.8	0	0	0.0648	2.01	1.0766	2.54	0.1205	1.56	0.61	767	42	742	13	734	11	4.4
12SZ20@05	195	280	1.4	2.87E-05	0.05	0.0670	1.75	1.1083	2.31	0.1199	1.50	0.65	839	36	757	12	730	10	13.0
12SZ20@07	187	360	1.9	8.62E-05	0.16	0.0643	1.83	1.0471	2.36	0.1181	1.50	0.63	753	38	727	12	719	10	4.4
12SZ20@08	326	510	1.6	1.25E-04	0.23	0.0643	1.27	1.0768	1.97	0.1215	1.51	0.76	750	27	742	10	739	11	1.4
12SZ20@09	160	148	0.9	2.96E-05	0.06	0.0619	1.60	1.0471	2.20	0.1227	1.51	0.68	670	34	727	12	746	11	-11.3
12SZ20@10	186	336	1.8	0	0	0.0647	1.47	1.0745	2.10	0.1204	1.51	0.72	765	31	741	11	733	10	4.2
12SZ20@11	638	1646	2.6	7.62E-06	0.01	0.0636	0.83	1.0737	1.72	0.1224	1.50	0.87	728	18	741	9	745	11	-2.3
12SZ20@12	104	75	0.7	6.62E-05	0.12	0.0645	2.10	1.0929	2.58	0.1229	1.50	0.58	758	44	750	14	747	11	1.5
12SZ20@13	261	408	1.6	6.43E-05	0.12	0.0633	1.38	1.0572	2.05	0.1212	1.52	0.74	718	29	732	11	737	11	-2.7
12SZ20@14	257	307	1.2	4.00E-05	0.07	0.0641	1.61	1.0408	2.20	0.1178	1.50	0.68	744	34	724	11	718	10	3.5
12SZ20@15	300	342	1.1	4.82E-05	0.09	0.0633	1.32	1.0284	2.00	0.1178	1.50	0.75	718	28	718	10	718	10	0.0
12SZ20@16	95	99	1.0	7.79E-05	0.15	0.0648	2.72	1.0960	3.11	0.1227	1.50	0.48	767	56	751	17	746	11	2.7
12SZ24 (sandstone, 31°28'26.73"N, 113°41'48.10"E)																			
12SZ24@01	440	363	0.8	1.33E-04	0.25	0.0636	0.92	1.0812	1.77	0.1233	1.51	0.85	728	19	744	9	750	11	-3.0
12SZ24@02	211	323	1.5	7.01E-05	0.13	0.0636	1.62	1.0656	2.20	0.1215	1.50	0.68	729	34	737	12	739	10	-1.3
12SZ24@03	51	131	2.6	1.94E-04	0.36	0.0654	2.14	1.1489	2.62	0.1273	1.50	0.57	788	44	777	14	773	11	2.0
12SZ24@04	284	264	0.9	3.49E-05	0.07	0.0679	0.88	1.3094	1.74	0.1398	1.50	0.86	867	18	850	10	843	12	2.7
12SZ24@05	868	1819	2.1	1.18E-03	2.20	0.0639	4.74	1.0515	4.98	0.1193	1.52	0.31	738	97	730	26	727	10	1.6

12SZ24@06	168	118	0.7	1.27E-04	0.24	0.0652	1.89	1.1422	2.42	0.1271	1.51	0.62	781	39	774	13	771	11	1.2
12SZ24@07	448	805	1.8	2.04E-04	0.38	0.0650	1.07	1.1689	1.85	0.1305	1.50	0.81	773	22	786	10	791	11	-2.2
12SZ24@08	141	161	1.1	1.72E-04	0.32	0.0643	1.35	1.1177	2.02	0.1260	1.50	0.74	752	28	762	11	765	11	-1.8
12SZ24@09	59	37	0.6	1.14E-04	0.21	0.0619	2.00	1.0854	2.50	0.1272	1.51	0.60	670	42	746	13	772	11	-15.3
12SZ24@10	130	198	1.5	4.47E-05	0.08	0.0638	1.84	1.0599	2.38	0.1204	1.50	0.63	736	39	734	12	733	10	0.4
12SZ24@11	157	210	1.3	0	0	0.0647	1.25	1.0631	1.96	0.1192	1.51	0.77	764	26	735	10	726	10	4.9
12SZ24@12	162	635	3.9	3.39E-05	0.06	0.0639	1.27	1.0768	1.98	0.1221	1.53	0.77	740	27	742	11	743	11	-0.4
12SZ24@13	65	101	1.6	4.81E-05	0.09	0.0639	1.98	1.0878	2.49	0.1235	1.50	0.60	738	41	747	13	751	11	-1.7
12SZ24@14	186	226	1.2	4.37E-05	0.08	0.0645	1.18	1.1440	1.92	0.1286	1.51	0.79	758	25	774	10	780	11	-2.9

12SZ28 (sandstone, 31°30'55.29''N, 113°35'44.97''E)

12SZ28@01	187	134	0.7	4.10E-05	0.08	0.0644	1.56	1.1084	2.16	0.1248	1.50	0.69	756	33	757	12	758	11	-0.2
12SZ28@02	85	59	0.7	0	0	0.0658	2.23	1.1002	2.69	0.1212	1.51	0.56	800	46	753	14	738	11	7.8
12SZ28@03	139	157	1.1	5.43E-05	0.10	0.0662	1.86	1.1614	2.42	0.1272	1.55	0.64	814	38	783	13	772	11	5.2
12SZ28@04	267	403	1.5	1.95E-05	0.04	0.0642	1.28	1.0846	1.97	0.1224	1.50	0.76	750	27	746	10	745	11	0.7
12SZ28@05	203	414	2.0	0	0	0.0643	1.98	1.0810	2.48	0.1220	1.50	0.60	751	41	744	13	742	11	1.2
12SZ28@06	163	248	1.5	5.32E-04	0.99	0.0642	2.61	1.1051	3.03	0.1248	1.54	0.51	749	54	756	16	758	11	-1.3
12SZ28@07	507	312	0.6	1.57E-05	0.03	0.0647	0.96	1.0742	1.78	0.1205	1.51	0.84	763	20	741	9	733	10	3.9
12SZ28@08	146	125	0.9	0	0	0.1125	0.81	5.1278	1.71	0.3306	1.50	0.88	1840	15	1841	15	1841	24	0.0
12SZ28@09	190	495	2.6	0	0	0.0638	1.51	1.0783	2.13	0.1225	1.50	0.70	736	32	743	11	745	11	-1.2
12SZ28@10	232	194	0.8	3.36E-05	0.06	0.0641	1.44	1.0614	2.08	0.1202	1.50	0.72	744	30	735	11	732	10	1.6
12SZ28@11	190	227	1.2	9.59E-05	0.18	0.0611	1.88	1.0114	2.41	0.1200	1.50	0.62	644	40	710	12	730	10	-13.4
12SZ28@13	169	370	2.2	4.62E-05	0.09	0.0646	1.72	1.0718	2.31	0.1203	1.55	0.67	763	36	740	12	732	11	4.0
12SZ28@14	92	95	1.0	1.81E-04	0.34	0.0638	2.98	1.0941	3.45	0.1244	1.73	0.50	735	62	750	18	756	12	-2.8
12SZ28@15	74	57	0.8	1.37E-04	0.26	0.0653	2.89	1.1154	3.25	0.1239	1.50	0.46	784	60	761	18	753	11	3.9
12SZ28@16	151	147	1.0	3.26E-05	0.06	0.0668	1.79	1.1213	2.34	0.1217	1.50	0.64	833	37	764	13	740	10	11.1
12SZ28@17	136	155	1.1	5.35E-05	0.10	0.0646	1.87	1.0939	2.40	0.1227	1.50	0.63	763	39	750	13	746	11	2.2

12SZ28@18	139	122	0.9	1.10E-04	0.21	0.0632	1.77	1.0303	2.33	0.1183	1.51	0.65	714	37	719	12	721	10	-0.9
12SZ28@19	135	182	1.3	3.71E-05	0.07	0.0634	1.78	1.1033	2.33	0.1262	1.50	0.64	721	37	755	12	766	11	-6.2
12SZ28@20	141	183	1.3	3.17E-05	0.06	0.0647	1.63	1.2112	2.23	0.1357	1.52	0.68	765	34	806	12	820	12	-7.2
Liulin Formation, middle part of Suixian Group																			
12SZ06 (sandstone, 31°31'45.39"N, 113°14'11.91"E)																			
12SZ06@01	154	155	1.0	3.48E-05	0.07	0.0642	1.47	1.1329	2.13	0.1279	1.55	0.73	749	31	769	12	776	11	-3.6
12SZ06@02	133	143	1.1	3.06E-05	0.06	0.0659	1.53	1.1920	2.14	0.1312	1.51	0.70	803	32	797	12	795	11	1.1
12SZ06@03	151	159	1.0	0	0	0.0679	1.37	1.1922	2.03	0.1273	1.50	0.74	866	28	797	11	772	11	10.9
12SZ06@04	68	38	0.6	7.72E-05	0.14	0.0680	2.17	1.2021	2.64	0.1283	1.50	0.57	868	44	802	15	778	11	10.3
12SZ06@05	287	134	0.5	0	0	0.0677	0.98	1.2419	1.81	0.1330	1.52	0.84	860	20	820	10	805	12	6.4
12SZ06@06	95	64	0.7	0	0	0.0699	1.55	1.4949	2.22	0.1550	1.59	0.72	926	31	928	14	929	14	-0.3
12SZ06@07	252	108	0.4	1.37E-05	0.03	0.0661	1.06	1.1913	1.84	0.1307	1.50	0.82	810	22	797	10	792	11	2.2
12SZ06@08	131	62	0.5	0	0	0.0671	1.49	1.1613	2.12	0.1255	1.51	0.71	842	31	783	12	762	11	9.5
12SZ06@09	97	52	0.5	0	0	0.0656	1.74	1.1215	2.30	0.1240	1.51	0.65	793	36	764	12	754	11	5.0
12SZ06@10	102	87	0.8	6.69E-05	0.13	0.0656	1.91	1.1690	2.48	0.1292	1.59	0.64	794	39	786	14	783	12	1.4
12SZ06@11	148	113	0.8	4.42E-05	0.08	0.0666	1.43	1.2304	2.09	0.1339	1.52	0.73	827	30	815	12	810	12	2.0
12SZ06@12	186	180	1.0	0	0	0.0656	1.22	1.1914	1.94	0.1318	1.50	0.77	793	25	797	11	798	11	-0.6
12SZ06@13	549	279	0.5	8.95E-06	0.02	0.0661	0.96	1.2396	1.78	0.1360	1.50	0.84	809	20	819	10	822	12	-1.6
12SZ06@14	156	103	0.7	0	0	0.0658	1.32	1.2119	2.00	0.1336	1.51	0.75	800	27	806	11	808	11	-1.1
12SZ06@15	200	176	0.9	1.67E-05	0.03	0.0640	1.39	1.1694	2.04	0.1324	1.50	0.73	743	29	786	11	802	11	-7.9
12SZ06@16	205	135	0.7	3.25E-05	0.06	0.0661	1.21	1.2038	1.93	0.1320	1.50	0.78	810	25	802	11	799	11	1.4
12SZ06@17	437	453	1.0	1.46E-05	0.03	0.0659	0.80	1.2459	1.70	0.1370	1.50	0.88	805	17	822	10	828	12	-2.9
12SZ06@18	77	58	0.8	1.58E-05	0.03	0.1232	0.87	6.0740	1.73	0.3575	1.50	0.87	2003	15	1987	15	1970	26	1.7
12SZ06@19	103	75	0.7	0	0	0.0645	1.68	1.1163	2.26	0.1254	1.50	0.67	759	35	761	12	762	11	-0.3
12SZ06@20	192	197	1.0	2.50E-05	0.05	0.0670	1.20	1.2584	1.93	0.1362	1.50	0.78	838	25	827	11	823	12	1.7
12SZ06@21	144	172	1.2	0	0	0.0652	1.50	1.1886	2.12	0.1321	1.50	0.71	782	31	795	12	800	11	-2.3
12SZ06@22	53	31	0.6	0	0	0.0675	2.24	1.2051	2.70	0.1296	1.51	0.56	852	46	803	15	785	11	7.8

12SZ06@23	143	206	1.4	2.41E-05	0.05	0.0656	1.45	1.1399	2.09	0.1260	1.50	0.72	793	30	772	11	765	11	3.5
12SZ06@24	189	209	1.1	4.76E-05	0.09	0.0637	1.36	1.0705	2.06	0.1219	1.55	0.75	731	28	739	11	742	11	-1.4
12SZ06@25	662	197	0.3	1.11E-05	0.02	0.0651	1.16	1.2607	2.10	0.1404	1.76	0.83	778	24	828	12	847	14	-8.9
12SZ06@26	248	241	1.0	1.54E-05	0.03	0.0667	1.06	1.2139	1.85	0.1319	1.52	0.82	829	22	807	10	799	11	3.7
12SZ06@27	752	488	0.6	1.46E-05	0.03	0.0663	0.60	1.2606	1.62	0.1378	1.51	0.93	817	12	828	9	832	12	-1.9
12SZ06@28	32	18	0.6	1.06E-04	0.20	0.0671	3.61	1.1694	3.93	0.1264	1.54	0.39	841	73	786	22	767	11	8.7
12SZ07(sandstone, 31°34’26.46’’N, 113°21’38.28’’E)																			
12SZ07@01	174	121	0.7	4.33E-05	0.08	0.0689	1.75	1.3525	2.31	0.1425	1.51	0.65	894	36	869	14	859	12	4.0
12SZ07@02	206	180	0.9	2.51E-05	0.05	0.0646	1.63	1.1827	2.21	0.1327	1.50	0.68	762	34	793	12	803	11	-5.4
12SZ07@03	378	143	0.4	0	0	0.0654	0.89	1.1321	1.75	0.1255	1.51	0.86	788	19	769	9	762	11	3.3
12SZ07@04	59	61	1.0	0	0	0.1221	1.12	6.1520	1.88	0.3653	1.51	0.80	1988	20	1998	17	2007	26	-1.0
12SZ07@05	85	52	0.6	6.13E-05	0.11	0.0650	1.99	1.1738	2.50	0.1309	1.50	0.60	775	41	788	14	793	11	-2.3
12SZ07@06	80	85	1.1	0	0	0.1237	1.20	6.0200	1.92	0.3529	1.51	0.78	2011	21	1979	17	1948	25	3.1
12SZ07@07	201	170	0.8	1.68E-05	0.03	0.0678	1.16	1.2631	1.90	0.1352	1.51	0.79	862	24	829	11	817	12	5.2
12SZ07@08	92	95	1.0	4.75E-05	0.09	0.1243	0.90	6.1997	1.76	0.3616	1.51	0.86	2019	16	2004	15	1990	26	1.5
12SZ07@09	153	280	1.8	3.64E-05	0.07	0.0650	1.49	1.0923	2.13	0.1219	1.52	0.71	773	31	750	11	742	11	4.1
12SZ07@10	677	1167	1.7	0	0	0.0665	1.01	1.2306	1.81	0.1342	1.50	0.83	823	21	815	10	812	11	1.4
12SZ07@11	353	250	0.7	1.46E-05	0.03	0.0660	0.91	1.2037	1.76	0.1323	1.50	0.85	806	19	802	10	801	11	0.6
12SZ07@12	114	131	1.1	3.52E-05	0.07	0.0648	1.78	1.1583	2.33	0.1297	1.51	0.65	768	37	781	13	786	11	-2.4
12SZ07@13	212	203	1.0	2.96E-04	0.55	0.0652	1.68	1.1072	2.26	0.1232	1.52	0.67	781	35	757	12	749	11	4.1
12SZ07@14	159	228	1.4	2.29E-05	0.04	0.0650	1.37	1.1393	2.03	0.1271	1.50	0.74	775	29	772	11	771	11	0.5
12SZ07@15	176	132	0.8	0	0	0.0656	1.42	1.1910	2.06	0.1317	1.50	0.73	793	29	796	11	798	11	-0.6
12SZ07@16	252	241	1.0	0	0	0.0659	1.07	1.2034	1.84	0.1325	1.50	0.82	802	22	802	10	802	11	0.0
12SZ07@17	594	670	1.1	1.01E-05	0.02	0.0622	1.07	0.9969	1.85	0.1162	1.50	0.81	682	23	702	9	709	10	-4.0
12SZ07@18	60	104	1.7	1.82E-04	0.34	0.0624	3.18	1.0496	3.55	0.1219	1.57	0.44	689	66	729	19	742	11	-7.6
12SZ07@19	615	859	1.4	8.59E-06	0.02	0.0658	0.89	1.1955	1.75	0.1317	1.51	0.86	801	19	799	10	798	11	0.4

12SZ07@20	362	419	1.2	1.75E-05	0.03	0.0680	0.86	1.3582	1.73	0.1449	1.50	0.87	868	18	871	10	872	12	-0.6
12SZ07@21	37	26	0.7	8.35E-05	0.16	0.1028	1.63	4.2431	2.33	0.2994	1.66	0.71	1675	30	1682	19	1688	25	-0.8
12SZ07@22	138	171	1.2	0	0	0.0651	1.50	1.1691	2.12	0.1303	1.50	0.71	777	31	786	12	789	11	-1.6
12SZ07@23	93	104	1.1	0	0	0.1244	0.92	6.1489	1.79	0.3586	1.53	0.86	2020	16	1997	16	1975	26	2.2
12SZ07@24	168	199	1.2	2.09E-05	0.04	0.0643	1.33	1.1764	2.00	0.1327	1.50	0.75	751	28	790	11	804	11	-7.0
12SZ07@25	371	531	1.4	2.44E-05	0.05	0.0641	0.94	1.1328	1.77	0.1281	1.50	0.85	746	20	769	10	777	11	-4.1
12SZ07@26	205	153	0.7	0	0	0.0663	1.20	1.1753	1.93	0.1286	1.51	0.78	815	25	789	11	780	11	4.3
12SZ07@27	44	33	0.7	5.78E-05	0.11	0.1215	1.69	6.0634	2.29	0.3619	1.55	0.68	1979	30	1985	20	1991	27	-0.6
12SZ07@28	45	50	1.1	0	0	0.1219	1.16	6.0729	1.91	0.3613	1.51	0.79	1984	21	1986	17	1988	26	-0.2
12SZ07@29	86	78	0.9	0	0	0.0644	2.02	1.1514	2.51	0.1296	1.50	0.60	756	42	778	14	786	11	-4.0
12SZ07@30	110	212	1.9	3.25E-05	0.06	0.0647	2.41	1.1483	2.85	0.1288	1.51	0.53	763	50	776	16	781	11	-2.4
12SZ07@31	111	220	2.0	3.24E-05	0.06	0.0673	1.62	1.2004	2.22	0.1293	1.53	0.69	847	33	801	12	784	11	7.5
12SZ07@32	63	44	0.7	0	0	0.1214	1.06	6.0925	1.84	0.3639	1.51	0.82	1977	19	1989	16	2001	26	-1.2
12SZ07@33	137	161	1.2	0	0	0.0640	1.48	1.1437	2.11	0.1296	1.51	0.71	742	31	774	12	785	11	-5.8
12SZ07@34	231	326	1.4	3.05E-05	0.06	0.0653	1.17	1.1849	1.91	0.1316	1.50	0.79	783	24	794	11	797	11	-1.8
12SZ07@35	41	31	0.8	4.94E-05	0.09	0.1248	1.28	6.0469	2.02	0.3515	1.57	0.78	2025	22	1983	18	1942	26	4.1
12SZ07@36	139	161	1.2	8.66E-05	0.16	0.0687	1.56	1.3790	2.17	0.1455	1.51	0.69	891	32	880	13	876	12	1.7
12SZ07@37	219	299	1.4	3.57E-05	0.07	0.0645	1.29	1.1179	1.98	0.1257	1.51	0.76	758	27	762	11	763	11	-0.6
12SZ07@38	127	125	1.0	0	0	0.0665	1.54	1.2208	2.15	0.1331	1.50	0.70	823	32	810	12	805	11	2.2
12SZ07@39	372	255	0.7	1.55E-05	0.03	0.0645	0.95	1.1419	1.78	0.1284	1.50	0.84	758	20	773	10	779	11	-2.8
12SZ07@40	201	181	0.9	1.82E-05	0.03	0.0659	1.81	1.2165	2.35	0.1340	1.50	0.64	802	38	808	13	811	11	-1.1
12SZ07@41	217	138	0.6	4.19E-06	0.01	0.1896	0.59	13.9295	1.61	0.5328	1.50	0.93	2739	10	2745	15	2753	34	-0.5
12SZ07@42	190	141	0.7	3.93E-05	0.07	0.0659	2.35	1.1995	2.79	0.1319	1.51	0.54	804	48	800	16	799	11	0.7
12SZ07@43	212	135	0.6	9.76E-06	0.02	0.1648	0.43	10.4834	1.57	0.4613	1.51	0.96	2506	7	2478	15	2445	31	2.4
12SZ07@44	1919	1486	0.8	2.37E-04	0.44	0.0639	0.63	1.1040	1.63	0.1252	1.50	0.92	739	13	755	9	761	11	-2.9
12SZ07@45	356	189	0.5	4.55E-05	0.09	0.0656	1.38	1.2194	2.04	0.1349	1.50	0.74	792	29	810	11	816	12	-2.9
12SZ07@46	77	45	0.6	0	0	0.1247	0.90	6.2073	1.75	0.3610	1.50	0.86	2025	16	2005	15	1987	26	1.9

12SZ07@47	70	77	1.1	1.04E-04	0.19	0.0617	2.46	1.1104	2.88	0.1306	1.50	0.52	662	52	758	16	791	11	-19.5
13SZ14 (sandstone, 31°34'59.08"N, 113°21'52.34"E)																			
13SZ14@01	303	172	0.6	3.89E-05	0.07	0.0658	1.13	1.2509	1.89	0.1380	1.51	0.80	799	24	824	11	833	12	-4.3
13SZ14@02	459	52	0.1	1.56E-05	0.03	0.0731	0.95	1.7781	1.77	0.1763	1.50	0.85	1018	19	1037	12	1047	15	-2.9
13SZ14@03	187	162	0.9	4.90E-05	0.09	0.0661	1.53	1.2394	2.18	0.1361	1.55	0.71	808	32	819	12	822	12	-1.8
13SZ14@04	312	244	0.8	1.60E-05	0.03	0.0638	1.20	1.1293	1.97	0.1283	1.56	0.79	736	25	767	11	778	11	-5.8
13SZ14@05	240	392	1.6	3.80E-05	0.07	0.0661	1.56	1.1230	2.18	0.1231	1.52	0.70	811	32	764	12	749	11	7.7
13SZ14@06	76	89	1.2	2.26E-04	0.42	0.0642	3.71	1.1363	4.01	0.1283	1.52	0.38	749	76	771	22	778	11	-4.0
13SZ14@07	108	75	0.7	0	0	0.0673	2.03	1.2906	2.59	0.1391	1.60	0.62	847	42	842	15	839	13	0.9
13SZ14@08	109	80	0.7	1.58E-04	0.29	0.0655	2.11	1.2217	2.59	0.1352	1.50	0.58	791	44	811	15	818	12	-3.4
13SZ14@09	58	54	0.9	9.28E-05	0.17	0.0702	2.97	1.3002	3.33	0.1343	1.50	0.45	935	60	846	19	812	11	13.1
13SZ14@10	234	221	0.9	2.90E-05	0.05	0.0674	1.54	1.2784	2.29	0.1376	1.70	0.74	850	32	836	13	831	13	2.3
13SZ14@11	117	100	0.9	7.76E-05	0.15	0.0661	2.17	1.1683	2.68	0.1283	1.57	0.59	808	45	786	15	778	12	3.7
13SZ14@12	107	84	0.8	7.86E-05	0.15	0.0653	2.38	1.1781	2.82	0.1308	1.51	0.53	785	49	790	16	792	11	-0.9
13SZ14@13	90	66	0.7	9.35E-05	0.17	0.0668	3.49	1.2225	3.80	0.1328	1.50	0.40	831	71	811	21	804	11	3.2
13SZ14@14	193	120	0.6	2.97E-05	0.06	0.0628	1.61	1.0955	2.20	0.1266	1.50	0.68	700	34	751	12	768	11	-9.7
13SZ14@15	176	107	0.6	3.25E-05	0.06	0.0673	1.95	1.2061	2.48	0.1300	1.52	0.61	847	40	803	14	788	11	7.1
13SZ14@16	92	54	0.6	0	0	0.0692	2.11	1.3920	2.59	0.1459	1.50	0.58	904	43	886	15	878	12	2.8
13SZ14@17	98	47	0.5	8.55E-05	0.16	0.0653	3.97	1.2002	4.25	0.1334	1.50	0.35	783	81	801	24	807	11	-3.1
13SZ14@18	130	102	0.8	0	0	0.0663	2.26	1.1770	2.71	0.1287	1.50	0.55	817	47	790	15	780	11	4.5
13SZ14@19	65	52	0.8	4.11E-04	0.77	0.0607	4.68	1.0746	4.94	0.1284	1.59	0.32	629	98	741	26	779	12	-23.9
13SZ14@20	72	147	2.0	1.97E-04	0.37	0.0634	2.61	1.1648	3.01	0.1331	1.51	0.50	723	54	784	17	806	11	-11.4
13SZ14@21	67	82	1.2	1.76E-04	0.33	0.0646	3.43	1.1485	3.75	0.1290	1.50	0.40	760	71	777	21	782	11	-3.0
13SZ14@22	156	217	1.4	3.08E-05	0.06	0.0668	2.55	1.2217	3.10	0.1326	1.75	0.57	832	52	811	17	803	13	3.5
13SZ14@23	39	26	0.7	1.21E-04	0.23	0.0675	3.14	1.1895	3.49	0.1278	1.51	0.43	853	64	796	19	775	11	9.2
13SZ14@24	43	34	0.8	0	0	0.1247	1.71	6.1139	2.29	0.3555	1.51	0.66	2025	30	1992	20	1961	26	3.2

13SZ14@25	41	22	0.5	2.96E-05	0.06	0.1757	1.03	11.8214	1.85	0.4880	1.53	0.83	2613	17	2590	17	2562	32	1.9
13SZ14@26	30	44	1.5	0	0	0.0687	4.13	1.2080	4.43	0.1275	1.60	0.36	890	83	804	25	773	12	13.1
13SZ14@27	46	36	0.8	0	0	0.0684	2.75	1.1999	3.14	0.1272	1.50	0.48	881	56	801	18	772	11	12.4
13SZ14@28	89	81	0.9	4.94E-05	0.09	0.0643	2.23	1.1106	2.68	0.1252	1.50	0.56	752	46	758	14	761	11	-1.2
13SZ14@29	55	60	1.1	0	0	0.0645	2.61	1.0929	3.06	0.1229	1.60	0.52	758	54	750	16	747	11	1.4
13SZ14@30	68	41	0.6	4.48E-05	0.08	0.0727	1.85	1.7572	2.38	0.1754	1.50	0.63	1004	37	1030	16	1042	14	-3.7
13SZ19 (sandstone, 31°35'19.81"N,113°12'2.19"E)																			
13SZ19@01	97	76	0.8	1.45E-04	0.27	0.0629	2.45	1.0590	2.88	0.1221	1.50	0.52	706	51	733	15	742	11	-5.2
13SZ19@02	126	99	0.8	1.86E-05	0.03	0.1226	0.78	5.9494	1.71	0.3519	1.52	0.89	1995	14	1968	15	1944	26	2.6
13SZ19@03	48	52	1.1	7.95E-05	0.15	0.1223	1.40	6.0561	2.05	0.3590	1.50	0.73	1991	25	1984	18	1977	26	0.7
13SZ19@04	68	56	0.8	0	0	0.0650	2.90	1.1690	3.29	0.1304	1.56	0.48	774	60	786	18	790	12	-2.1
13SZ19@05	137	138	1.0	6.26E-05	0.12	0.0637	1.78	1.0888	2.35	0.1239	1.53	0.65	733	37	748	13	753	11	-2.8
13SZ19@06	229	143	0.6	1.94E-04	0.36	0.0657	1.31	1.1333	2.03	0.1252	1.54	0.76	795	27	769	11	760	11	4.4
13SZ19@07	55	69	1.2	3.27E-05	0.06	0.1052	1.48	4.3123	2.15	0.2972	1.56	0.72	1719	27	1696	18	1677	23	2.4
13SZ19@08	213	137	0.6	3.78E-05	0.07	0.0664	1.33	1.2462	2.01	0.1361	1.51	0.75	819	28	822	11	823	12	-0.4
13SZ19@09	194	107	0.6	3.06E-05	0.06	0.0673	1.35	1.1923	2.05	0.1286	1.54	0.75	846	28	797	11	780	11	7.9
13SZ19@10	154	201	1.3	5.08E-05	0.09	0.0653	1.57	1.1918	2.17	0.1324	1.50	0.69	783	33	797	12	802	11	-2.4
13SZ19@11	57	77	1.3	7.10E-05	0.13	0.0624	2.47	1.0670	2.91	0.1241	1.54	0.53	687	52	737	15	754	11	-9.8
13SZ19@12	89	74	0.8	4.30E-05	0.08	0.0695	2.20	1.2910	2.67	0.1347	1.51	0.57	914	45	842	15	815	12	10.8
13SZ19@13	102	103	1.0	3.95E-05	0.07	0.0652	1.81	1.1719	2.35	0.1304	1.51	0.64	780	38	788	13	790	11	-1.2
13SZ19@14	516	534	1.0	5.11E-04	0.96	0.0641	1.43	1.0487	2.09	0.1187	1.52	0.73	744	30	728	11	723	10	2.7
13SZ19@15	54	47	0.9	0	0	0.1244	1.40	6.0957	2.05	0.3554	1.50	0.73	2020	25	1990	18	1960	25	3.0
13SZ19@16	110	79	0.7	0	0	0.0661	1.83	1.1739	2.37	0.1288	1.50	0.63	810	38	788	13	781	11	3.5
13SZ19@17	34	29	0.9	5.32E-05	0.10	0.1265	1.78	6.2314	2.38	0.3573	1.58	0.66	2050	31	2009	21	1969	27	3.9
13SZ19@18	227	189	0.8	2.04E-05	0.04	0.0643	1.32	1.1018	2.01	0.1244	1.52	0.76	750	28	754	11	756	11	-0.7
13SZ19@19	43	36	0.8	1.52E-04	0.29	0.1202	1.51	5.9461	2.13	0.3587	1.50	0.70	1960	27	1968	19	1976	26	-0.8

13SZ19@20	222	92	0.4	1.06E-04	0.20	0.0646	1.27	1.2048	2.03	0.1353	1.58	0.78	761	27	803	11	818	12	-7.5
13SZ19@21	60	27	0.4	1.52E-04	0.29	0.0632	2.55	1.0987	2.96	0.1262	1.52	0.51	714	53	753	16	766	11	-7.3
13SZ19@22	267	211	0.8	1.57E-05	0.03	0.0668	1.32	1.2678	2.03	0.1377	1.54	0.76	831	27	831	12	831	12	0.0
13SZ19@23	168	97	0.6	2.61E-05	0.05	0.1670	0.80	10.9714	1.71	0.4766	1.51	0.88	2527	13	2521	16	2512	31	0.6
13SZ19@24	79	81	1.0	1.13E-04	0.21	0.0660	2.47	1.1733	2.90	0.1290	1.51	0.52	805	51	788	16	782	11	2.8
13SZ19@25	69	59	0.9	1.68E-04	0.31	0.0642	2.67	1.1739	3.06	0.1326	1.50	0.49	749	55	788	17	803	11	-7.2
13SZ19@26	107	89	0.8	1.54E-04	0.29	0.0638	2.77	1.1923	3.15	0.1356	1.50	0.48	735	57	797	18	819	12	-11.5
13SZ19@27	35	21	0.6	2.12E-04	0.40	0.0598	5.06	1.0344	5.28	0.1255	1.52	0.29	596	106	721	28	762	11	-28.0
13SZ19@28	107	109	1.0	0	0	0.0656	1.90	1.1979	2.57	0.1324	1.73	0.67	794	39	800	14	802	13	-1.0
13SZ19@29	240	184	0.8	3.86E-05	0.07	0.0652	1.28	1.2498	1.97	0.1389	1.50	0.76	782	27	823	11	839	12	-7.2
13SZ19@30	33	7	0.2	2.47E-05	0.05	0.1559	2.29	9.7319	2.74	0.4528	1.50	0.55	2412	38	2410	26	2408	30	0.2
13SZ19@31	78	64	0.8	1.56E-04	0.29	0.0637	2.91	1.1568	3.31	0.1317	1.57	0.47	731	61	780	18	798	12	-9.1
13SZ19@32	116	91	0.8	0	0	0.0671	1.79	1.2810	2.34	0.1384	1.50	0.64	842	37	837	13	836	12	0.7
13SZ19@33	78	42	0.5	0	0	0.0642	2.37	1.1207	2.81	0.1266	1.50	0.54	748	49	763	15	769	11	-2.8
13SZ19@34	83	64	0.8	1.18E-04	0.22	0.0656	2.74	1.1973	3.13	0.1324	1.51	0.48	793	56	799	17	802	11	-1.0
13SZ19@35	86	65	0.8	0	0	0.0636	2.20	1.1893	2.78	0.1357	1.70	0.61	727	46	796	15	820	13	-12.9
13SZ19@36	60	52	0.9	1.28E-04	0.24	0.0629	3.20	1.1513	3.54	0.1328	1.52	0.43	704	67	778	19	804	12	-14.3
13SZ19@37	26	26	1.0	7.27E-05	0.14	0.1238	3.07	6.3265	3.47	0.3708	1.62	0.47	2011	54	2022	31	2033	28	-1.1
13SZ19@38	72	130	1.8	1.06E-04	0.20	0.0651	3.74	1.2072	4.04	0.1345	1.54	0.38	777	77	804	23	814	12	-4.8
13SZ19@39	152	185	1.2	5.55E-05	0.10	0.0649	1.91	1.1265	2.43	0.1258	1.50	0.62	772	40	766	13	764	11	1.1
12SZ14 (metaryolite, 31°49’10.09”N, 113°22’22.17”E)																		
12SZ14@01	70	51	0.7	0	0	0.0631	1.72	1.0470	2.28	0.1204	1.50	0.66	711	36	727	12	733	10	-3.1
12SZ14@02	132	138	1.0	2.78E-05	0.05	0.0638	2.06	1.0511	2.55	0.1194	1.50	0.59	736	43	729	13	727	10	1.1
12SZ14@03	55	92	1.7	2.59E-05	0.05	0.0648	1.93	1.0714	2.46	0.1199	1.54	0.62	768	40	739	13	730	11	4.9
12SZ14@04	140	191	1.4	2.50E-05	0.05	0.0640	1.73	1.0821	2.29	0.1227	1.50	0.66	741	36	745	12	746	11	-0.7
12SZ14@05	112	97	0.9	3.18E-05	0.06	0.0634	1.43	1.0624	2.08	0.1215	1.51	0.72	721	30	735	11	739	11	-2.5

12SZ14@06	71	123	1.7	3.44E-04	0.64	0.0651	1.76	1.0871	2.31	0.1211	1.50	0.65	779	37	747	12	737	10	5.4
12SZ14@07	73	46	0.6	0	0	0.0651	1.64	1.0829	2.24	0.1207	1.52	0.68	777	34	745	12	734	11	5.5
12SZ14@08	137	154	1.1	1.01E-05	0.02	0.0628	1.22	1.0550	1.94	0.1218	1.50	0.77	701	26	731	10	741	11	-5.7
12SZ14@09	108	124	1.2	5.33E-05	0.10	0.0644	1.62	1.1105	2.21	0.1251	1.50	0.68	755	34	758	12	760	11	-0.6
12SZ14@10	205	224	1.1	2.81E-05	0.05	0.0631	1.53	1.0842	2.14	0.1246	1.51	0.70	711	32	746	11	757	11	-6.4
12SZ14@11	31	46	1.5	2.13E-04	0.40	0.0636	2.46	1.1118	2.88	0.1268	1.50	0.52	728	51	759	16	770	11	-5.7
12SZ14@12	90	152	1.7	7.58E-05	0.14	0.0641	1.46	1.1221	2.09	0.1269	1.50	0.72	746	31	764	11	770	11	-3.2
12SZ14@13	136	279	2.0	4.19E-05	0.08	0.0642	1.19	1.0985	1.92	0.1241	1.50	0.78	749	25	753	10	754	11	-0.7
12SZ14@14	68	57	0.8	8.64E-05	0.16	0.0637	1.71	1.0553	2.28	0.1201	1.50	0.66	733	36	732	12	731	10	0.2
12SZ14@15	66	79	1.2	7.24E-05	0.14	0.0638	2.15	1.0331	2.62	0.1174	1.50	0.57	736	45	720	14	716	10	2.8
12SZ14@16	50	83	1.7	9.33E-05	0.17	0.0627	2.00	1.0561	2.50	0.1222	1.50	0.60	698	42	732	13	743	11	-6.4
12SZ14@17	107	157	1.5	2.21E-05	0.04	0.0640	1.42	1.0705	2.08	0.1214	1.51	0.73	741	30	739	11	738	11	0.3
12SZ14@18	91	93	1.0	1.60E-04	0.30	0.0658	1.42	1.1331	2.07	0.1249	1.50	0.73	800	30	769	11	759	11	5.1
12SZ14@19	80	162	2.0	6.82E-05	0.13	0.0633	1.53	1.1133	2.15	0.1277	1.51	0.70	717	32	760	12	774	11	-8.1
12SZ14@20	111	197	1.8	2.12E-05	0.04	0.0646	1.32	1.0831	2.00	0.1216	1.50	0.75	761	28	745	11	740	11	2.9
12SZ14@21	144	58	0.4	1.74E-05	0.03	0.0725	0.93	1.7090	1.79	0.1710	1.52	0.85	999	19	1012	12	1018	14	-1.9
12SZ14@22	131	127	1.0	2.65E-05	0.05	0.0642	1.27	1.0761	1.96	0.1216	1.50	0.76	747	27	742	10	740	11	0.9
12SZ14@23	113	86	0.8	2.09E-05	0.04	0.0629	1.46	1.0485	2.09	0.1209	1.50	0.72	705	31	728	11	736	10	-4.3
12SZ14@25	178	245	1.4	5.32E-05	0.10	0.0635	1.31	1.0682	1.99	0.1220	1.50	0.75	725	28	738	11	742	11	-2.3
12SZ17(tuffaceous siltstone, 31°39'45.83''N, 113°34'43.75''E)																		
12SZ17@01	364	244	0.7	9.28E-06	0.02	0.0635	0.89	1.0659	1.75	0.1217	1.50	0.86	726	19	737	9	740	11	-2.0
12SZ17@02	283	183	0.6	1.86E-05	0.03	0.0628	1.07	1.0266	1.85	0.1185	1.51	0.82	703	23	717	10	722	10	-2.6
12SZ17@03	232	122	0.5	2.26E-05	0.04	0.0632	1.31	1.0424	1.99	0.1196	1.50	0.75	716	28	725	10	728	10	-1.7
12SZ17@04	670	757	1.1	3.45E-05	0.06	0.0632	0.71	1.0287	1.66	0.1181	1.50	0.90	714	15	718	9	720	10	-0.9
12SZ17@05	315	193	0.6	3.39E-05	0.06	0.0653	1.02	1.0558	1.82	0.1172	1.51	0.83	785	21	732	10	715	10	9.0
12SZ17@06	303	188	0.6	1.13E-05	0.02	0.0630	0.99	1.0585	1.81	0.1218	1.51	0.84	710	21	733	9	741	11	-4.4

12SZ17@07	257	119	0.5	2.78E-05	0.05	0.0627	1.15	1.0211	1.89	0.1181	1.50	0.79	699	24	714	10	719	10	-3.0
12SZ17@08	201	122	0.6	5.06E-05	0.09	0.0633	1.29	1.0417	1.98	0.1194	1.50	0.76	717	27	725	10	727	10	-1.5
12SZ17@09	271	130	0.5	1.31E-05	0.02	0.0633	1.13	1.0396	1.89	0.1191	1.51	0.80	719	24	724	10	725	10	-0.8
12SZ17@10	400	237	0.6	1.71E-05	0.03	0.0631	0.88	1.0482	1.74	0.1204	1.50	0.86	713	19	728	9	733	10	-2.8
12SZ17@11	314	173	0.6	2.80E-05	0.05	0.0628	1.12	1.0032	1.87	0.1158	1.50	0.80	702	24	705	10	706	10	-0.6
12SZ17@12	402	303	0.8	8.55E-06	0.02	0.0633	0.85	1.0447	1.73	0.1196	1.50	0.87	719	18	726	9	729	10	-1.3
12SZ17@13	492	375	0.8	3.89E-05	0.07	0.0649	0.83	1.0596	1.71	0.1185	1.50	0.87	769	17	734	9	722	10	6.2
12SZ17@14	308	139	0.5	1.13E-05	0.02	0.0641	0.98	1.0477	1.79	0.1186	1.50	0.84	745	21	728	9	722	10	3.0
12SZ17@15	386	277	0.7	8.71E-06	0.02	0.0637	0.86	1.0685	1.73	0.1216	1.50	0.87	733	18	738	9	740	11	-1.0
12SZ17@16	161	78	0.5	0	0	0.0653	1.31	1.1076	2.00	0.1230	1.51	0.76	785	27	757	11	748	11	4.7
12SZ17@17	163	52	0.3	5.09E-05	0.10	0.0618	1.44	1.0200	2.08	0.1198	1.50	0.72	666	31	714	11	729	10	-9.6
12SZ17@19	291	145	0.5	0	0	0.0630	0.98	1.0565	1.80	0.1216	1.51	0.84	709	21	732	9	740	11	-4.4
12SZ17@20	84	27	0.3	0.00E+00	0.00	0.0634	2.48	1.0528	2.90	0.1204	1.50	0.52	723	52	730	15	733	10	-1.4
12SZ17@21	398	310	0.8	4.18E-05	0.08	0.0633	0.90	1.0596	1.76	0.1214	1.50	0.86	718	19	734	9	739	11	-2.9
12SZ17@22	129	67	0.5	0	0	0.0644	2.13	1.0510	2.60	0.1183	1.50	0.58	756	44	729	14	721	10	4.7
12SZ17@23	187	73	0.4	1.80E-05	0.03	0.0649	1.23	1.0551	1.94	0.1180	1.50	0.77	770	26	731	10	719	10	6.6
12SZ17@24	176	78	0.4	5.72E-05	0.11	0.0643	1.43	1.0521	2.07	0.1186	1.50	0.72	753	30	730	11	722	10	4.1
12SZ17@25	133	56	0.4	2.08E-04	0.39	0.0625	1.95	0.9904	2.48	0.1150	1.52	0.61	690	41	699	13	702	10	-1.7
12SZ17@26	245	146	0.6	0	0	0.0641	1.07	1.0565	1.85	0.1196	1.50	0.81	743	23	732	10	728	10	2.0
12SZ17@27	145	56	0.4	4.54E-05	0.08	0.0624	1.51	1.0520	2.16	0.1222	1.54	0.71	690	32	730	11	743	11	-7.8
12SZ17@28	433	165	0.4	6.72E-06	0.01	0.0668	0.74	1.2668	1.68	0.1376	1.51	0.90	831	15	831	10	831	12	0.0
Yuanziwan Formation, upper part of Suixian Group																			
12SZ10 (siltstone, 31°39'17.21''N, 113°21'44.9''E)																			
12SZ10@01	90	126	1.4	7.71E-05	0.14	0.0652	1.99	1.1137	2.49	0.1238	1.50	0.60	782	41	760	13	752	11	3.8
12SZ10@02	139	186	1.3	1.64E-04	0.31	0.0604	2.10	1.0225	2.62	0.1228	1.57	0.60	617	45	715	14	747	11	-21.0
12SZ10@03	137	189	1.4	2.52E-05	0.05	0.0643	1.74	1.1139	2.30	0.1256	1.50	0.65	753	36	760	12	763	11	-1.3
12SZ10@04	100	115	1.1	0	0	0.0627	1.77	1.0373	2.33	0.1200	1.52	0.65	698	37	723	12	730	10	-4.6

12SZ10@05	392	600	1.5	4.18E-05	0.08	0.0646	1.21	1.0787	1.94	0.1211	1.52	0.78	762	25	743	10	737	11	3.3
12SZ10@06	207	207	1.0	3.62E-04	0.68	0.0621	4.56	1.0590	4.80	0.1238	1.50	0.31	676	95	733	25	752	11	-11.3
12SZ10@07	80	140	1.7	1.09E-04	0.20	0.0626	2.25	1.0632	2.71	0.1232	1.50	0.55	695	47	735	14	749	11	-7.8
12SZ10@08	122	176	1.4	0	0	0.0640	1.62	1.0707	2.21	0.1214	1.50	0.68	741	34	739	12	738	10	0.4
12SZ10@09	273	313	1.1	1.29E-05	0.02	0.0642	1.04	1.0670	1.84	0.1205	1.52	0.83	749	22	737	10	734	11	2.0
12SZ10@10	228	199	0.9	5.74E-05	0.11	0.0648	1.32	1.0634	2.00	0.1190	1.50	0.75	768	28	735	11	725	10	5.5
12SZ10@11	175	104	0.6	3.05E-05	0.06	0.0637	1.64	1.0585	2.22	0.1204	1.50	0.68	733	34	733	12	733	10	0.0
12SZ10@12	185	152	0.8	1.25E-04	0.23	0.0645	1.50	1.0827	2.12	0.1217	1.50	0.71	759	31	745	11	740	11	2.5
12SZ10@13	168	327	2.0	5.11E-05	0.10	0.0636	1.87	1.1020	2.40	0.1257	1.50	0.63	728	39	754	13	763	11	-4.9
12SZ10@14	157	222	1.4	2.26E-05	0.04	0.0635	1.47	1.0592	2.10	0.1210	1.50	0.72	724	31	733	11	736	10	-1.7
12SZ10@15	115	189	1.6	7.90E-05	0.15	0.0626	2.14	1.0169	2.62	0.1178	1.51	0.58	694	45	712	13	718	10	-3.4
12SZ10@16	218	129	0.6	4.87E-05	0.09	0.0645	1.42	1.0694	2.07	0.1202	1.50	0.73	760	30	738	11	731	10	3.7
12SZ10@17	65	97	1.5	5.58E-05	0.10	0.0662	2.14	1.0792	2.62	0.1182	1.51	0.58	813	44	743	14	720	10	11.5
12SZ10@18	69	131	1.9	9.60E-05	0.18	0.0633	2.36	1.1001	2.80	0.1260	1.50	0.54	719	49	753	15	765	11	-6.5
12SZ10@20	79	93	1.2	6.61E-05	0.12	0.0619	2.14	1.0204	2.61	0.1195	1.50	0.57	672	45	714	13	728	10	-8.4
12SZ10@22	144	78	0.5	3.69E-05	0.07	0.0631	1.56	1.0706	2.17	0.1231	1.50	0.69	710	33	739	11	749	11	-5.4
12SZ10@23	253	104	0.4	3.47E-05	0.06	0.0644	1.47	1.0808	2.11	0.1217	1.51	0.72	756	31	744	11	740	11	2.0
12SZ10@24	62	112	1.8	5.74E-05	0.11	0.0648	2.19	1.0739	2.69	0.1202	1.57	0.58	769	45	741	14	731	11	4.8
12SZ10@25	149	463	3.1	2.23E-05	0.04	0.0642	1.38	1.1339	2.04	0.1281	1.51	0.74	748	29	770	11	777	11	-3.9
12SZ10@26	90	157	1.8	3.98E-05	0.07	0.0650	1.82	1.0782	2.36	0.1203	1.50	0.64	774	38	743	13	732	10	5.4
12SZ10@27	86	124	1.4	2.28E-05	0.04	0.0673	3.45	1.1563	3.77	0.1247	1.52	0.40	846	70	780	21	757	11	10.5
12SZ10@28	87	141	1.6	0	0	0.0641	2.04	1.0902	2.53	0.1234	1.50	0.59	745	43	749	14	750	11	-0.7
13SZ17 (sandstone, 31°39'45.17"N, 113°15'3.30"E)																			
13SZ17@01	626	1258	2.0	1.25E-04	0.23	0.0631	0.99	1.0522	1.80	0.1209	1.50	0.84	712	21	730	9	736	10	-3.3
13SZ17@02	65	118	1.8	1.31E-04	0.24	0.0640	2.36	1.0579	2.79	0.1200	1.50	0.54	740	49	733	15	730	10	1.3
13SZ17@03	72	92	1.3	1.16E-04	0.22	0.0639	2.26	1.0562	2.71	0.1199	1.50	0.55	738	47	732	14	730	10	1.1

13SZ17@04	63	94	1.5	6.68E-05	0.13	0.0642	2.59	1.0391	3.00	0.1174	1.52	0.51	749	54	723	16	715	10	4.4
13SZ17@05	66	75	1.1	3.18E-04	0.59	0.0645	2.92	1.0486	3.29	0.1179	1.51	0.46	759	60	728	17	718	10	5.4
13SZ17@06	97	123	1.3	1.08E-04	0.20	0.0672	2.17	1.0780	2.64	0.1164	1.51	0.57	843	44	743	14	710	10	15.7
13SZ17@07	56	88	1.6	1.12E-04	0.21	0.0639	2.90	1.0604	3.26	0.1204	1.50	0.46	737	60	734	17	733	10	0.6
13SZ17@08	82	172	2.1	5.18E-05	0.10	0.0673	2.20	1.0836	2.67	0.1167	1.51	0.57	848	45	745	14	712	10	16.1
13SZ17@09	67	37	0.6	3.62E-05	0.07	0.0657	2.38	1.0866	2.82	0.1199	1.50	0.53	798	49	747	15	730	10	8.6
13SZ17@10	71	145	2.0	2.34E-04	0.44	0.0616	3.02	1.0084	3.37	0.1188	1.51	0.45	659	63	708	17	724	10	-9.9
13SZ17@11	123	73	0.6	1.51E-04	0.28	0.0630	1.71	1.0572	2.27	0.1217	1.50	0.66	708	36	732	12	741	11	-4.6
13SZ17@12	121	210	1.7	3.45E-05	0.06	0.0654	2.00	1.0949	2.50	0.1215	1.50	0.60	786	41	751	13	739	10	6.0
13SZ17@13	42	80	1.9	0	0	0.0663	2.87	1.1091	3.25	0.1213	1.52	0.47	816	59	758	18	738	11	9.6
13SZ17@14	50	62	1.2	1.60E-04	0.30	0.0623	3.41	1.0215	3.72	0.1188	1.50	0.40	686	71	715	19	724	10	-5.5
13SZ17@15	69	89	1.3	1.18E-04	0.22	0.0642	3.42	1.0487	3.73	0.1184	1.51	0.40	749	71	728	20	722	10	3.6
13SZ17@16	164	262	1.6	4.56E-05	0.09	0.0651	1.48	1.1756	2.11	0.1309	1.50	0.71	779	31	789	12	793	11	-1.8
13SZ17@17	95	183	1.9	1.67E-04	0.31	0.0633	1.97	1.0585	2.48	0.1213	1.50	0.61	718	41	733	13	738	10	-2.7
13SZ17@18	80	134	1.7	1.03E-04	0.19	0.0629	2.87	1.0236	3.23	0.1179	1.50	0.46	706	60	716	17	719	10	-1.7
13SZ17@19	30	36	1.2	2.60E-04	0.49	0.0644	3.32	1.0668	3.65	0.1201	1.50	0.41	755	69	737	19	731	10	3.1
13SZ17@20	195	154	0.8	0	0	0.0640	1.33	1.1642	2.02	0.1320	1.53	0.75	741	28	784	11	799	11	-7.8
13SZ17@21	110	222	2.0	6.11E-05	0.11	0.0645	2.15	1.0912	2.63	0.1227	1.52	0.58	758	45	749	14	746	11	1.5
13SZ17@22	102	217	2.1	1.10E-04	0.21	0.0637	2.25	1.0547	2.70	0.1200	1.50	0.56	732	47	731	14	731	10	0.2
13SZ17@23	79	165	2.1	1.14E-04	0.21	0.0668	2.52	1.0989	2.93	0.1193	1.50	0.51	832	52	753	16	727	10	12.6
13SZ17@24	69	83	1.2	0	0	0.0663	2.31	1.1083	2.76	0.1212	1.51	0.55	816	47	757	15	738	11	9.6
13SZ17@25	77	142	1.8	1.47E-04	0.27	0.0634	2.73	1.0352	3.11	0.1183	1.50	0.48	723	57	722	16	721	10	0.3
13SZ17@26	95	189	2.0	4.33E-05	0.08	0.0639	2.32	1.0233	2.77	0.1162	1.50	0.54	737	48	716	14	709	10	3.9
Qinghu U-Pb working reference zircon																			
Qinghu@01	862	350	0.405	0.00008	0.16	0.0492	2.27	0.1614	2.82	0.0238	1.67	0.59	156	52	152	4	152	3	
Qinghu@02	1952	1151	0.590	0.00001	0.02	0.0492	1.05	0.1776	2.03	0.0262	1.73	0.86	159	24	166	3	167	3	
Qinghu@03	1176	556	0.473	0.00018	0.34	0.0493	1.92	0.1687	2.44	0.0248	1.50	0.62	164	44	158	4	158	2	

Qinghu@04	1794	1215	0.677	0.00001	0.02	0.0491	1.14	0.1741	1.88	0.0257	1.50	0.80	155	26	163	3	164	2
Qinghu@05	2213	1223	0.553	0.00001	0.02	0.0496	1.02	0.1709	1.82	0.0250	1.51	0.83	174	24	160	3	159	2
Qinghu@06	1728	756	0.437	0.00001	0.02	0.0491	1.16	0.1688	1.90	0.0249	1.50	0.79	151	27	158	3	159	2
Qinghu@07	2076	1194	0.575	0.00001	0.02	0.0495	1.00	0.1735	1.82	0.0254	1.51	0.83	173	23	162	3	162	2
Qinghu@08	2078	964	0.464	0.00001	0.02	0.0490	0.99	0.1690	1.80	0.0250	1.51	0.84	147	23	159	3	159	2
Qinghu@09	1757	797	0.453	0.00001	0.02	0.0499	1.07	0.1703	1.85	0.0248	1.51	0.82	188	25	160	3	158	2
Qinghu@10	2030	1088	0.536	0.00001	0.02	0.0492	0.99	0.1691	1.84	0.0249	1.56	0.84	156	23	159	3	159	2
Qinghu@11	1107	451	0.407	0.00003	0.06	0.0481	1.43	0.1662	2.08	0.0251	1.51	0.73	104	33	156	3	160	2
Qinghu@12	1627	722	0.444	0.00001	0.02	0.0499	1.08	0.1704	1.85	0.0247	1.50	0.81	192	25	160	3	158	2
Qinghu@13	1007	448	0.445	0.00002	0.03	0.0490	1.40	0.1682	2.05	0.0249	1.50	0.73	147	33	158	3	159	2
Qinghu@14	1712	1041	0.608	0.00002	0.04	0.0487	1.51	0.1741	2.13	0.0259	1.50	0.70	132	35	163	3	165	2
Qinghu@15	1304	555	0.425	0.00001	0.02	0.0486	1.21	0.1702	1.93	0.0254	1.50	0.78	130	28	160	3	162	2
Qinghu@16	1251	537	0.429	0.00001	0.02	0.0488	1.22	0.1713	1.94	0.0255	1.50	0.78	137	28	161	3	162	2
Qinghu@17	1666	937	0.562	0.00001	0.03	0.0483	1.10	0.1686	1.92	0.0253	1.58	0.82	115	26	158	3	161	3
Qinghu@18	1514	760	0.502	0.00001	0.01	0.0494	1.10	0.1722	1.87	0.0253	1.51	0.81	168	26	161	3	161	2
Qinghu@19	458	156	0.341	0.00001	0.02	0.0487	2.09	0.1661	2.61	0.0248	1.56	0.60	132	48	156	4	158	2
Qinghu@20	1679	804	0.479	0.00001	0.03	0.0490	1.29	0.1718	1.98	0.0254	1.50	0.76	148	30	161	3	162	2
Qinghu@21	1546	580	0.375	0.00001	0.02	0.0492	1.06	0.1699	1.84	0.0250	1.50	0.82	157	25	159	3	159	2
Qinghu@22	2558	1596	0.624	0.00001	0.03	0.0500	0.91	0.1710	1.76	0.0248	1.51	0.86	195	21	160	3	158	2
Qinghu@23	1918	1026	0.535	0.00002	0.03	0.0488	1.08	0.1677	1.87	0.0249	1.53	0.82	140	25	157	3	159	2
Qinghu@24	1086	474	0.437	0.00001	0.02	0.0482	1.37	0.1674	2.04	0.0252	1.51	0.74	111	32	157	3	160	2
Qinghu@25	2264	1337	0.590	0.00001	0.02	0.0486	1.32	0.1715	2.02	0.0256	1.53	0.76	126	31	161	3	163	2
Qinghu@26	1940	988	0.509	0.00001	0.02	0.0504	1.06	0.1771	1.85	0.0255	1.52	0.82	212	24	166	3	162	2
Qinghu@27	1295	667	0.515	0.00002	0.04	0.0478	1.31	0.1700	1.99	0.0258	1.50	0.75	90	31	159	3	164	2
Qinghu@28	1670	991	0.593	0.00003	0.05	0.0479	1.18	0.1639	1.92	0.0248	1.51	0.79	96	28	154	3	158	2
Qinghu@29	1052	555	0.528	0.00003	0.06	0.0491	1.84	0.1700	2.37	0.0251	1.50	0.63	154	42	159	4	160	2
Qinghu@30	2329	1261	0.541	0.00001	0.01	0.0496	1.14	0.1779	1.90	0.0260	1.51	0.80	174	26	166	3	166	2
Qinghu@31	1040	446	0.429	0.00002	0.04	0.0495	1.63	0.1717	2.22	0.0252	1.50	0.68	170	38	161	3	160	2
Qinghu@32	1316	532	0.404	0.00001	0.02	0.0497	1.44	0.1715	2.08	0.0250	1.51	0.72	182	33	161	3	159	2
Qinghu@33	1331	636	0.478	0.00001	0.02	0.0489	1.86	0.1689	2.39	0.0250	1.50	0.63	145	43	158	4	159	2
Qinghu@34	1528	699	0.458	0.00001	0.02	0.0489	1.69	0.1704	2.26	0.0253	1.51	0.67	143	39	160	3	161	2
Qinghu@35	1192	484	0.406	0.00002	0.04	0.0481	1.61	0.1658	2.20	0.0250	1.50	0.68	106	38	156	3	159	2
Qinghu@36	1172	594	0.507	0.00003	0.05	0.0497	1.56	0.1696	2.17	0.0248	1.50	0.69	181	36	159	3	158	2

Qinghu@37	1316	792	0.602	0.00001	0.02	0.0503	1.35	0.1792	2.03	0.0258	1.51	0.75	211	31	167	3	164	2
Qinghu@38	1062	432	0.407	0.00001	0.02	0.0494	1.52	0.1713	2.13	0.0252	1.50	0.70	165	35	161	3	160	2
Qinghu@39	410	23	0.528	0.00005	0.10	0.0492	1.88	0.1636	2.48	0.0241	1.61	0.65	156	44	154	4	154	2
Qinghu@40	177	13	0.392	0.00059	1.11	0.0491	5.11	0.1642	5.36	0.0243	1.62	0.30	151	116	154	8	155	2
Qinghu@41	694	33	0.670	0.00002	0.04	0.0499	1.86	0.1742	2.44	0.0253	1.58	0.65	192	43	163	4	161	3
Qinghu@42	187	17	0.320	0.00007	0.13	0.0488	2.24	0.1671	2.71	0.0248	1.52	0.56	137	52	157	4	158	2
Qinghu@43	339	24	0.415	0.00002	0.04	0.0485	1.70	0.1667	2.27	0.0249	1.51	0.66	123	40	157	3	159	2
Qinghu@44	602	29	0.643	0.00089	1.66	0.0471	4.15	0.1628	4.48	0.0251	1.70	0.38	53	96	153	6	160	3
Qinghu@45	408	24	0.510	0.00001	0.02	0.0494	1.71	0.1709	2.31	0.0251	1.55	0.67	166	40	160	3	160	2
Qinghu@46	505	27	0.593	0.00003	0.07	0.0491	1.93	0.1707	2.46	0.0252	1.53	0.62	150	45	160	4	161	2
Qinghu@47	714	53	0.405	0.00001	0.02	0.0486	1.13	0.1702	1.89	0.0254	1.51	0.80	127	26	160	3	162	2
Qinghu@48	487	43	0.331	0.00003	0.05	0.0495	1.33	0.1729	2.02	0.0254	1.52	0.75	169	31	162	3	161	2
Qinghu@49	575	33	0.528	0.00003	0.06	0.0495	1.52	0.1691	2.28	0.0248	1.70	0.75	170	35	159	3	158	3
Qinghu@50	327	21	0.449	0.00004	0.08	0.0487	2.52	0.1676	2.94	0.0250	1.52	0.52	132	58	157	4	159	2
Qinghu@51	756	42	0.542	0.00001	0.02	0.0498	1.68	0.1706	2.30	0.0248	1.57	0.68	187	39	160	3	158	2
Qinghu@52	439	25	0.512	0.00011	0.20	0.0483	2.79	0.1644	3.21	0.0247	1.59	0.50	116	64	155	5	157	2
Qinghu@53	529	39	0.410	0.00004	0.08	0.0490	1.72	0.1737	2.29	0.0257	1.51	0.66	147	40	163	3	164	2
Qinghu@54	373	20	0.567	0.00004	0.08	0.0489	2.25	0.1685	2.79	0.0250	1.64	0.59	144	52	158	4	159	3
Qinghu@55	379	22	0.518	0.00009	0.17	0.0489	2.21	0.1676	2.73	0.0248	1.61	0.59	145	51	157	4	158	3

[a] The value of $^{204}Pb/^{206}Pbm$ is the measured value;

[b] f_{206} is the percentage of common ^{206}Pb in total ^{206}Pb assuming present-day Stacey-Kramers commom Pb;

[c] ρ denotes error correlation between $^{207}Pb/^{235}U$ and $^{206}Pb/^{238}U$.

Appendix S3 SIMS Zircon oxygen isotopic data

Sample Spot	U-Pb age[&] (Ma)	±1σ	$\delta^{18}O$ (‰)	2SE	Discordance[d] (%)
Gujing Formation, lower part of Suixian Group					
12SZ20@01	769	11	3.3	0.2	-2.7
12SZ20@02	749	11	4.3	0.2	0.2
12SZ20@03	746	11	5.3	0.3	5.6
12SZ20@04	734	11	2.5	0.3	4.4
12SZ20@05	730	10	4.6	0.3	13.0
12SZ20@07	719	10	4.7	0.2	4.4
12SZ20@08	739	11	5.1	0.2	1.4
12SZ20@09	746	11	3.4	0.3	-11.3
12SZ20@10	733	10	1.8	0.4	4.2
12SZ20@11	745	11	3.9	0.3	-2.3
12SZ20@12	747	11	3.3	0.4	1.5
12SZ20@13	737	11	2.8	0.2	-2.7
12SZ20@14	718	10	3.5	0.4	3.5
12SZ20@15	718	10	4.0	0.3	0.0
12SZ20@16	746	11	5.6	0.3	2.7
12SZ24@01	750	11	4.8	0.4	-3.0
12SZ24@02	739	10	5.0	0.3	-1.3
12SZ24@03	773	11	3.5	0.3	2.0
12SZ24@04	843	12	6.0	0.4	2.7
12SZ24@05	727	10	2.4	0.3	1.6
12SZ24@06	771	11	5.1	0.3	1.2
12SZ24@07	791	11	3.7	0.3	-2.2
12SZ24@08	765	11	1.4	0.3	-1.8
12SZ24@09	772	11	4.9	0.3	-15.3
12SZ24@10	733	10	3.2	0.4	0.4
12SZ24@11	726	10	5.5	0.3	4.9
12SZ24@12	743	11	4.3	0.4	-0.4
12SZ24@13	751	11	1.8	0.3	-1.7
12SZ24@14	780	11	4.7	0.2	-2.9
12SZ28@01	758	11	3.9	0.3	-0.2
12SZ28@02	738	11	4.4	0.2	7.8
12SZ28@03	772	11	1.6	0.2	5.2
12SZ28@04	745	11	5.5	0.3	0.7
12SZ28@05	742	11	2.8	0.4	1.2

12SZ28@06	758	11	3.9	0.3	-1.3
12SZ28@07	733	10	5.7	0.4	3.9
12SZ28@08	1840	15	7.6	0.3	0.0
12SZ28@09	745	11	2.8	0.2	-1.2
12SZ28@10	732	10	3.6	0.3	1.6
12SZ28@11	730	10	2.2	0.4	-13.4
12SZ28@13	732	11	3.9	0.2	4.0
12SZ28@14	756	12	4.7	0.3	-2.8
12SZ28@15	753	11	4.1	0.2	3.9
12SZ28@16	740	10	1.9	0.2	11.1
12SZ28@17	746	11	3.1	0.3	2.2
12SZ28@18	721	10	5.3	0.4	-0.9
12SZ28@19	766	11	1.7	0.2	-6.2
12SZ28@20	820	12	6.0	0.2	-7.2
Liulin Formation, middle part of Suixian Group					
12SZ06@01	776	11	6.0	0.4	-3.6
12SZ06@02	795	11	6.4	0.3	1.1
12SZ06@03	772	11	4.7	0.3	10.9
12SZ06@04	778	11	6.0	0.4	10.3
12SZ06@05	805	12	6.2	0.4	6.4
12SZ06@06	929	14	5.5	0.3	-0.3
12SZ06@07	792	11	7.3	0.3	2.2
12SZ06@08	762	11	5.7	0.4	9.5
12SZ06@09	754	11	5.1	0.2	5.0
12SZ06@10	783	12	5.4	0.4	1.4
12SZ06@11	810	12	5.0	0.2	2.0
12SZ06@12	798	11	5.2	0.3	-0.6
12SZ06@13	822	12	6.1	0.3	-1.6
12SZ06@14	808	11	5.4	0.2	-1.1
12SZ06@15	802	11	5.6	0.4	-7.9
12SZ06@16	799	11	5.8	0.3	1.4
12SZ06@17	828	12	6.9	0.4	-2.9
12SZ06@18	2003	15	7.0	0.3	1.7
12SZ06@19	762	11	4.7	0.2	-0.3
12SZ06@20	823	12	6.4	0.4	1.7
12SZ06@21	800	11	5.6	0.2	-2.3
12SZ06@22	785	11	6.0	0.3	7.8
12SZ06@23	765	11	5.4	0.2	3.5
12SZ06@24	742	11	5.2	0.3	-1.4
12SZ06@25	847	14	7.1	0.3	-8.9
12SZ06@26	799	11	6.4	0.3	3.7

12SZ06@27	832	12	6.0	0.4	-1.9
12SZ06@28	767	11	5.7	0.2	8.7
12SZ07@01	859	12	6.0	0.3	4.0
12SZ07@02	803	11	6.0	0.3	-5.4
12SZ07@03	762	11	5.5	0.2	3.3
12SZ07@04	1988	20	7.0	0.3	-1.0
12SZ07@05	793	11	5.8	0.3	-2.3
12SZ07@06	2011	21	7.0	0.2	3.1
12SZ07@07	817	12	7.5	0.2	5.2
12SZ07@08	2019	16	7.0	0.2	1.5
12SZ07@09	742	11	3.0	0.2	4.1
12SZ07@10	812	11	5.4	0.2	1.4
12SZ07@11	801	11	6.6	0.3	0.6
12SZ07@12	786	11	5.5	0.3	-2.4
12SZ07@13	749	11	6.5	0.3	4.1
12SZ07@14	771	11	5.2	0.3	0.5
12SZ07@15	798	11	5.1	0.3	-0.6
12SZ07@16	802	11	7.1	0.2	0.0
12SZ07@17	709	10	5.1	0.3	-4.0
12SZ07@18	742	11	6.0	0.3	-7.6
12SZ07@19	798	11	6.0	0.3	0.4
12SZ07@20	872	12	8.4	0.3	-0.6
12SZ07@21	1675	30	6.4	0.2	-0.8
12SZ07@22	789	11	6.7	0.3	-1.6
12SZ07@23	2020	16	6.8	0.3	2.2
12SZ07@24	804	11	5.8	0.3	-7.0
12SZ07@25	777	11	3.4	0.3	-4.1
12SZ07@26	780	11	5.4	0.3	4.3
12SZ07@27	1979	30	7.0	0.3	-0.6
12SZ07@28	1984	21	7.0	0.3	-0.2
12SZ07@29	786	11	5.6	0.2	-4.0
12SZ07@30	781	11	5.7	0.3	-2.4
12SZ07@31	784	11	3.7	0.3	7.5
12SZ07@32	1977	19	6.5	0.4	-1.2
12SZ07@33	785	11	6.1	0.2	-5.8
12SZ07@34	797	11	5.8	0.3	-1.8
12SZ07@35	2025	22	6.6	0.3	4.1
12SZ07@36	876	12	5.8	0.4	1.7
12SZ07@37	763	11	4.6	0.4	-0.6
12SZ07@38	805	11	5.6	0.3	2.2

12SZ07@39	779	11	6.0	0.4	-2.8
12SZ07@40	811	11	6.7	0.4	-1.1
12SZ07@41	2739	10	6.0	0.5	-0.5
12SZ07@42	799	11	6.7	0.3	0.7
12SZ07@43	2506	7	6.0	0.4	2.4
12SZ07@44	761	11	6.4	0.3	-2.9
12SZ07@45	816	12	10.5	0.3	-2.9
12SZ07@46	2025	16	7.1	0.3	1.9
12SZ07@47	791	11	4.8	0.4	-19.5
13SZ14@01	833	12	6.3	0.3	-4.3
13SZ14@02	1018	19	10.3	0.4	-2.9
13SZ14@03	822	12	6.5	0.2	-1.8
13SZ14@04	778	11	5.7	0.2	-5.8
13SZ14@05	749	11	5.4	0.1	7.7
13SZ14@06	778	11	3.7	0.3	-4.0
13SZ14@07	839	13	10.0	0.4	0.9
13SZ14@08	818	12	6.4	0.3	-3.4
13SZ14@09	812	11	4.7	0.4	13.1
13SZ14@10	831	13	5.2	0.2	2.3
13SZ14@11	778	12	5.5	0.3	3.7
13SZ14@12	792	11	5.7	0.3	-0.9
13SZ14@13	804	11	7.0	0.3	3.2
13SZ14@14	768	11	5.1	0.3	-9.7
13SZ14@15	788	11	5.3	0.4	7.1
13SZ14@16	878	12	6.0	0.2	2.8
13SZ14@17	807	11	9.9	0.3	-3.1
13SZ14@18	780	11	5.5	0.4	4.5
13SZ14@19	779	12	3.4	0.3	-23.9
13SZ14@20	806	11	5.6	0.3	-11.4
13SZ14@21	782	11	5.7	0.4	-3.0
13SZ14@22	803	13	5.2	0.3	3.5
13SZ14@23	775	11	3.5	0.4	9.2
13SZ14@24	2025	30	7.5	0.3	3.2
13SZ14@25	2613	17	5.9	0.3	1.9
13SZ14@26	773	12	6.0	0.2	13.1
13SZ14@27	772	11	5.5	0.4	12.4
13SZ14@28	761	11	5.5	0.2	-1.2
13SZ14@29	747	11	5.4	0.4	1.4
13SZ14@30	1004	37	10.0	0.3	-3.7

13SZ19@01	742	11	3.8	0.4	-5.2
13SZ19@02	1995	14	6.6	0.2	2.6
13SZ19@03	1991	25	6.4	0.4	0.7
13SZ19@04	790	12	5.6	0.2	-2.1
13SZ19@05	753	11	3.9	0.3	-2.8
13SZ19@06	760	11	5.2	0.3	4.4
13SZ19@07	1719	27	6.1	0.3	2.4
13SZ19@08	823	12	9.2	0.3	-0.4
13SZ19@09	780	11	6.8	0.3	7.9
13SZ19@10	802	11	6.1	0.4	-2.4
13SZ19@11	754	11	6.3	0.2	-9.8
13SZ19@12	815	12	6.9	0.2	10.8
13SZ19@13	790	11	5.6	0.3	-1.2
13SZ19@14	723	10	3.7	0.2	2.7
13SZ19@15	2020	25	6.9	0.4	3.0
13SZ19@16	781	11	3.1	0.4	3.5
13SZ19@17	2050	31	6.8	0.3	3.9
13SZ19@18	756	11	7.2	0.3	-0.7
13SZ19@19	1960	27	6.9	0.2	-0.8
13SZ19@20	818	12	6.2	0.3	-7.5
13SZ19@21	766	11	5.0	0.3	-7.3
13SZ19@22	831	12	8.8	0.4	0.0
13SZ19@23	2527	13	6.1	0.3	0.6
13SZ19@24	782	11	5.1	0.2	2.8
13SZ19@25	803	11	6.3	0.4	-7.2
13SZ19@26	819	12	4.1	0.3	-11.5
13SZ19@27	762	11	5.8	0.3	-28.0
13SZ19@28	802	13	5.9	0.4	-1.0
13SZ19@29	839	12	5.6	0.4	-7.2
13SZ19@30	2412	38	7.4	0.3	0.2
13SZ19@31	798	12	7.6	0.2	-9.1
13SZ19@32	836	12	4.1	0.3	0.7
13SZ19@33	769	11	6.3	0.4	-2.8
13SZ19@34	802	11	6.0	0.4	-1.0
13SZ19@35	820	13	6.8	0.2	-12.9
13SZ19@36	804	12	5.8	0.3	-14.3
13SZ19@37	2011	54	7.2	0.4	-1.1
13SZ19@38	814	12	5.3	0.3	-4.8
13SZ19@39	764	11	3.8	0.2	1.1
12SZ14@01	733	10	4.5	0.5	-3.1

12SZ14@02	727	10	6.1	0.3	1.1
12SZ14@03	730	11	1.4	0.5	4.9
12SZ14@04	746	11	2.4	0.3	-0.7
12SZ14@05	739	11	6.1	0.2	-2.5
12SZ14@06	737	10	2.4	0.1	5.4
12SZ14@07	734	11	7.3	0.3	5.5
12SZ14@08	741	11	4.2	0.2	-5.7
12SZ14@09	760	11	4.2	0.2	-0.6
12SZ14@10	757	11	5.1	0.2	-6.4
12SZ14@11	770	11	4.7	0.2	-5.7
12SZ14@12	770	11	3.3	0.2	-3.2
12SZ14@13	754	11	4.1	0.2	-0.7
12SZ14@14	731	10	4.5	0.2	0.2
12SZ14@15	716	10	5.1	0.2	2.8
12SZ14@16	743	11	5.2	0.1	-6.4
12SZ14@17	738	11	3.8	0.3	0.3
12SZ14@18	759	11	6.3	0.2	5.1
12SZ14@19	774	11	4.9	0.3	-8.1
12SZ14@20	740	11	5.6	0.3	2.9
12SZ14@21	999	19	6.3	0.2	-1.9
12SZ14@22	740	11	5.2	0.2	0.9
12SZ14@23	736	10	4.2	0.2	-4.3
12SZ14@25	742	11	4.6	0.2	-2.3
12SZ17@01	740	11	5.0	0.1	-2.0
12SZ17@02	722	10	4.6	0.3	-2.6
12SZ17@03	728	10	4.2	0.3	-1.7
12SZ17@04	720	10	4.8	0.3	-0.9
12SZ17@05	715	10	4.7	0.2	9.0
12SZ17@06	741	11	3.6	0.3	-4.4
12SZ17@07	719	10	3.9	0.3	-3.0
12SZ17@08	727	10	4.9	0.2	-1.5
12SZ17@09	725	10	3.7	0.4	-0.8
12SZ17@10	733	10	3.8	0.2	-2.8
12SZ17@11	706	10	3.5	0.3	-0.6
12SZ17@12	729	10	6.2	0.2	-1.3
12SZ17@13	722	10	3.9	0.3	6.2
12SZ17@14	722	10	4.2	0.2	3.0
12SZ17@15	740	11	3.9	0.2	-1.0
12SZ17@16	748	11	4.1	0.3	4.7
12SZ17@17	729	10	4.1	0.2	-9.6

12SZ17@19	740	11	4.9	0.2	-4.4
12SZ17@20	733	10	3.8	0.3	-1.4
12SZ17@21	739	11	3.8	0.3	-2.9
12SZ17@22	721	10	3.9	0.3	4.7
12SZ17@23	719	10	4.0	0.2	6.6
12SZ17@24	722	10	5.8	0.3	4.1
12SZ17@25	702	10	4.4	0.2	-1.7
12SZ17@26	728	10	2.3	0.3	2.0
12SZ17@27	743	11	3.6	0.2	-7.8
12SZ17@28	831	12	8.3	0.3	0.0
Yuanziwan Formation, upper part of Suixian Group					
12SZ10@01	752	11	3.1	0.2	3.8
12SZ10@02	747	11	3.8	0.3	-21.0
12SZ10@03	763	11	2.3	0.4	-1.3
12SZ10@04	730	10	4.3	0.3	-4.6
12SZ10@05	737	11	6.0	0.4	3.3
12SZ10@06	752	11	3.9	0.2	-11.3
12SZ10@07	749	11	2.2	0.2	-7.8
12SZ10@08	738	10	5.2	0.2	0.4
12SZ10@09	734	11	5.5	0.3	2.0
12SZ10@10	725	10	4.9	0.4	5.5
12SZ10@11	733	10	6.9	0.4	0.0
12SZ10@12	740	11	6.6	0.2	2.5
12SZ10@13	763	11	1.3	0.4	-4.9
12SZ10@14	736	10	6.2	0.4	-1.7
12SZ10@15	718	10	2.2	0.3	-3.4
12SZ10@16	731	10	5.7	0.4	3.7
12SZ10@17	720	10	4.4	0.3	11.5
12SZ10@18	765	11	4.1	0.4	-6.5
12SZ10@20	728	10	5.5	0.2	-8.4
12SZ10@22	749	11	4.5	0.2	-5.4
12SZ10@23	740	11	3.9	0.3	2.0
12SZ10@24	731	11	4.7	0.4	4.8
12SZ10@25	777	11	2.8	0.3	-3.9
12SZ10@26	732	10	2.9	0.4	5.4
12SZ10@27	757	11	5.3	0.4	10.5
12SZ10@28	750	11	4.3	0.3	-0.7
13SZ17@01	736	10	6.1	0.3	-3.3
13SZ17@02	730	10	2.4	0.4	1.3

13SZ17@03	730	10	2.5	0.3	1.1
13SZ17@04	715	10	2.3	0.3	4.4
13SZ17@05	718	10	3.4	0.3	5.4
13SZ17@06	710	10	3.6	0.3	15.7
13SZ17@07	733	10	2.6	0.4	0.6
13SZ17@08	712	10	4.0	0.3	16.1
13SZ17@09	730	10	2.5	0.2	8.6
13SZ17@10	724	10	3.6	0.4	-9.9
13SZ17@11	741	11	8.6	0.3	-4.6
13SZ17@12	739	10	3.3	0.3	6.0
13SZ17@13	738	11	3.9	0.3	9.6
13SZ17@14	724	10	3.4	0.2	-5.5
13SZ17@15	722	10	2.7	0.4	3.6
13SZ17@16	793	11	6.2	0.4	-1.8
13SZ17@17	738	10	3.6	0.3	-2.7
13SZ17@18	719	10	2.6	0.2	-1.7
13SZ17@19	731	10	2.6	0.3	3.1
13SZ17@20	799	11	6.7	0.4	-7.8
13SZ17@21	746	11	4.1	0.2	1.5
13SZ17@22	731	10	4.2	0.3	0.2
13SZ17@23	727	10	3.3	0.3	12.6
13SZ17@24	738	11	4.7	0.4	9.6
13SZ17@25	721	10	3.7	0.3	0.3
13SZ17@26	709	10	2.5	0.4	3.9

[&] The "U-Pb age: listed here refers to $^{206}Pb/^{238}U$ age (＜1000 Ma) or $^{207}Pb/^{206}Pb$ age (＞1000 Ma);

* indicates undated spots whose U-Pb ages are derived from weighted mean of $^{206}Pb/^{238}U$ ages given the concodance of almost all of other spots within one sample;

[d] discordance difined as percent diviation of $t_{206/238}$ relative to $t_{207/206}$ using the equation $(1-t_{206/238}/t_{207/206})*100$; data marked in red are not included in the oxygen isotope plot.

Note: The $^{206}Pb/^{238}U$ age listed here with aboslute discordance ＜12% are used for plotting U-Pb age vs. $\delta^{18}O$ diagram.

Appendix S3 Zircon LA-ICP-MS Hf isotopic results

Sample spot	U-Pb (Ma)	±1σ (Ma)	$^{176}Yb/^{177}Hf$	2σ	$^{176}Lu/^{177}Hf$	2σ	$^{176}Hf/^{177}Hf$	2σ	$^{176}Yb/^{176}Lu$	$\varepsilon_{Hf}(0)$	2σ	$\varepsilon_{Hf}(t)$	2σ	T_{DM1} #(Ma)	T_{DM2} #(Ma)
Gujing Formation, lower part of Suixian Group															
12SZ20@01	769	11	0.036764	0.000423	0.001393	0.000015	0.282154	0.000022	26	-21.9	1.3	-5.6	1.4	1564	1779
12SZ20@03	746	11	0.073106	0.000425	0.002710	0.000018	0.282161	0.000018	27	-21.6	1.2	-6.5	1.3	1610	1806
12SZ20@04	734	11	0.036631	0.000198	0.001354	0.000007	0.282122	0.000019	27	-23.0	1.2	-7.5	1.3	1607	1846
12SZ20@07	719	10	0.042143	0.000575	0.001587	0.000019	0.282233	0.000027	27	-19.1	1.4	-3.9	1.5	1459	1655
12SZ20@08	739	11	0.040897	0.000487	0.001528	0.000016	0.282194	0.000030	27	-20.4	1.5	-4.9	1.5	1513	1719
12SZ20@09	746	11	0.049729	0.001622	0.001630	0.000043	0.282167	0.000024	31	-21.4	1.3	-5.7	1.4	1555	1768
12SZ20@10	733	10	0.046115	0.000370	0.001733	0.000017	0.282166	0.000022	27	-21.4	1.3	-6.1	1.4	1560	1775
12SZ20@11	745	11	0.041064	0.000208	0.001577	0.000007	0.282229	0.000035	26	-19.2	1.6	-3.6	1.7	1465	1656
12SZ20@12	747	11	0.109882	0.003230	0.004029	0.000112	0.282214	0.000035	27	-19.7	1.6	-5.3	1.7	1591	1744
12SZ20@13	737	11	0.060591	0.000481	0.002322	0.000017	0.282031	0.000026	26	-26.2	1.4	-11.1	1.5	1780	2030
12SZ20@14	718	10	0.041774	0.000260	0.001583	0.000009	0.282168	0.000027	26	-21.4	1.4	-6.3	1.5	1551	1772
12SZ20@15	718	10	0.045421	0.000222	0.001722	0.000008	0.282155	0.000042	26	-21.8	1.8	-6.8	1.8	1576	1799
12SZ20@16	746	11	0.037484	0.000274	0.001431	0.000010	0.282140	0.000018	26	-22.4	1.2	-6.6	1.3	1585	1811
12SZ24@01	750	11	0.111279	0.002162	0.004046	0.000073	0.282098	0.000027	28	-23.8	1.4	-9.3	1.5	1766	1950
12SZ24@02	739	10	0.086027	0.000733	0.003162	0.000024	0.281929	0.000030	27	-29.8	1.5	-15.1	1.5	1972	2232
12SZ24@03	773	11	0.065178	0.000601	0.002374	0.000022	0.282132	0.000022	27	-22.6	1.3	-6.8	1.4	1637	1842
12SZ24@04	843	12	0.075827	0.001827	0.002740	0.000068	0.282563	0.000021	28	-7.4	1.3	9.7	1.4	1021	1062
12SZ24@05	727	10	0.198478	0.004143	0.006956	0.000146	0.282267	0.000037	29	-17.9	1.7	-5.2	1.7	1649	1723
12SZ24@06	771	11	0.044770	0.000642	0.001586	0.000021	0.282046	0.000020	28	-25.7	1.2	-9.5	1.3	1724	1976
12SZ24@07	791	11	0.096539	0.001373	0.003459	0.000054	0.282398	0.000034	28	-13.2	1.6	2.4	1.6	1290	1391
12SZ24@08	765	11	0.079833	0.002571	0.002955	0.000096	0.282233	0.000061	27	-19.1	2.4	-3.7	2.4	1515	1678
12SZ24@10	733	10	0.104013	0.002257	0.003754	0.000073	0.282615	0.000059	28	-5.5	2.3	8.8	2.4	972	1018
12SZ24@11	726	10	0.057028	0.000811	0.002068	0.000029	0.281896	0.000019	28	-31.0	1.2	-16.0	1.3	1960	2266

12SZ24@12	743	11	0.108808	0.001265	0.003845	0.000039	0.282123	0.000033	28	-23.0	1.5	-8.5	1.6	1720	1903
12SZ24@13	751	11	0.055899	0.000564	0.002082	0.000022	0.282169	0.000017	27	-21.3	1.2	-5.8	1.3	1571	1774
12SZ24@14	780	11	0.072078	0.001688	0.002778	0.000064	0.282437	0.000023	26	-11.9	1.3	3.9	1.4	1209	1305
12SZ28@01	758	11	0.034713	0.000276	0.001310	0.000011	0.282099	0.000014	26	-23.8	1.1	-7.7	1.2	1637	1878
12SZ28@02	738	11	0.058605	0.000883	0.002313	0.000034	0.282328	0.000015	25	-15.7	1.2	-0.6	1.2	1352	1499
12SZ28@03	772	11	0.069203	0.000458	0.002568	0.000016	0.282218	0.000017	27	-19.6	1.2	-3.9	1.3	1521	1694
12SZ28@04	745	11	0.040002	0.000744	0.001493	0.000026	0.282024	0.000014	27	-26.4	1.1	-10.8	1.2	1750	2020
12SZ28@05	742	11	0.074720	0.000271	0.002677	0.000008	0.282107	0.000019	28	-23.5	1.2	-8.5	1.3	1687	1902
12SZ28@06	758	11	0.034936	0.000248	0.001306	0.000011	0.282015	0.000017	27	-26.8	1.2	-10.7	1.3	1754	2027
12SZ28@07	733	10	0.101130	0.002839	0.003534	0.000096	0.282266	0.000019	29	-17.9	1.2	-3.4	1.3	1491	1641
12SZ28@08	1840	15	0.014352	0.000262	0.000487	0.000008	0.281403	0.000019	29	-48.4	1.2	-8.0	1.4	2548	2762
12SZ28@09	745	11	0.086533	0.002199	0.003228	0.000078	0.282089	0.000023	27	-24.1	1.3	-9.3	1.4	1739	1946
12SZ28@10	732	10	0.040283	0.000117	0.001506	0.000004	0.282142	0.000015	27	-22.3	1.2	-6.9	1.2	1585	1814
12SZ28@13	732	11	0.060840	0.000745	0.002210	0.000025	0.282115	0.000017	28	-23.2	1.2	-8.2	1.3	1655	1879
12SZ28@14	756	12	0.043531	0.000201	0.001599	0.000007	0.282138	0.000018	27	-22.4	1.2	-6.6	1.3	1594	1816
12SZ28@15	753	11	0.043918	0.000381	0.001587	0.000014	0.282209	0.000016	28	-19.9	1.2	-4.1	1.3	1494	1690
12SZ28@16	740	10	0.072778	0.000284	0.002575	0.000011	0.282142	0.000017	28	-22.3	1.2	-7.2	1.3	1631	1837
12SZ28@17	746	11	0.069520	0.000851	0.002425	0.000030	0.282244	0.000026	29	-18.7	1.4	-3.4	1.4	1478	1650
12SZ28@18	721	10	0.027884	0.000130	0.001032	0.000005	0.282526	0.000017	27	-8.7	1.2	6.7	1.3	1028	1115
12SZ28@19	766	11	0.072672	0.000803	0.002555	0.000032	0.282166	0.000018	28	-21.4	1.2	-5.8	1.3	1596	1788
Liulin Formation, middle part of Suixian Group															
12SZ06@01	776	11	0.043751	0.000180	0.001669	0.000004	0.282533	0.000018	26	-8.5	1.2	7.8	1.3	1036	1104
12SZ06@02	795	11	0.051678	0.000155	0.002088	0.000008	0.282498	0.000019	25	-9.7	1.2	6.8	1.3	1097	1172
12SZ06@03	772	11	0.025994	0.000295	0.001055	0.000010	0.282437	0.000017	25	-11.8	1.2	4.7	1.3	1153	1261
12SZ06@04	778	11	0.065069	0.001910	0.002374	0.000068	0.282362	0.000018	27	-14.5	1.2	1.4	1.3	1305	1430
12SZ06@05	805	12	0.036244	0.000238	0.001443	0.000008	0.282480	0.000017	25	-10.3	1.2	6.7	1.3	1105	1186
12SZ06@06	929	14	0.033358	0.000110	0.001300	0.000005	0.282549	0.000017	26	-7.9	1.2	11.9	1.3	1003	1023

12SZ06@07	792	11	0.055073	0.000777	0.002126	0.000034	0.282502	0.000021	26	-9.5	1.3	6.8	1.3	1093	1168
12SZ06@08	762	11	0.026042	0.000522	0.001178	0.000023	0.282494	0.000016	22	-9.8	1.2	6.4	1.3	1077	1164
12SZ06@09	754	11	0.026238	0.000297	0.001195	0.000014	0.282454	0.000020	22	-11.3	1.2	4.8	1.3	1134	1241
12SZ06@10	783	12	0.034496	0.000160	0.001344	0.000004	0.282027	0.000017	26	-26.3	1.2	-9.8	1.3	1739	2000
12SZ06@11	810	12	0.049974	0.000186	0.001898	0.000006	0.282474	0.000019	26	-10.5	1.2	6.3	1.3	1127	1207
12SZ06@12	798	11	0.041558	0.000434	0.001599	0.000016	0.282433	0.000018	26	-12.0	1.2	4.8	1.3	1176	1276
12SZ06@13	822	12	0.038504	0.000226	0.001418	0.000008	0.282294	0.000017	27	-16.9	1.2	0.5	1.3	1367	1514
12SZ06@14	808	11	0.039390	0.000780	0.001601	0.000029	0.282466	0.000016	25	-10.8	1.2	6.2	1.3	1129	1214
12SZ06@15	802	11	0.039310	0.000429	0.001387	0.000016	0.282604	0.000019	28	-6.0	1.2	11.0	1.3	927	961
12SZ06@16	799	11	0.038032	0.000643	0.001567	0.000026	0.282466	0.000018	24	-10.8	1.2	6.0	1.3	1127	1215
12SZ06@17	828	12	0.023693	0.000176	0.000940	0.000007	0.282383	0.000013	25	-13.8	1.1	4.0	1.2	1226	1340
12SZ06@18	2003	15	0.010834	0.000098	0.000397	0.000003	0.281249	0.000020	27	-53.9	1.2	-9.7	1.5	2749	2977
12SZ06@19	762	11	0.013727	0.000099	0.000526	0.000004	0.282538	0.000017	26	-8.3	1.2	8.3	1.3	997	1068
12SZ06@20	823	12	0.038257	0.000199	0.001357	0.000006	0.282512	0.000017	28	-9.2	1.2	8.3	1.3	1056	1120
12SZ06@21	800	11	0.027513	0.000402	0.000982	0.000015	0.282414	0.000017	28	-12.7	1.2	4.5	1.3	1184	1294
12SZ06@22	785	11	0.041945	0.001410	0.001651	0.000055	0.282432	0.000018	25	-12.0	1.2	4.5	1.3	1179	1282
12SZ06@23	765	11	0.068959	0.000398	0.002661	0.000015	0.282603	0.000019	26	-6.0	1.2	9.6	1.3	961	1006
12SZ06@24	742	11	0.053700	0.001382	0.001944	0.000050	0.282504	0.000017	28	-9.5	1.2	5.9	1.3	1085	1172
12SZ06@25	847	14	0.055558	0.000600	0.002091	0.000023	0.282511	0.000017	27	-9.2	1.2	8.3	1.3	1079	1136
12SZ06@26	799	11	0.023662	0.000086	0.000891	0.000003	0.282523	0.000016	27	-8.8	1.2	8.4	1.3	1028	1094
12SZ06@27	832	12	0.030755	0.000043	0.001088	0.000001	0.282325	0.000016	28	-15.8	1.2	2.0	1.3	1311	1446
12SZ07@01	859	12	0.017967	0.000045	0.000769	0.000002	0.282579	0.000016	23	-6.8	1.2	11.7	1.3	947	973
12SZ07@02	803	11	0.033787	0.000126	0.001318	0.000003	0.282444	0.000017	26	-11.6	1.2	5.4	1.3	1152	1247
12SZ07@03	762	11	0.045247	0.000584	0.001977	0.000025	0.282484	0.000016	23	-10.2	1.2	5.6	1.3	1115	1204
12SZ07@04	1988	20	0.015515	0.000071	0.000540	0.000002	0.281248	0.000016	29	-53.9	1.2	-10.3	1.5	2760	2992
12SZ07@05	793	11	0.016135	0.000105	0.000615	0.000004	0.282398	0.000019	26	-13.2	1.2	4.0	1.3	1194	1314
12SZ07@06	2011	21	0.007570	0.000021	0.000269	0.000001	0.281217	0.000018	28	-55.0	1.2	-10.5	1.6	2782	3021

12SZ07@07	817	12	0.023691	0.000279	0.000879	0.000010	0.282346	0.000016	27	-15.1	1.2	2.5	1.3	1276	1408
12SZ07@08	2019	16	0.018398	0.000032	0.000635	0.000001	0.281261	0.000018	29	-53.4	1.2	-9.2	1.4	2749	2966
12SZ07@09	742	11	0.061450	0.000172	0.002250	0.000006	0.282164	0.000016	27	-21.5	1.2	-6.3	1.3	1585	1790
12SZ07@10	812	11	0.077384	0.000553	0.002828	0.000019	0.282263	0.000019	27	-18.0	1.2	-1.6	1.3	1466	1611
12SZ07@11	801	11	0.027270	0.000172	0.001125	0.000008	0.282477	0.000017	24	-10.4	1.2	6.7	1.3	1100	1184
12SZ07@12	786	11	0.069088	0.000254	0.002520	0.000009	0.281855	0.000022	27	-32.4	1.3	-16.4	1.4	2043	2336
12SZ07@13	749	11	0.046233	0.000933	0.001783	0.000037	0.282459	0.000020	26	-11.1	1.2	4.6	1.3	1144	1247
12SZ07@14	771	11	0.024720	0.000148	0.000974	0.000006	0.282418	0.000016	25	-12.5	1.2	4.0	1.3	1178	1294
12SZ07@15	798	11	0.020424	0.000088	0.000769	0.000003	0.282402	0.000015	27	-13.1	1.2	4.1	1.3	1194	1310
12SZ07@16	802	11	0.030142	0.000214	0.001149	0.000006	0.282484	0.000016	26	-10.2	1.2	6.9	1.3	1090	1170
12SZ07@17	709	10	0.054018	0.000358	0.002096	0.000010	0.282585	0.000016	26	-6.6	1.2	8.1	1.2	972	1037
12SZ07@18	742	11	0.035039	0.000068	0.001329	0.000001	0.282075	0.000020	26	-24.7	1.3	-9.0	1.3	1671	1926
12SZ07@19	798	11	0.041317	0.000424	0.001347	0.000012	0.281844	0.000019	31	-32.8	1.2	-16.0	1.3	1995	2322
12SZ07@20	872	12	0.051332	0.000458	0.002046	0.000016	0.282410	0.000018	25	-12.8	1.2	5.3	1.3	1224	1312
12SZ07@21	1675	30	0.011010	0.000134	0.000401	0.000004	0.281427	0.000017	27	-47.6	1.2	-10.7	1.8	2509	2765
12SZ07@22	789	11	0.040154	0.000044	0.001467	0.000002	0.282540	0.000019	27	-8.2	1.2	8.5	1.3	1021	1083
12SZ07@24	804	11	0.077275	0.000622	0.002592	0.000019	0.281859	0.000019	30	-32.3	1.2	-15.9	1.3	2041	2326
12SZ07@25	777	11	0.057851	0.000719	0.002140	0.000027	0.281921	0.000020	27	-30.1	1.2	-14.1	1.3	1928	2212
12SZ07@26	780	11	0.022666	0.000183	0.000939	0.000008	0.281975	0.000016	24	-28.2	1.2	-11.5	1.3	1793	2084
12SZ07@27	1979	30	0.007732	0.000015	0.000285	0.000001	0.281217	0.000018	27	-55.0	1.2	-11.2	1.8	2783	3033
12SZ07@28	1984	21	0.018174	0.000008	0.000641	0.000001	0.281247	0.000018	28	-53.9	1.2	-10.5	1.6	2768	3002
12SZ07@29	786	11	0.019318	0.000015	0.000712	0.000001	0.282422	0.000017	27	-12.4	1.2	4.6	1.3	1164	1276
12SZ07@30	781	11	0.045280	0.000865	0.001680	0.000031	0.281815	0.000019	27	-33.8	1.2	-17.5	1.3	2054	2387
12SZ07@31	784	11	0.100071	0.001016	0.003486	0.000037	0.281994	0.000022	29	-27.5	1.3	-12.0	1.4	1893	2115
12SZ07@32	1977	19	0.008555	0.000014	0.000312	0.000000	0.281206	0.000016	27	-55.4	1.2	-11.7	1.5	2800	3054
12SZ07@33	785	11	0.022794	0.000137	0.000808	0.000006	0.282439	0.000017	28	-11.8	1.2	5.2	1.3	1143	1247
12SZ07@34	797	11	0.099458	0.000145	0.003948	0.000008	0.282503	0.000022	25	-9.5	1.3	6.0	1.4	1148	1213
12SZ07@35	2025	22	0.011918	0.000032	0.000428	0.000001	0.281230	0.000021	28	-54.5	1.3	-9.9	1.6	2776	3005

12SZ07@36	876	12	0.022705	0.000120	0.000816	0.000005	0.282588	0.000017	28	-6.5	1.2	12.4	1.3	935	952
12SZ07@37	763	11	0.027681	0.000199	0.000983	0.000006	0.282587	0.000016	28	-6.5	1.2	9.8	1.3	940	991
12SZ07@38	805	11	0.053640	0.000238	0.001785	0.000006	0.281876	0.000021	30	-31.7	1.3	-14.9	1.3	1973	2274
12SZ07@39	779	11	0.016154	0.000071	0.000616	0.000003	0.282399	0.000018	26	-13.2	1.2	3.7	1.3	1193	1317
12SZ07@40	811	11	0.024651	0.000481	0.000968	0.000018	0.282470	0.000018	25	-10.7	1.2	6.7	1.3	1105	1189
12SZ07@41	2739	10	0.011829	0.000049	0.000437	0.000002	0.281022	0.000016	27	-61.9	1.2	-1.1	1.3	3055	3151
12SZ07@42	799	11	0.035114	0.000067	0.001421	0.000005	0.282504	0.000017	25	-9.5	1.2	7.4	1.3	1069	1142
12SZ07@43	2506	7	0.033509	0.000451	0.001276	0.000015	0.281004	0.000018	26	-62.5	1.2	-8.5	1.3	3146	3322
12SZ07@44	761	11	0.063071	0.000222	0.002301	0.000008	0.282102	0.000015	27	-23.7	1.1	-8.1	1.2	1677	1898
12SZ07@45	816	12	0.026878	0.000207	0.000973	0.000007	0.282058	0.000015	28	-25.3	1.2	-7.8	1.3	1680	1927
12SZ07@46	2025	16	0.008255	0.000043	0.000305	0.000002	0.281241	0.000016	27	-54.1	1.2	-9.4	1.4	2752	2977
13SZ14@01	833	12	0.024011	0.000053	0.000870	0.000001	0.282361	0.000015	28	-14.5	1.2	3.4	1.3	1253	1375
13SZ14@02	1018	19	0.046201	0.000159	0.001596	0.000005	0.282119	0.000015	29	-23.1	1.2	-1.7	1.4	1621	1781
13SZ14@03	822	12	0.078049	0.000103	0.002537	0.000004	0.282150	0.000020	31	-22.0	1.2	-5.2	1.3	1618	1802
13SZ14@04	778	11	0.032495	0.000148	0.001355	0.000005	0.282272	0.000014	24	-17.7	1.1	-1.2	1.3	1396	1565
13SZ14@05	749	11	0.062625	0.000522	0.002167	0.000015	0.282495	0.000019	29	-9.8	1.2	5.7	1.3	1105	1192
13SZ14@06	778	11	0.033555	0.000612	0.001224	0.000020	0.282527	0.000016	27	-8.7	1.2	7.9	1.3	1032	1102
13SZ14@07	839	13	0.025967	0.000396	0.000943	0.000013	0.282127	0.000017	28	-22.8	1.2	-4.8	1.3	1582	1796
13SZ14@08	818	12	0.022418	0.000376	0.000829	0.000014	0.282548	0.000014	27	-7.9	1.1	9.7	1.2	991	1042
13SZ14@10	831	13	0.043375	0.000091	0.001518	0.000003	0.282388	0.000019	29	-13.6	1.2	4.0	1.4	1237	1345
13SZ14@11	778	12	0.049626	0.000636	0.001687	0.000021	0.281922	0.000017	29	-30.1	1.2	-13.8	1.3	1904	2198
13SZ14@12	792	11	0.042034	0.000389	0.001541	0.000015	0.282437	0.000017	27	-11.8	1.2	4.9	1.3	1168	1268
13SZ14@13	804	11	0.029531	0.000248	0.001099	0.000009	0.282529	0.000017	27	-8.6	1.2	8.6	1.3	1025	1087
13SZ14@14	768	11	0.022630	0.000064	0.001037	0.000002	0.282622	0.000014	22	-5.3	1.1	11.1	1.2	893	929
13SZ14@15	788	11	0.028274	0.000162	0.001005	0.000004	0.282357	0.000014	28	-14.7	1.1	2.2	1.2	1264	1400
13SZ14@16	878	12	0.031029	0.000151	0.001240	0.000006	0.282557	0.000016	25	-7.6	1.2	11.1	1.3	990	1021
13SZ14@17	807	11	0.018789	0.000068	0.000648	0.000003	0.282175	0.000017	29	-21.1	1.2	-3.7	1.3	1504	1712

13SZ14@18	780	11	0.023933	0.000042	0.000941	0.000001	0.282427	0.000014	25	-12.2	1.1	4.5	1.2	1165	1275
13SZ14@20	806	11	0.105023	0.002055	0.003468	0.000068	0.281810	0.000019	30	-34.0	1.2	-18.1	1.3	2163	2435
13SZ14@21	782	11	0.040887	0.000519	0.001606	0.000017	0.282570	0.000015	25	-7.1	1.2	9.3	1.3	981	1033
13SZ14@22	803	13	0.057196	0.000446	0.002145	0.000013	0.282438	0.000018	27	-11.8	1.2	4.8	1.3	1186	1281
13SZ14@23	775	11	0.037076	0.000925	0.001330	0.000033	0.282412	0.000017	28	-12.7	1.2	3.7	1.3	1198	1313
13SZ14@24	2025	30	0.014609	0.000223	0.000519	0.000008	0.281284	0.000018	28	-52.6	1.2	-8.1	1.8	2710	2916
13SZ14@25	2613	17	0.018008	0.000054	0.000671	0.000002	0.281250	0.000018	27	-53.8	1.2	3.7	1.5	2766	2812
13SZ14@28	761	11	0.016478	0.000046	0.000712	0.000002	0.282364	0.000016	23	-14.4	1.2	2.0	1.3	1245	1387
13SZ14@29	747	11	0.020404	0.000243	0.000746	0.000008	0.282532	0.000016	27	-8.5	1.2	7.6	1.3	1012	1090
13SZ14@30	1004	37	0.041933	0.000374	0.001461	0.000015	0.282213	0.000014	29	-19.8	1.1	1.5	2.0	1483	1612
13SZ19@01	742	11	0.042756	0.000596	0.001565	0.000021	0.282274	0.000019	27	-17.6	1.2	-2.0	1.3	1401	1576
13SZ19@02	1995	14	0.072792	0.002247	0.002018	0.000054	0.281268	0.000015	36	-53.2	1.2	-11.4	1.3	2842	3054
13SZ19@03	1991	25	0.013792	0.000119	0.000461	0.000004	0.281189	0.000018	30	-56.0	1.2	-12.2	1.7	2833	3089
13SZ19@04	790	12	0.023048	0.000216	0.000937	0.000007	0.282422	0.000016	25	-12.4	1.2	4.6	1.3	1171	1280
13SZ19@05	753	11	0.024583	0.000189	0.000966	0.000006	0.282435	0.000016	25	-11.9	1.2	4.2	1.3	1154	1269
13SZ19@06	760	11	0.031241	0.000039	0.001340	0.000002	0.282476	0.000016	23	-10.5	1.2	5.7	1.3	1107	1202
13SZ19@07	1719	27	0.034047	0.000166	0.001143	0.000004	0.281444	0.000016	30	-47.0	1.2	-10.0	1.7	2535	2764
13SZ19@08	823	12	0.026063	0.000332	0.000938	0.000011	0.281992	0.000019	28	-27.6	1.2	-10.0	1.3	1770	2042
13SZ19@09	780	11	0.050596	0.000206	0.001951	0.000008	0.282527	0.000019	26	-8.7	1.2	7.6	1.3	1051	1120
13SZ19@10	802	11	0.031590	0.000096	0.001210	0.000001	0.282480	0.000019	26	-10.3	1.2	6.7	1.3	1098	1180
13SZ19@11	754	11	0.026543	0.000117	0.000977	0.000005	0.282306	0.000017	27	-16.5	1.2	-0.3	1.3	1334	1500
13SZ19@12	815	12	0.019906	0.000025	0.000737	0.000001	0.282319	0.000016	27	-16.0	1.2	1.6	1.3	1308	1453
13SZ19@13	790	11	0.017670	0.000067	0.000643	0.000003	0.282415	0.000015	27	-12.6	1.2	4.5	1.3	1171	1284
13SZ19@14	723	10	0.118362	0.003226	0.003863	0.000102	0.282048	0.000020	31	-25.6	1.2	-11.5	1.3	1832	2039
13SZ19@15	2020	25	0.009780	0.000023	0.000347	0.000001	0.281196	0.000015	28	-55.7	1.1	-11.1	1.6	2815	3060
13SZ19@16	781	11	0.049390	0.000127	0.001869	0.000006	0.282614	0.000016	26	-5.6	1.2	10.7	1.3	925	961
13SZ19@17	2050	31	0.011695	0.000086	0.000416	0.000003	0.281237	0.000018	28	-54.3	1.2	-9.1	1.9	2766	2984

13SZ19@18	756	11	0.052039	0.000184	0.001834	0.000004	0.282174	0.000019	28	-21.1	1.2	-5.4	1.3	1553	1758
13SZ19@19	1960	27	0.008639	0.000034	0.000308	0.000001	0.281224	0.000016	28	-54.7	1.2	-11.4	1.7	2775	3027
13SZ19@20	818	12	0.037479	0.000129	0.001377	0.000004	0.282489	0.000016	27	-10.0	1.2	7.3	1.3	1090	1164
13SZ19@21	766	11	0.014520	0.000044	0.000689	0.000002	0.282459	0.000016	21	-11.1	1.2	5.5	1.3	1112	1215
13SZ19@22	831	12	0.021692	0.000599	0.000738	0.000019	0.282168	0.000015	29	-21.4	1.1	-3.4	1.3	1517	1719
13SZ19@23	2527	13	0.017812	0.000034	0.000669	0.000001	0.280904	0.000018	27	-66.1	1.2	-10.5	1.4	3231	3440
13SZ19@24	782	11	0.061467	0.000760	0.002329	0.000024	0.282433	0.000018	26	-12.0	1.2	4.1	1.3	1199	1299
13SZ19@25	803	11	0.037403	0.000358	0.001366	0.000011	0.282501	0.000019	27	-9.6	1.2	7.4	1.3	1072	1145
13SZ19@26	819	12	0.031315	0.000574	0.001142	0.000019	0.282437	0.000015	27	-11.9	1.2	5.6	1.3	1157	1251
13SZ19@28	802	13	0.030455	0.000793	0.001111	0.000028	0.282419	0.000013	27	-12.5	1.1	4.7	1.3	1180	1286
13SZ19@29	839	12	0.052792	0.001217	0.001827	0.000040	0.282297	0.000015	29	-16.8	1.2	0.7	1.3	1378	1517
13SZ19@30	2412	38	0.016355	0.000006	0.000575	0.000000	0.281164	0.000014	28	-56.8	1.1	-3.7	2.1	2875	3014
13SZ19@31	798	12	0.025888	0.000172	0.000960	0.000006	0.282465	0.000014	27	-10.9	1.1	6.3	1.3	1112	1202
13SZ19@32	836	12	0.033137	0.000151	0.001274	0.000005	0.282423	0.000015	26	-12.4	1.2	5.4	1.3	1181	1276
13SZ19@33	769	11	0.032423	0.000246	0.001251	0.000008	0.282177	0.000014	26	-21.1	1.1	-4.7	1.2	1526	1735
13SZ19@34	802	11	0.036051	0.000164	0.001339	0.000004	0.282362	0.000017	27	-14.5	1.2	2.5	1.3	1268	1396
13SZ19@37	2011	54	0.011767	0.000061	0.000411	0.000002	0.281192	0.000016	29	-55.9	1.2	-11.6	2.7	2826	3075
13SZ19@39	764	11	0.086390	0.000297	0.002967	0.000005	0.282086	0.000017	29	-24.2	1.2	-8.9	1.3	1731	1941
12SZ14@01	733	10	0.035093	0.000281	0.001368	0.000011	0.282333	0.000018	26	-15.5	1.2	-0.02	1.3	1310	1468
12SZ14@02	727	10	0.042978	0.000674	0.001720	0.000026	0.282287	0.000017	25	-17.1	1.2	-1.9	1.3	1388	1560
12SZ14@04	746	11	0.037656	0.000429	0.001375	0.000016	0.282155	0.000019	27	-21.8	1.2	-6.0	1.3	1561	1782
12SZ14@05	739	11	0.032427	0.000076	0.001278	0.000002	0.281824	0.000018	25	-33.5	1.2	-17.9	1.3	2020	2373
12SZ14@06	737	10	0.046917	0.000228	0.001739	0.000010	0.282282	0.000019	27	-17.3	1.2	-1.9	1.3	1396	1567
12SZ14@07	734	11	0.023374	0.000108	0.001028	0.000006	0.282196	0.000017	23	-20.4	1.2	-4.7	1.3	1490	1705
12SZ14@08	741	11	0.052199	0.000353	0.002007	0.000012	0.282217	0.000018	26	-19.6	1.2	-4.3	1.3	1499	1689
12SZ14@09	760	11	0.031623	0.000139	0.001225	0.000005	0.282046	0.000017	26	-25.7	1.2	-9.5	1.3	1708	1971
12SZ14@10	757	11	0.058644	0.000468	0.002238	0.000020	0.282129	0.000020	26	-22.7	1.2	-7.2	1.3	1635	1849

12SZ14@11	770	11	0.030616	0.000484	0.001228	0.000018	0.282117	0.000020	25	-23.1	1.2	-6.8	1.3	1608	1840
12SZ14@12	770	11	0.047340	0.000341	0.001777	0.000011	0.282100	0.000019	27	-23.8	1.2	-7.7	1.3	1656	1884
12SZ14@13	754	11	0.133482	0.000489	0.004833	0.000020	0.281978	0.000028	28	-28.1	1.4	-13.9	1.5	1992	2182
12SZ14@14	731	10	0.037274	0.000162	0.001405	0.000006	0.282268	0.000018	27	-17.8	1.2	-2.4	1.3	1403	1586
12SZ14@15	716	10	0.069728	0.002742	0.002586	0.000102	0.282300	0.000021	27	-16.7	1.3	-2.1	1.3	1402	1560
12SZ14@16	743	11	0.055338	0.000734	0.002066	0.000024	0.282098	0.000021	27	-23.9	1.3	-8.5	1.4	1673	1904
12SZ14@17	738	11	0.055829	0.000697	0.002059	0.000025	0.282292	0.000017	27	-17.0	1.2	-1.7	1.3	1393	1556
12SZ14@18	759	11	0.023667	0.000339	0.000894	0.000011	0.282117	0.000021	26	-23.2	1.3	-6.9	1.4	1594	1835
12SZ14@19	774	11	0.050163	0.000273	0.001863	0.000010	0.282222	0.000019	27	-19.4	1.2	-3.3	1.3	1486	1667
12SZ14@20	740	11	0.053658	0.001042	0.002000	0.000033	0.282112	0.000018	27	-23.4	1.2	-8.0	1.3	1649	1878
12SZ14@22	740	11	0.021091	0.000091	0.000814	0.000004	0.282110	0.000016	26	-23.4	1.2	-7.5	1.3	1600	1851
12SZ14@25	742	11	0.060526	0.001853	0.002190	0.000064	0.282161	0.000019	28	-21.6	1.2	-6.3	1.3	1586	1793
12SZ17@01	740	11	0.040931	0.000286	0.001635	0.000010	0.282382	0.000016	25	-13.8	1.2	1.7	1.3	1250	1384
12SZ17@02	722	10	0.072149	0.001487	0.002731	0.000046	0.282417	0.000019	26	-12.6	1.2	2.1	1.3	1236	1353
12SZ17@03	728	10	0.066287	0.000217	0.002329	0.000008	0.282600	0.000018	28	-6.1	1.2	8.9	1.3	957	1012
12SZ17@04	720	10	0.073143	0.000455	0.002839	0.000016	0.282465	0.000017	26	-10.9	1.2	3.7	1.3	1170	1269
12SZ17@05	715	10	0.064435	0.001130	0.002373	0.000038	0.282453	0.000017	27	-11.3	1.2	3.4	1.3	1172	1281
12SZ17@06	741	11	0.063826	0.000845	0.002222	0.000027	0.282541	0.000019	29	-8.2	1.2	7.1	1.3	1039	1112
12SZ17@07	719	10	0.058456	0.000312	0.002050	0.000012	0.282583	0.000020	29	-6.7	1.2	8.2	1.3	973	1036
12SZ17@08	727	10	0.058396	0.002087	0.002166	0.000075	0.282612	0.000024	27	-5.7	1.3	9.4	1.4	935	986
12SZ17@09	725	10	0.066150	0.000892	0.002329	0.000030	0.282547	0.000018	28	-7.9	1.2	6.9	1.3	1033	1107
12SZ17@10	733	10	0.069504	0.000390	0.002436	0.000013	0.282545	0.000019	29	-8.0	1.2	7.0	1.3	1040	1113
12SZ17@11	706	10	0.065143	0.001095	0.002321	0.000035	0.282574	0.000017	28	-7.0	1.2	7.5	1.3	994	1063
12SZ17@12	729	10	0.062647	0.000648	0.002262	0.000025	0.282318	0.000022	28	-16.1	1.3	-1.1	1.4	1364	1518
12SZ17@13	722	10	0.055339	0.000309	0.001983	0.000011	0.282583	0.000022	28	-6.7	1.3	8.3	1.4	972	1034
12SZ17@14	722	10	0.053305	0.000296	0.001902	0.000010	0.282567	0.000017	28	-7.3	1.2	7.8	1.3	994	1063
12SZ17@15	740	11	0.113026	0.000830	0.003856	0.000028	0.282596	0.000019	29	-6.2	1.2	8.2	1.3	1005	1054

12SZ17@16	748	11	0.103767	0.001118	0.003578	0.000038	0.282644	0.000023	29	-4.5	1.3	10.2	1.4	923	958
12SZ17@17	729	10	0.049780	0.000249	0.001781	0.000009	0.282543	0.000018	28	-8.1	1.2	7.1	1.3	1024	1100
12SZ17@19	740	11	0.047699	0.000651	0.001883	0.000019	0.282419	0.000017	25	-12.5	1.2	2.9	1.3	1205	1323
12SZ17@20	733	10	0.068174	0.000166	0.002423	0.000007	0.282614	0.000019	28	-5.6	1.2	9.4	1.3	938	987
12SZ17@21	739	11	0.159032	0.002896	0.005405	0.000099	0.282635	0.000025	29	-4.9	1.3	8.8	1.4	990	1023
12SZ17@22	721	10	0.070116	0.002272	0.002478	0.000080	0.282600	0.000019	28	-6.1	1.2	8.7	1.3	960	1017
12SZ17@23	719	10	0.033889	0.000559	0.001217	0.000020	0.282510	0.000016	28	-9.3	1.2	6.0	1.3	1055	1149
12SZ17@24	722	10	0.032064	0.000495	0.001275	0.000018	0.282426	0.000019	25	-12.3	1.2	3.1	1.3	1176	1302
12SZ17@25	702	10	0.065464	0.000802	0.002302	0.000028	0.282603	0.000019	28	-6.0	1.2	8.5	1.3	951	1011
12SZ17@26	728	10	0.050851	0.000505	0.001851	0.000019	0.282481	0.000019	27	-10.3	1.2	4.9	1.3	1116	1215
12SZ17@27	743	11	0.030444	0.000120	0.001090	0.000005	0.282172	0.000016	28	-21.2	1.2	-5.4	1.3	1526	1747
12SZ17@28	831	12	0.053706	0.000337	0.001870	0.000011	0.282510	0.000017	29	-9.3	1.2	8.1	1.3	1074	1136
Yuanziwan Formation, upper part of Suixian Group															
12SZ10@01	752	11	0.053345	0.000218	0.002020	0.000009	0.282136	0.000024	26	-22.5	1.3	-6.9	1.4	1615.7	1830.7
12SZ10@02	747	11	0.072090	0.000460	0.002543	0.000016	0.282189	0.000031	28	-20.6	1.5	-5.4	1.6	1562.4	1750.9
12SZ10@03	763	11	0.026471	0.000147	0.001018	0.000005	0.282214	0.000019	26	-19.7	1.2	-3.4	1.3	1464.2	1663.0
12SZ10@04	730	10	0.052742	0.000691	0.001891	0.000024	0.281953	0.000022	28	-29.0	1.3	-13.8	1.4	1869.6	2158.3
12SZ10@05	737	11	0.043154	0.000215	0.001603	0.000008	0.282044	0.000020	27	-25.8	1.2	-10.3	1.3	1727.8	1988.8
12SZ10@07	749	11	0.046471	0.000642	0.001746	0.000023	0.282115	0.000020	27	-23.2	1.3	-7.6	1.3	1633.6	1862.2
12SZ10@08	738	10	0.041047	0.000246	0.001579	0.000011	0.281984	0.000019	26	-27.9	1.2	-12.4	1.3	1810.9	2094.1
12SZ10@09	734	11	0.040728	0.000098	0.001537	0.000002	0.282183	0.000017	26	-20.8	1.2	-5.4	1.3	1528.0	1739.0
12SZ10@10	725	10	0.022914	0.000208	0.000945	0.000009	0.282050	0.000017	24	-25.5	1.2	-10.0	1.3	1688.8	1964.3
12SZ10@11	733	10	0.097772	0.000826	0.003335	0.000036	0.282047	0.000024	29	-25.7	1.3	-11.1	1.4	1807.3	2026.5
12SZ10@13	763	11	0.069837	0.000796	0.002562	0.000030	0.281896	0.000020	27	-31.0	1.3	-15.5	1.3	1986.5	2268.4
12SZ10@14	736	10	0.043564	0.000319	0.001620	0.000012	0.282126	0.000018	27	-22.8	1.2	-7.4	1.3	1612.1	1842.2
12SZ10@16	731	10	0.036856	0.000239	0.001398	0.000008	0.281992	0.000017	26	-27.6	1.2	-12.1	1.3	1790.9	2077.3

12SZ10@17	720	10	0.041915	0.000210	0.001594	0.000007	0.282121	0.000017	26	-23.0	1.2	-7.9	1.3	1618.8	1855.7
12SZ10@18	765	11	0.042009	0.000378	0.001609	0.000013	0.282188	0.000022	26	-20.7	1.3	-4.6	1.4	1524.3	1724.0
12SZ10@20	728	10	0.116227	0.000388	0.003953	0.000014	0.282374	0.000037	29	-14.1	1.7	0.1	1.7	1345.1	1458.0
12SZ10@22	749	11	0.061955	0.002685	0.002284	0.000092	0.281949	0.000027	27	-29.1	1.4	-13.7	1.5	1895.8	2171.2
12SZ10@23	740	11	0.048112	0.001423	0.001710	0.000045	0.282293	0.000018	28	-16.9	1.2	-1.4	1.3	1379.1	1545.0
12SZ10@24	731	11	0.048567	0.000809	0.001772	0.000029	0.281936	0.000025	27	-29.6	1.4	-14.3	1.4	1888.4	2186.3
12SZ10@25	777	11	0.088392	0.002324	0.003201	0.000083	0.282206	0.000024	28	-20.0	1.3	-4.5	1.4	1564.9	1729.3
12SZ10@26	732	10	0.047685	0.000186	0.001769	0.000007	0.282181	0.000019	27	-20.9	1.2	-5.6	1.3	1540.9	1749.2
12SZ10@27	757	11	0.028810	0.000442	0.001085	0.000016	0.282200	0.000019	27	-20.2	1.2	-4.1	1.3	1486.4	1691.3
12SZ10@28	750	11	0.065030	0.000965	0.002411	0.000034	0.282131	0.000026	27	-22.7	1.4	-7.3	1.4	1639.3	1849.0
13SZ17@01	736	10	0.141088	0.001771	0.004996	0.000048	0.282213	0.000022	28	-19.8	1.3	-6.0	1.4	1638	1771
13SZ17@02	730	10	0.041076	0.000152	0.001500	0.000005	0.282152	0.000019	27	-21.9	1.2	-6.5	1.3	1570	1795
13SZ17@03	730	10	0.050014	0.000291	0.001813	0.000011	0.282128	0.000020	28	-22.8	1.2	-7.6	1.3	1618	1846
13SZ17@04	715	10	0.041864	0.000165	0.001560	0.000006	0.282161	0.000019	27	-21.6	1.2	-6.6	1.3	1560	1785
13SZ17@05	718	10	0.044161	0.000315	0.001632	0.000012	0.282142	0.000021	27	-22.3	1.3	-7.2	1.3	1591	1821
13SZ17@07	733	10	0.042965	0.000251	0.001573	0.000009	0.282184	0.000020	27	-20.8	1.2	-5.4	1.3	1528	1739
13SZ17@09	730	10	0.089549	0.000818	0.003420	0.000031	0.282327	0.000019	26	-15.7	1.2	-1.3	1.3	1395	1529
13SZ17@10	724	10	0.056921	0.000292	0.002091	0.000011	0.282223	0.000019	27	-19.4	1.2	-4.5	1.3	1494	1685
13SZ17@11	741	11	0.034624	0.000408	0.001295	0.000016	0.282161	0.000021	27	-21.6	1.3	-5.9	1.4	1550	1772
13SZ17@12	739	10	0.057143	0.000567	0.002082	0.000019	0.282243	0.000024	27	-18.7	1.3	-3.4	1.4	1465	1645
13SZ17@13	738	11	0.065614	0.000739	0.002403	0.000028	0.282157	0.000025	27	-21.8	1.4	-6.7	1.4	1602	1807
13SZ17@14	724	10	0.035576	0.000159	0.001313	0.000007	0.282181	0.000023	27	-20.9	1.3	-5.6	1.4	1521	1740
13SZ17@15	722	10	0.049282	0.000293	0.001832	0.000010	0.282178	0.000032	27	-21.0	1.5	-6.0	1.6	1547	1759
13SZ17@16	793	11	0.058614	0.001197	0.002147	0.000040	0.282486	0.000022	27	-10.1	1.3	6.3	1.4	1117	1197
13SZ17@17	738	10	0.060346	0.000139	0.002222	0.000005	0.282169	0.000020	27	-21.3	1.2	-6.1	1.3	1577	1781
13SZ17@18	719	10	0.052510	0.000398	0.001921	0.000016	0.282138	0.000021	27	-22.4	1.3	-7.5	1.3	1608	1834
13SZ17@19	731	10	0.039832	0.000447	0.001474	0.000017	0.282197	0.000021	27	-20.3	1.3	-4.9	1.3	1506	1714

13SZ17@20	799	11	0.031427	0.000353	0.001320	0.000014	0.282471	0.000017	24	-10.6	1.2	6.3	1.3	1113	1199
13SZ17@21	746	11	0.074815	0.000180	0.002697	0.000007	0.282210	0.000028	28	-19.9	1.4	-4.7	1.5	1538	1717
13SZ17@22	731	10	0.054128	0.000135	0.001967	0.000005	0.282177	0.000023	28	-21.0	1.3	-5.9	1.4	1554	1762
13SZ17@24	738	11	0.031422	0.000099	0.001170	0.000004	0.282127	0.000019	27	-22.8	1.2	-7.1	1.3	1592	1831
13SZ17@25	721	10	0.056329	0.000318	0.002067	0.000013	0.282232	0.000027	27	-19.1	1.4	-4.2	1.5	1480	1668
13SZ17@26	709	10	0.043505	0.000166	0.001590	0.000005	0.282190	0.000021	27	-20.6	1.3	-5.7	1.3	1521	1736

T_{DM1} and T_{DM2} were calculated according o the following equations and parameters:
$T_{DM1} = (1/\lambda) \times \ln[1+(^{176}Hf/^{177}Hf_{DM} - {}^{176}Hf/^{177}Hf_S)/(^{176}Lu/^{177}Hf_{DM} - {}^{176}Lu/^{177}Hf_S)]$;
$T_{DM2} = T_{DM1} - (T_{DM1} - T) \times [(f_{cc}-f_s)/(f_{cc}-f_{DM})]$;
$f_{Lu/Hf} = (^{176}Lu/^{177}Hf)_s/(^{176}Lu/^{177}Hf)_{CHUR}-1$;
where f_{cc},f_{DM},and f_s are the $f_{Lu/Hf}$ values of the continental crust, the depleted mantle, and the zircon grains, respectively; S, CHUR, DM,and T refer to sample, chondritic uniform reservoir, depleted mantle, and zircon U-Pb age, respectively.
Decay constant of ^{176}Lu $\lambda = 1.867 \times 10^{-11}$ $year^{-1}$(Söderlund et al., 2004).
$^{176}Hf/^{177}Hf_{DM} = 0.28325$, $^{176}Lu/^{177}Hf_{DM} = 0.0384$ (Griffin et al., 2000).
Present-day $^{176}Hf/^{177}Hf_{CHUR}(0) = 0.282772$; $^{176}Lu/^{177}Hf_{CHUR} = 0.0332$ (Blichert and Albarède, 1997).
$(^{176}Lu/^{177}Hf)_{CC} = 0.015$, $(^{176}Hf/^{177}Hf)_{CC} = 0.28325$ (Amelin et al., 1999).

References:

Amelin, Y., Lee, D-C., Halliday, A. N. and Pidgeon, R. T. ,1999, Nature of the Earth's earliest crust from hafnium isotopes in single detrital zircons, Nature 399, 252-255.
Blichert-Toft, J. and Albarède, F., 1997. The Lu–Hf isotope geochemistry of chondrites and the evolution of the mantle–crust system. Earth and Planetary Science Letters 148, 243–258.
Griffin, W., Pearson, N.J., Belousova, E., Jackson, S.E., Van Achterbergh, E., O'Reilly, S.Y. and Shee, S.R., 2000. The Hf isotope composition of cratonic mantle: LAM–MC–ICPMS analysis of zircon megacrysts in kimberlites. Geochimica et Cosmochimica Acta 64, 133–148.
Söderlund, U., Patchett, P.J., Vervoort, J.D. and Isachsen, C.E., 2004. The ^{176}Lu decay constant determined by Lu-Hf and U-Pb isotope systematics of Precambrian mafic intrusions. Earth and Planetary Science Letters 219, 311-324.

Appendix S4 Atlas of cathodoluminescence images

12SZ20 siltstone Gujing Formation lower part of Suixian Group

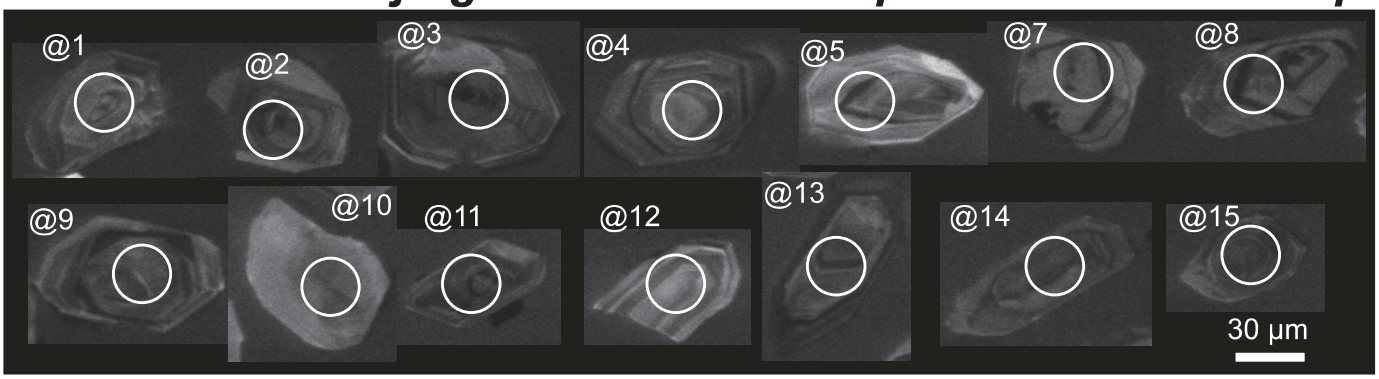

12SZ24 sandstone Gujing Formation lower part of Suixian Group

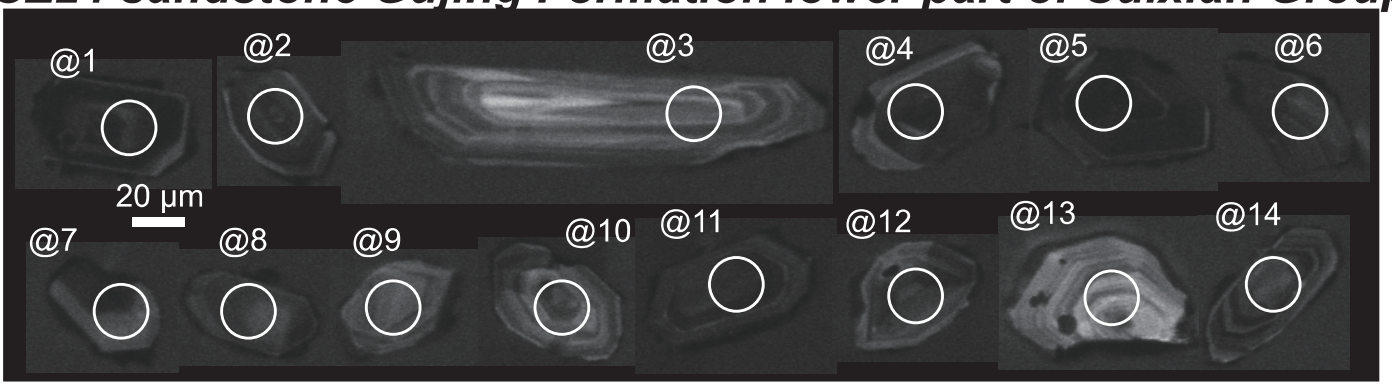

12SZ28 sandstone Gujing Formation lower part of Suixian Group

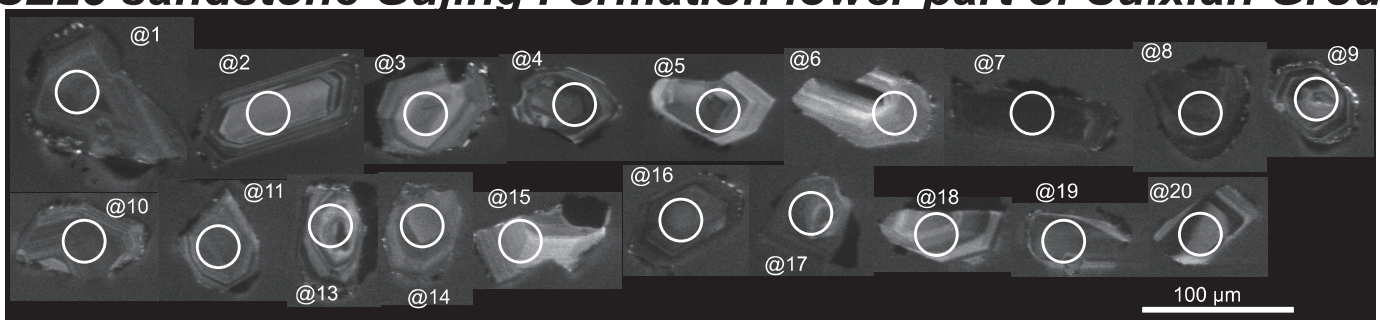

12SZ06 sandstone Liulin Formation middle part of Suixian Group

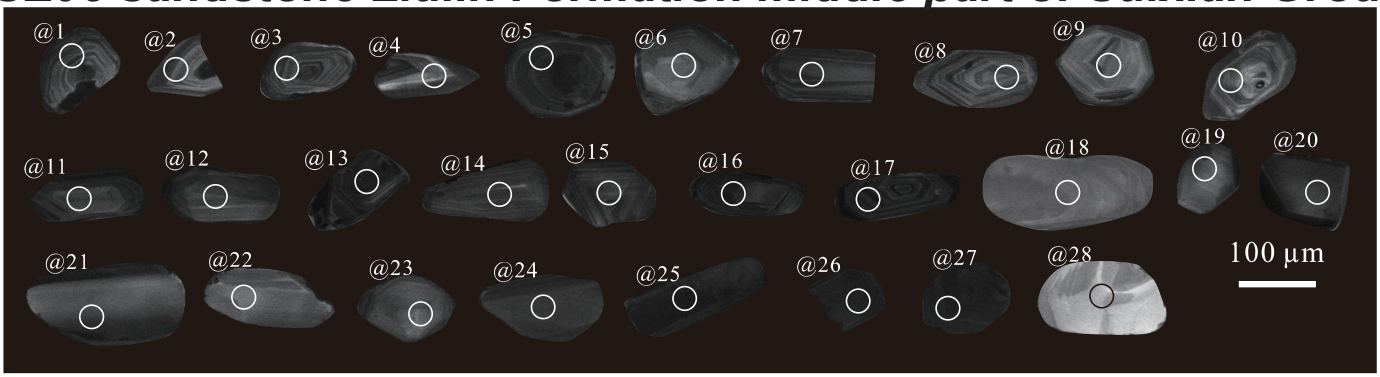

12SZ07 sandstone Liulin Formation middle part of Suixian Group

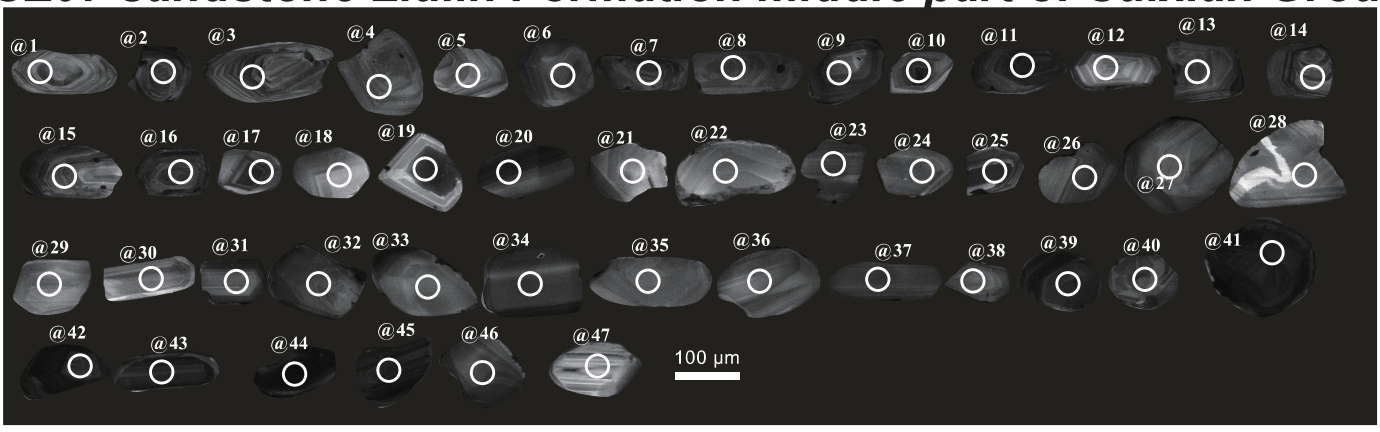

13SZ14 sandstone Liulin Formation middle part of Suixian Group

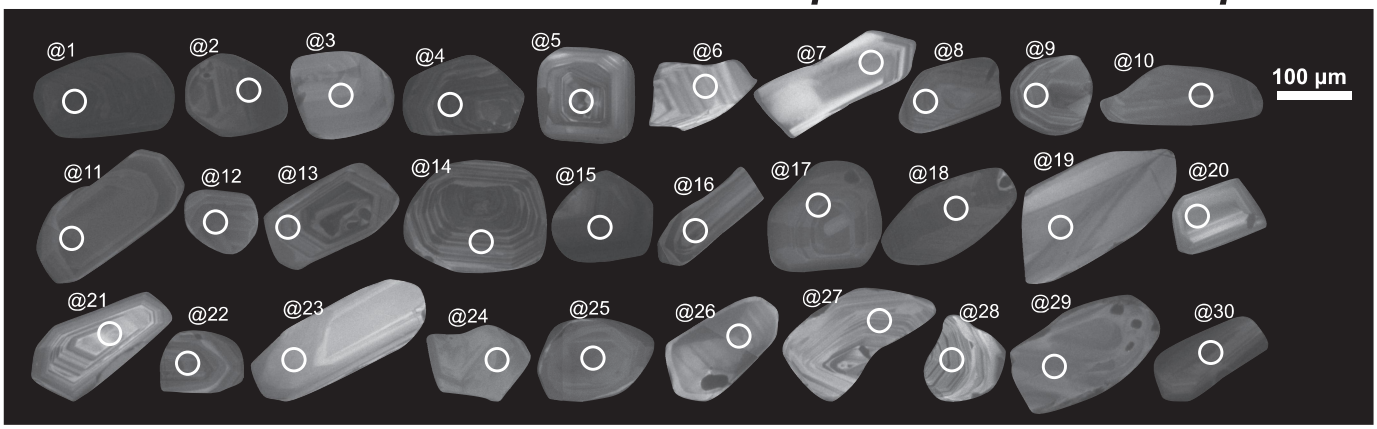

13SZ19 sandstone Liulin Formation middle part of Suixian Group

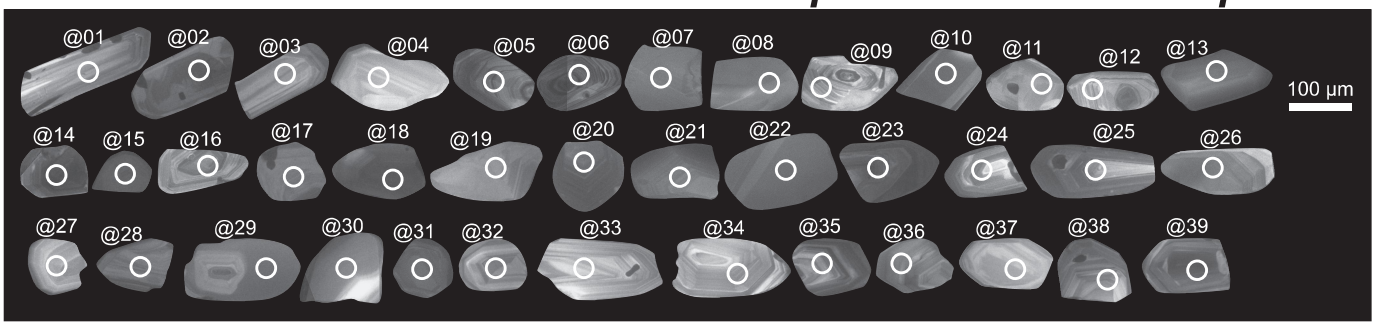

12SZ14 metarhyolite Liulin Formation middle part of Suixian Group

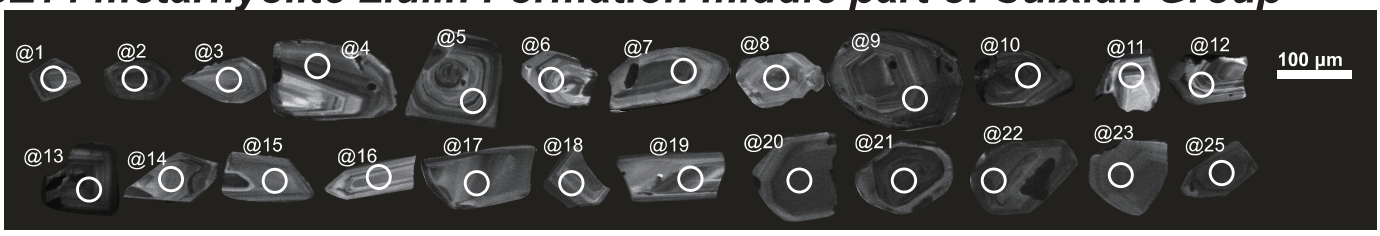

12SZ17 tuffaceous siltestone Liulin Formation middle part of Suixian Group

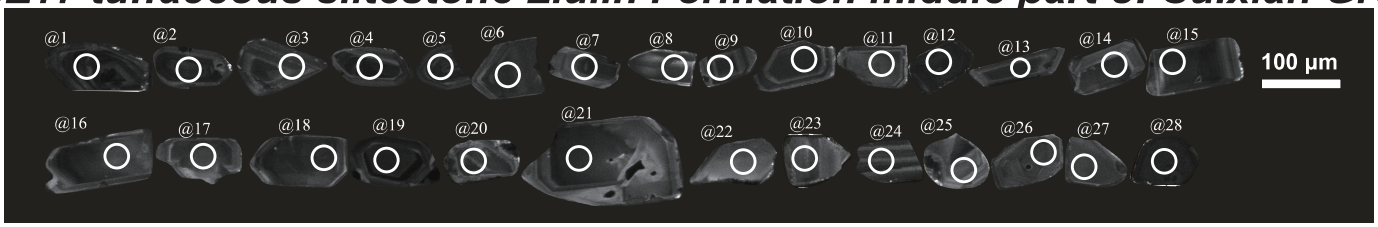

12SZ10 siltstone Yuanziwan Formation upper part of Suixian Group

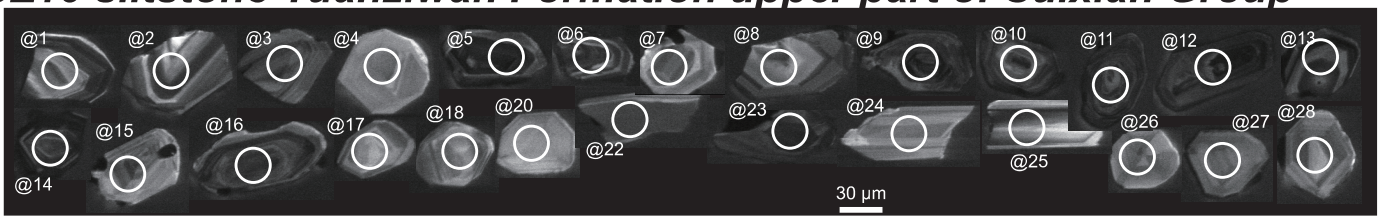

13SZ17 sandstone Yuanziwan Formation upper part of Suixian Group